Effect of Mechanical Environment on the Differentiation of Bone Marrow Stromal Cells for Functional Bone Tissue Engineering

Katherine Dulaney Kavlock

Dissertation Submitted to the Faculty of the Virginia Tech-Wake Forest School of Biomedical Engineering and Sciences in fulfillment of the requirements for the degree of

Doctor of Philosophy
In
Biomedical Engineering

Committee Members:

Aaron S. Goldstein, Ph.D., Chairman
William R. Huckle, Ph.D.
Yong W. Lee, Ph.D.
Brian J. Love, Ph.D.
Pavlos P. Vlachos, Ph.D

March 27, 2009
Blacksburg VA

Keywords: Bone Marrow Stromal Cells, Osteoblastic Differentiation, Polyurethane, Perfusion

Effect of Mechanical Environment on the Differentiation of Bone Marrow Stromal Cells for Functional Bone Tissue Engineering

Katherine Dulaney Kavlock

Abstract

Bone is the second most transplanted tissue after blood and the need for bone graft materials continues to rise at an average annual growth rate of over 18%. An engineered bone substitute consisting of a bone-like extracellular matrix deposited on the internal pores of a resorbable biomaterial scaffold is postulated to stimulate normal bone remodeling when implanted *in vivo*. Part one of this engineering strategy, the deposition of bone-like extracellular matrix, can be achieved by the directed differentiation of progenitor cells such as bone marrow stromal cells (BMSCs). Part two of the engineering strategy, the biomaterial scaffold, can be fabricated with the appropriate mechanical properties using a synthetic polymer system with tunable properties like polyurethanes. Finally, BMSCs seeded within the biomaterial scaffold can be cultured in a perfusion flow bioreactor to stimulate osteoblastic differentiation and the deposition of bioactive factors. Using the three-part engineering strategy described, I hypothesize that the extracellular matrix produced by BMSCs can be modulated by two stimuli: the stiffness of the scaffold and perfusion flow. First, I propose that culturing BMSCs on polyurethane scaffolds with increasing stiffness will increase markers of osteoblastic differentiation. Secondly, I suggest that mechanically stimulating BMSCs with novel perfusion strategies will also increase markers of osteoblastic differentiation.

In aim 1, a family of segmented degradable poly(esterurethane urea)s (PEUURs) were synthesized. The modulus of the PEUUR materials was systematically increased from 0.18 to 0.80 MPa by systematically increasing the molecular weight of the poly(ε-caprolactone) (PCL) soft segment from 1425 to 2700 Da. BMSCs were cultured on both rigid polymer films and on porous foam scaffolds to dissociate the effect of variation in polymer chemistry from the effect of scaffold modulus on cell phenotype. These studies demonstrated changes in osteoblastic differentiation as measured by prostaglandin E_2 production, alkaline phosphatase activity (ALP) activity, and osteopontin gene expression.

However, the increased levels of these phenotypic markers on the PCL 2700 material could not be attributed to scaffold chemistry or modulus. Instead, the differences may be related to polymer crystallinity or surface topography.

In aim 2, novel dynamic perfusion strategies were used to investigate the influence of frequency on osteoblastic differentiation. BMSCs were seeded on porous foam scaffolds and exposed to both steady perfusion and pulsatile perfusion at 0.017, 0.050, and 0.083 Hz frequencies. The data presented here demonstrated that while some markers of osteoblastic phenotype such as ALP activity are enhanced by 0.05 Hz pulsatile flow over continuous flow, they are insensitive to frequency at low frequencies. Therefore, future studies will continue to investigate the effect of a larger range of frequencies.

Additionally, fluid flow has also been shown to stimulate the deposition of bioactive factors such as BMP-2 and VEGF-A, and these growth factors are known to significantly enhance healing in bone defect models. Therefore, we plan to investigate the effect of dynamic flow strategies on the deposition of these bioactive factors. We propose that an engineered bone graft material containing a bone-like extracellular matrix and producing these growth factors will show more rapid formation of bone when implanted *in vivo*.

Authors Acknowledgements

This work could not have been accomplished without the assistance and expertise of several people here at Virginia Tech. First and foremost, I am extremely grateful to my advisor, Dr. Aaron Goldstein, for his guidance throughout my graduate education here at Virginia Tech. I also want to acknowledge Dr. Brian Love, Dr. William Huckle, Dr. YongWoo Lee, and Dr. Pavlos Vlachos for their valuable support and advice while serving on my committee.

I want to thank Dr. Thomas Ward from the Department of Chemistry for the use of the goniometer and spin-coater. Additionally, I want to thank Dr. Garth Wilkes and Todd Pechar from the Department of Chemical Engineering and Sha Yang from the Department of Chemistry for assistance with DSC, DMA, and WAXS measurements as well as helpful conversations on materials characterization. Finally, I am grateful to Riley Chan and Mike Vaught for all their assistance in construction and programming of the flow system.

Last but not least, I want to express my sincere appreciation to all my lab mates, friends, and family for supporting me and keeping me balanced during the last 5 years.

This work has been funded by the National Institutes of Health (R21-AR015945 and R21-AR055200) as well as by a National Science Foundation Graduate Research Fellowship.

Table of Contents

Figures *Page Number*

Tables

Chapter 1: Introduction

1.1 Significance

Approximately half of the more 3 million musculoskeletal procedures performed annually in the US involve bone grafting [1]. In fact, the worldwide market for bone replacement and repair strategies in 2006 was estimated to be more than $2.3 billion and is projected to double by 2010 [2]. The growth of the market is fueled by several factors, including aging of the population, physiological problems associated with the increased incidence of obesity, and the emergence of new and minimally invasive procedures. Bone grafts are often used for spinal fusions, for filling defects following removal of bone tumors, or for the treatment of congenital diseases [3].

The four qualities that a bone graft should exhibit include: (1) osteointegration, the ability to promote union with the surface of the bone with no intervening fibrous layer; (2) osteoconduction, the ability to support the growth of bone over its surface; (3) osteoinduction, the ability to promote the differentiation of adult stem cells from surrounding tissue into an osteoblastic phenotype; and (4) osteogenesis, the ability to form new bone from osteoblasts present in the graft [4]. Autologous bone grafts (autografts) are currently the only graft material that exhibit all four of these desired characteristics.

Autologous cancellous bone and, to a lesser extent, cortical bone, harvested from the iliac crest, scapula, fibula, or rib, is currently the surgical "gold standard" for bone graft material. Cortical bone, also known as compact bone, makes up about 80% of the skeleton and is only 10% porous. Cancellous (or trabecular or spongy) bone is 50-90% porous, making its modulus of elasticity and ultimate strength much less than that of cortical bone [5]. Cortical bone can be used in bone graft procedures to provide structural support to a defect site, but is less osteogenic than cancellous bone. Cancellous bone contains more cells and is more metabolically active than cortical bone, allowing for faster healing and incorporation into surrounding bone [6]. However, autologous bone, both cortical and cancellous, is available in limited supply and its explantation incurs additional costs and risks, including additional surgical time, risk of infection, increased morbidity and weakened

bone at the donor site, and chronic pain at the donor site [7]. Additionally, reports indicate that up to 15% of patients with an iliac graft harvest have persisting pain at the harvest site for more than 3 months [4, 8].

The most commonly used alternative to autograft is allogenic bone graft (allograft), typically obtained from a cadaver. Allografts have all of the characteristics of an ideal bone graft with the exception of osteogenesis because the cells in allografts are eliminated to reduce risk of immune response and disease transfer. The greatest advantage of allograft material is the increased availability of donor material and avoidance of donor site morbidity. However, it does still carry the risk of viral disease transfer despite sterilization and screening. Also, the processing associated with sterilizing allografts, namely freezing and irradiation, affects the structural strength and the biochemical properties of the graft [3, 6]. In fact, because of processing conditions, allograft materials have a higher incidence of delayed union, fatigue fractures, and resorption of the graft material than autografts [7]. Therefore, the processing and preservation methods must strike a critical balance between being stringent enough to inactivate viruses, but not too stringent so as to negatively alter the biochemical and biomechanical properties of the tissue.

Currently autografts and allografts are used in 75% of bone grafting procedures; however, the rapidly rising demand for material, coupled with the inherent limitations of autografts and allografts, has led to increased use of alternative materials [2]. Consequently, orthobiologics, biologically based products for hard and soft tissue regeneration, is the fastest growing sector of the global orthopaedic market [1]. Substitutes to autograft and allograft vary widely in terms of composition and mechanism of action and include materials such as ceramics, metals, synthetic polymers, natural structural proteins, and demineralized bone matrix. Unfortunately, most of these substitute materials have one thing in common: they only possess two of the four characteristics of an ideal graft material (osteoconduction and osteointegration). Therefore, new graft materials must be developed. The next generation of bone graft substitutes must possess the increased availability of synthetic materials in addition to the osteoinductive and osteogenic potential of autograft materials. The field of tissue engineering seeks to address this need using an interdisciplinary approach that

combines aspects of medicine, biology, material science, and engineering fields of research. However, before a suitable bone tissue replacement can be engineered, the biology of bone must be better understood.

1.2 Bone Biology

Bone is a highly organized structure comprised of a central marrow cavity surrounded by cancellous bone which in turn is surrounded by dense cortical bone. Osteons (Figure 1.1) are the basic organizational unit of cortical bone. The center of each osteon is the haversian canal which encloses blood vessels, lymphatic vessels, and sometimes nerves. Surrounding each haversian canal are the osteocyte-containing lamellae. Osteocytes are non-dividing, mature bone cells and the most abundant cell type found in bone. Osteocytes extend processes through small canals called canaliculi which radiate outward from the haversian canal and link osteocytes to adjacent cells. These linkages, mediated by gap junctions, are thought to allow osteocytes to communicate. The canaliculi also allow for nutrient transport since diffusion through mineralized bone matrix is very difficult.

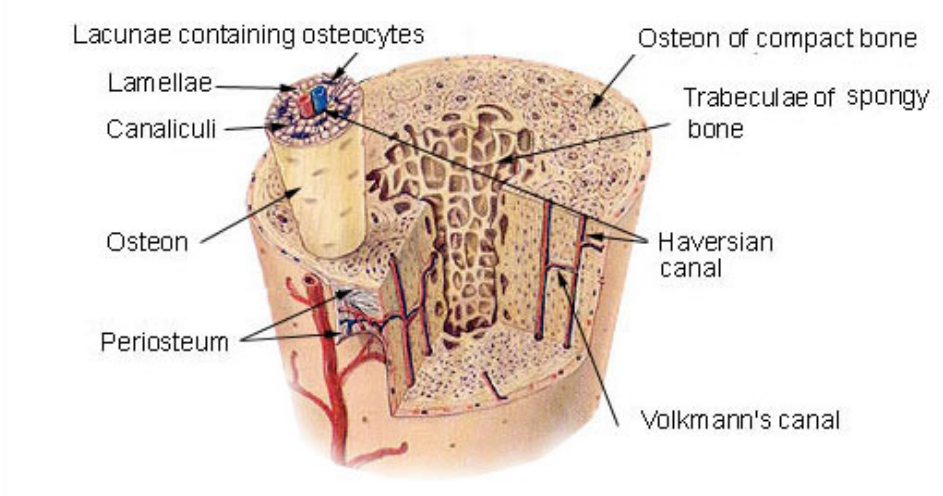

Figure 1.1: Organization of cortical bone [9] [fair use]

Bone tissue is comprised of two main components: bone extracellular matrix and bone cells. Bone extracellular matrix is comprised of both organic and inorganic components

and constitutes more than 90% of tissue volume [10]. The organic components of the extracellular matrix consist largely of type-I collagen fibrils and non-collagenous proteins such as osteopontin and osteocalcin. (Osteopontin also is found in plasma and a variety of organs suggesting that this molecule acts as both a structural molecule, as in the case of bone matrix, and as a cytokine.) Within the bone extracellular matrix, osteopontin is known to promote cell attachment through covalent binding with fibronectin and type I collagen [11]. Osteocalcin is a bone-specific protein that is synthesized by mature osteoblasts at the onset of matrix mineralization. Osteocalcin contains three residues of γ-carboxyglutamic acid (Gla), a calcium-binding amino acid, and is believed to interact with hydroxyapatite through its Gla residues [11]. Both osteopontin and osteocalcin have an affinity for calcium and may facilitate the nucleation of calcium phosphate during mineralization [11].

The inorganic components of the extracellular matrix consist of calcium, carbonate, and phosphate ions, which are arranged in a crystalline-like structure. This structure gives bone its compressive strength and also serves as an ion reservoir. Matrix mineralization occurs in a two step process: nucleation of calcium phosphate crystals, followed by crystal growth [5]. Non-collagenous proteins have high affinities for calcium and can be nucleation points for crystallization. After nucleation, amorphous calcium phosphate is deposited and eventually converted to hydroxyapatite.

Bone tissue houses three main cell types: osteoblasts, osteoclasts, and osteocytes. The three types of bone cells are responsible for formation, resorption, and the maintenance bone tissue respectively. The primary function of osteoblasts is synthesizing and secreting organic extracellular matrix molecules such as type I collagen. Osteoblasts also synthesize a variety of growth factors including transforming growth factor-β (TGF-β) and bone morphogenic proteins (BMPs) that can aid in both the recruitment and differentiation of stem cells [10]. TGF-β1 is a multifunctional cytokine that can acts to regulate cell growth, stimulate matrix production, and induce vascular endothelial growth factor (VEGF), a growth factor associated with the formation of blood vessels during bone development. BMPs are a member of the TGF-β superfamily and have been shown to be osteoinductive and mediators of fracture repair. Recombinant forms of BMP-2 and BMP-7 have been developed and are

used clinically in conjunction with bone grafting materials and for enhancing fixation of metal orthopaedic implants. With both metal implants and other bone grafting materials, BMPs initiate endochondral bone formation where mesenchymal stem cells lay down a cartilaginous matrix which is subsequently resorbed and replaced with bone [11]. As osteoblasts produce collagen matrix they become separated, less metabolically active, and they gradually lose the ability to produce matrix. When matrix is no longer actively being formed, the osteoblasts become embedded within the extracellular matrix and become osteocytes.

Osteoclasts originate from hematopoietic precursor cells are responsible for bone resorption [12]. These multinuclear cells attach to the surface of bone and lower the pH of the extracellular environment from 7 to 4. The acidity dissolves the mineral component of the extracellular matrix while proteases released from the osteoclasts degrade the organic components of the matrix. In this manner osteoclasts form cavities in the bone matrix to allow for new bone formation by osteoblasts [10].

Osteocytes are responsible for the maintenance of bone. The osteocytes have long processes that extend through the canaliculi and connect to other osteocytes. Through this cellular network, osteocytes can coordinate bone formation and resorption. As previously described, the canaliculi are filled with interstitial fluid to allow for nutrient transport. When bone undergoes deformation the fluid in the canaliculi flows causing shear stresses and streaming potentials to which the osteocytes sense and respond [5].

1.3 Mechanotransduction

The natural process of bone remodeling is the first indication that bone is mechanosensitive. For example, decreased mechanical loading from prolonged bed rest or exposure to the microgravity of outer space leads to decreased bone mass, while increased loading due to weight gain or exercise results in increased bone mass. Because of the variety of mechanical events that a bone cell experiences, theories about the nature of the receptors for mechanical force have also widely varied. Compressive forces applied on bone during movement cause not only direct strain to the cells but changes in hydrostatic pressure, fluid-

flow induced shear stress, and electrical potentials. Each of these phenomena may be sensed by the osteocytes.

The four primary theories about how mechanosensing occurs involve (1) stretch activated ion channels; (2) integrins; (3) deformation of the cytoskeleton; and (4) connexins [13, 14]. With stretch activated ion channels, strain of the cellular membrane due to macroscopic phenomena such as hydrodynamic shear stress in canaliculi causes Ca^{2+} channels to open. The influx of Ca^{2+} ions activates intracellular enzymes such as phospholipase C and protein kinase C while also causing membrane depolarization leading to the opening of voltage-gated channels and further ion entry [13]. Furthermore it has been shown that intracellular calcium is a critical second messenger molecule because when its mobilization is blocked during mechanical stimulation, the mechanically regulated changes in gene expression (COX-2, c-fos, and OPN) do not occur [15, 16].

Integrins are cell surface receptors that are activated when their binding partners (i.e. fibronectin, collagen, or osteopontin) in the extracellular matrix are deformed. Interestingly, studies have shown that integrin-mediated signaling of mechanical stimulation also involves release of calcium and that 1 Hz cyclic stress has been shown to be more effective at increasing calcium transients than 0.1 Hz or continuous stimulation in response to small mechanical forces (2×10^{-10} N) [17]. Additionally, osteoblasts and bone marrow stromal cells display different trends in calcium transients in response to mechanical stress. Osteoblasts exhibit single or oscillating intracellular calcium transients while bone marrow stromal cells demonstrate only a single calcium transients peak. This difference perhaps indicates significant differences in the transmission of signal with progression of differentiation [13]. Integrins also play a role in mechanotransduction by transmitting forces to the cytoskeleton.

As the cytoskeleton is deformed, it provides more sites for the formation of focal adhesions, which act as mechanical linkages to the extracellular matrix, and consequently increasing activation of focal adhesion kinase (FAK). FAK is believed to mediate adhesion-stimulated effects and plays an important role in the response of cells (i.e. migration) to the stiffness of their substrates [18]. At the cellular scale, cells anchor to and pull on their

surroundings. Actin filaments link focal adhesions and transmit strains through the cytoskeleton. The cell then responds to the resistance of the substrate by adjusting its adhesions and cytoskeleton organization [19]. It has been shown that ablation of FAK impairs the ability of cells to reorient and migrate in response to gradients in substrate compliance [18].

Finally, connexins are proteins that span the cell membrane. They form hemichannels that interact with similar hemichannels on adjacent cells allowing exchange of small molecules. Intercellular communication through connexins allows cells to transmit information about their mechanical environment to each other. This transmission allows a "sensing" cell to elicit changes in cells removed from the site of mechanical loading. Mechanical stimulation has also been shown to increase the expression of connexins both *in vitro* and *in vivo*. As cells become better connected to each other in response to mechanical stimulation they can transmit more information, acting as a positive feedback loop. Knockdown of connexins with connexins antisense results in inhibition of the release of the signaling molecule, prostaglandin E_2 (PGE_2), in the presence of shearing fluid flow [14]. The intercellular communication made possible by connexins may help explain how osteocytes communicate with osteoblasts and osteoclasts in bone remodeling.

Stimulation of mechanosensors by fluid flow result in intracellular events such as increases in intracellular calcium release [15], synthesis and release of nitric oxide and PGE_2 [20-22], and activation of mitogen-activated protein kinases (MAPKs) (Figure 1.2) [16, 23]. Extracellular regulated kinase (ERK) is a MAPK that has been shown to be activated by PGE_2 [24] which in turn has been shown to be synthesized in response to cytoplasmic calcium release [25]. ERK and c-jun kinase (JNK) activate the c-Fos and c-Jun subunits of AP-1 respectively [26, 27]. AP-1 is a transcription factor that binds to the promoter region upstream of several bone-related genes including collagen type I, alkaline phosphatase, osteopontin, and osteocalcin [28].

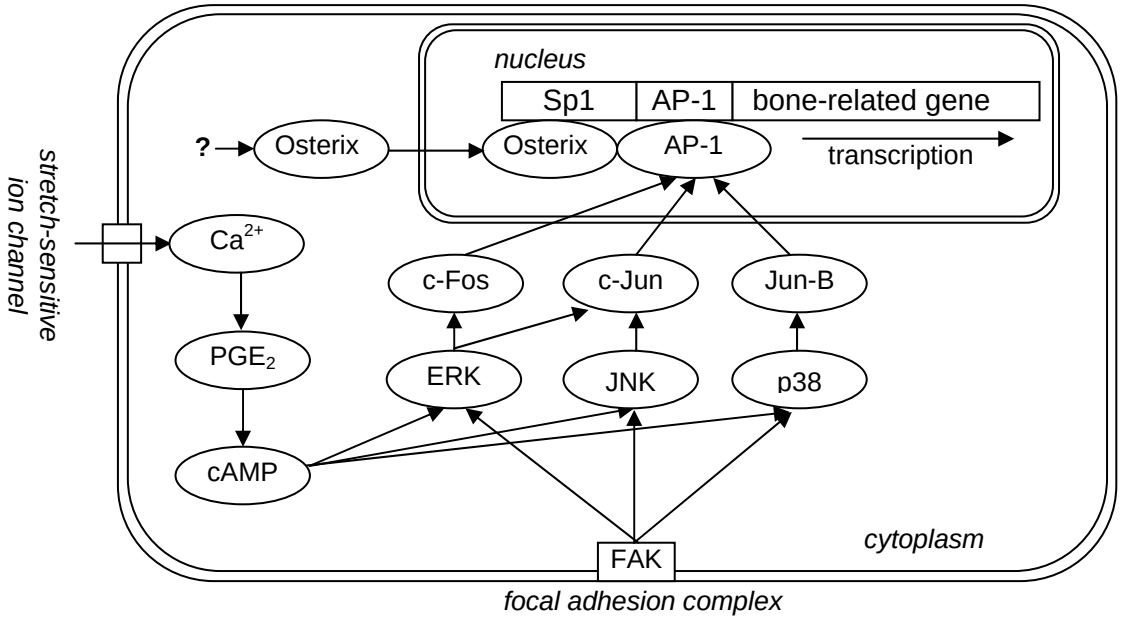

Figure 1.2: Mechanistic model of perfusion-induced expression of osteoblastic genes.

In reality, all of the theories outlined above are probably involved in mechanotransduction as cells sense mechanical events through multiple pathways. With a working understanding of bone biology and how bone cells sense their mechanical environment, a strategy for engineering a suitable bone graft substitute can be formed.

1.4 Tissue Engineering Strategy

The broad tissue engineering paradigm for creating bone tissue *in vitro* involves the use of cells, a biodegradable scaffold, and pharmaceutics either in combination or alone. The cells are the prime component of the paradigm and are the means by which new tissue is formed *in vitro*. The scaffold serves as both a space filler and a delivery vehicle for the cells and/or pharmaceutics. Since most primary organ cells are anchorage dependent, they cannot form new tissue on their own. Instead they need the biomaterial scaffold to provide a surface to attach to and serve as a template for guiding tissue regeneration [29]. The pharmaceutical agents used in the tissue engineering paradigm range from antibiotics to bioactive molecules such as growth factors; and their main function is to facilitate healing.

An engineered bone tissue consisting of a bone-like extracellular matrix deposited on the internal pores of a resorbable biomaterial scaffold is postulated to stimulate integration, vascular infiltration, and normal bone remodeling when implanted *in vivo* [29, 30]. Our approach for engineering a suitable bone graft material incorporates both cells and a biomaterial scaffold. However, instead of additional bioactive molecules, we plan to utilize the cells intrinsic ability to produce a bioactive extracellular matrix. Several *in vitro* conditioning techniques can be employed to facilitate the deposition of a bioactive matrix. For example, mechanical stimulation has been shown to aid in the development of tissue by organizing and stimulating the deposition of a bone-like extracellular matrix containing the growth factors necessary to stimulate native tissue integration and remodeling. Therefore, our tissue engineering approach also includes a bioreactor that supplies nutrients and applies mechanical stimulation to the cells [31, 32]. Our strategy also includes the addition of osteogenic supplements during *ex vivo* development of the engineered bone tissue. These osteogenic factors include ascorbic acid, β-glycerophosphate, and dexamethasone. Ascorbic acid induces collagen synthesis and deposition. β-glycerophosphate provides a source of inorganic phosphate for mineralization. And dexamethasone, a synthetic glucocorticoid, promotes bone nodule formation [10].

1.5 Osteoprogenitor Cells

Appropriate cells for our tissue engineering strategy must be highly proliferative and capable of producing the necessary extracellular matrix. Immortalized cell lines, such as the neonatal mouse MC3T3-E1 cell line, were developed by researchers to meet these needs. They can divide indefinitely and are known to display patterns of gene expression that resemble those of primary bone cells [33]. Primary cells are cells obtained and isolated directly from animal or human tissue. While cell lines can have features in common with primary osteogenic cells and can serve as reproducible models for studying osteoblastic function, primary cells are preferred because they are more representative of cells *in vivo* and are therefore more clinically relevant.

Primary osteoblasts can be very effective in depositing mineralized bone-like extracellular matrix, but have only limited capacity for proliferation, and are difficult to isolate due to their encasement within mature mineralized bone [34, 35]. An alternative strategy for obtaining large numbers of osteoblasts is to expand them from osteoprogenitor cells. Osteoprogenitor cells are immature, highly proliferative cells that can be obtained from a number of tissue types. Both osteoblasts and osteocytes originate from a population of mesenchymal stem cells (MSCs). MSCs are adult stem cells that can differentiate into a variety of skeletal tissue types (bone, cartilage, ligament/tendon, etc) and therefore represent a potential osteoprogenitor cell source for bone tissue engineering applications.

1.5.1 Cell Source

Researchers have shown that MSCs may be isolated from many sources including (but not limited to) blood, umbilical cord and placenta, amniotic fluid, skeletal muscle, and adipose tissue [36-41]. When MSCs are derived from the bone marrow they are commonly referred to as bone marrow stromal cells (BMSCs). Bone marrow remains the preferred cell source for bone engineering applications because the BMCSs predominantly differentiate into an osteoblastic phenotype [42-44]. Friedenstein *et al.* were first to isolate BMSCs and chronicle their multilineage differentiation potential in 1966 [45]. Since Friedenstein's discovery many researchers have described the ability of BMSCs to differentiate into different cell types found in skeletal tissues including fibroblasts, osteoblasts, chondrocytes, adipocytes and stroma, the connective tissue that houses the undifferentiated cells [45-49]. In addition to their multipotency, BMSCs have enormous capacity for self-replication. It has been reported that billions of BMSCs may be derived from marrow aspirates as small as 1 mL [50].

1.5.2 Osteoblastic Differentiation

Osteoblastic differentiation of BMSCs *in vitro* is marked by three phases: proliferation, extracellular matrix maturation, and extracellular matrix mineralization [51].

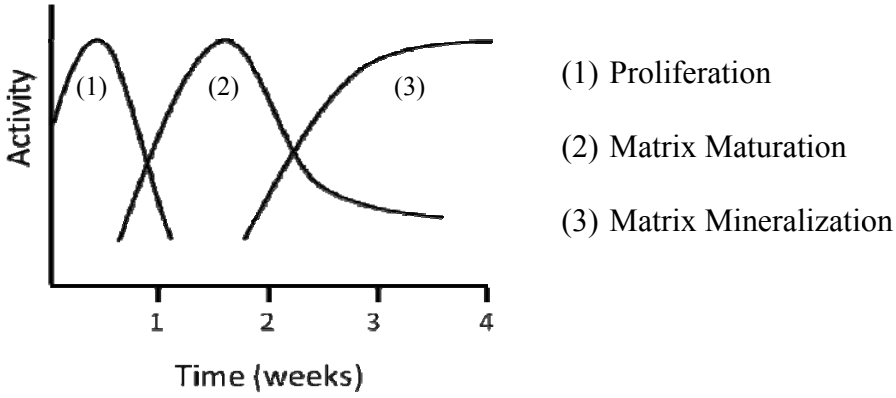

Figure 1.3: Graphical depiction of the timeline for osteoblastic differentiation of BMSCs

The proliferative phase is marked by expression of genes such as histones, protooncogenes and transforming growth factor-β (TGF-β) [10, 52]. As proliferation slows, phenotypic markers of matrix maturation, alkaline phosphatase (ALP) activity and collagen type-I expression, begin to increase [46, 53]. ALP is an enzyme that liberates phosphate ions from organic molecules and is thought to promote mineralization of the bone extracellular matrix. As the third phase of osteoblastic differentiation, matrix mineralization, progresses, ALP activity begins to wane [5]. Matrix mineralization is marked by expression of non-collagenous proteins such as osteopontin (OPN) and osteocalcin (OC) along with the deposition of calcium phosphate mineral [51]. OC has an affinity for calcium, is specific to bone, and only appears during the onset of matrix mineralization. While OPN is up-regulated throughout the differentiation process and is implicated in cell attachment to the bone matrix. Levels of these protein markers can be used to evaluate the effectiveness of *in vitro* strategies to stimulate osteogenic differentiation.

1.6 Biomaterial Scaffold

The role of the biomaterial scaffold in the tissue engineering paradigm is to provide structural support to a defect while providing surface area and void volume for new growth within and around the defect site. An ideal scaffold material would be biocompatible, have appropriate mechanical properties, and support the natural remodeling process *in vivo* [3, 4]. Many materials have been used as scaffolding in bone tissue engineering investigations,

including metals and alloys such as titanium, ceramic materials such as bioactive glass and hydroxyapatite [54-57], natural polymers including both proteins such as collagen, fibrin, and silk, and polysaccharides such as starch, alginate, chitosan/chitin, and hyaluronic acid derivatives [58-63], and synthetic polymers ranging from aliphatic polyesters (ex. PLA, PGA, and PCL) to polyhydroxylalkanoates (ex. PHB, PHBV, and PHO) to polyurethanes [64-66]. While titanium and ceramic materials have high mechanical strength, they have slow degradation rates or are not degradable (like titanium) and they are not inherently osteoinductive [67]. In contrast, much of the interest in natural polymeric materials stems from their inherent biocompatibility and, as in the case of collagen, the desire to mimic the extracellular matrix found in bone. In general, these materials lack mechanical strength of the same order of magnitude as that of natural bone [68]. The main benefit of synthetic polymers is that through careful control of the synthesis process, they can be tailored to exhibit desired mechanical and physical properties such as elastic modulus and degradation rate.

1.6.1 Polyurethanes

Polyurethanes are a class of synthetic polymer most commonly used for making blood contacting devices such as heart valves or vascular grafts [69]. Other applications include cardiovascular applications such as catheters and pacemaker leads, hemodialysis applications such as membranes and tubing, and tissue replacement/augmentation such as breast implants, synthetic bile ducts, wound healing materials, and facial reconstructions [69, 70].

Most polyurethanes are composed of alternating soft polyol segments and hard urethane segments. The most common synthesis method for these segmented polyurethanes is a two-step method where a diisocyanate and a macrodiol (1-5 kDa) are reacted first to form a prepolymer and then the prepolymer is chain extended with a short diamine or diol (< 1 kDa) [71].

Biocompatibility is of utmost importance in selection of polyurethane components and their degradation products. For example, commercial polyurethanes synthesized from

methylene bid diphenylisocyanate (MDI) may not be suitable for biomedical application where degradation of the polyurethane is desired because the degradation products have been shown to be carcinogenic and mutagenic. However, lysine ethyl ester diisocyanate (LDI) and 1,4-diisocyanatobutane (BDI) have been shown to be biocompatible alternatives to MDI [66, 72, 73].

Polyurethane biomaterials are an attractive means to examine the effect of scaffold mechanical properties on osteoblastic differentiation of BMSCs because the mechanical properties of segmented polyurethanes can be "tuned" to a desired range through careful choice of macrodiol, diisocyanate, and chain-extender and by controlling factors such as hard and soft segment contents [71, 74-76]. Recently it has been reported for several cell types that substrate compliance has a significant effect on behavior such as cell migration, morphology, and differentiation [19, 77-82]. Initial findings with pre-osteoblastic MC3T3-E1 cells on crosslinked hydrogels indicate that ALP activity levels as well as expression of osteocalcin and bone sialoprotein mRNA increase when grown on stiffer substrates [78, 79]. However, the effect of scaffold compliance has not been investigated in three dimensional scaffold architectures. To accomplish this, scaffolds with similar porosities and pore sizes must be fabricated from polymers with increasing stiffness.

1.6.2 Scaffold fabrication

Fabrication of scaffolds suitable for bone tissue engineering purposes should allow for high porosity and pore interconnectivity to allow for transport of nutrients and oxygen and the ingrowth of tissue. Several different documented schemes exist for producing porous scaffolds including solvent casting/particulate leaching, thermally induced phase separation (TIPS), CO_2 foaming, and microsphere sintering. Combinations of techniques such as phase separation/particulate leaching or CO_2 foaming/particulate leaching have also been investigated.

In solvent casting/particulate leaching techniques a high concentration of particles are mixed with a polymer solution and the solvent is allowed to evaporate. Once the particulates have been removed the resulting structure is a system of interconnected pores. Porosity and

therefore mechanical properties depends on the size and amount of particulates used. Many different particulates (e.g. paraffin spheres, sugar crystals, gelatin, lipid molecules) have been incorporated in these processing techniques [83-86]. Salt (NaCl) crystals are among the most common porogens used in particulate leaching techniques. NaCl leaching schemes have been shown to result in larger pore sizes and increased interconnectivity over processing schemes that do not involve porogen leaching [87].

In TIPS a polymer solution is cooled to induce the formation of two phases: a polymer-rich phase and a polymer-lean phase [88]. The solvent is then removed by solvent extraction or sublimation to form pores. However, pore shape and size is reported to be irregular and commonly less than 10 microns in diameter [89]. The small pore diameter likely limits the infiltration of tissue into the scaffold, thus limiting the usefulness of normal phase separation techniques for producing scaffolds suitable for bone tissue engineering applications. Gong *et al.* devised a coarsening protocol for a TIPS procedure that results in pore diameters ranging from a few microns to approximately 300 μm [90]. In addition to the network of macropores, many micropores were observed in the walls of the large pores and less than 100% interconnectivity was measured indicating the existence of isolated pores. This is unfavorable because cells cannot infiltrate isolated pores.

High pressure gas foaming techniques have also been employed to produce porous foam scaffolds. Polymer particles are tightly packed and then exposed to high pressure CO_2 which acts like a solvent to make the polymer fluid. As the gas pressure is reduced to ambient pressure the CO_2 expands to create pores [91]. This technique is advantageous in that it avoids the use of expensive and/or toxic organic solvents, which can affect cell viability, and high temperatures, which can undermine polymer properties. However, CO_2 foaming techniques typically result in a closed pore structure with only 10-30% interconnectivity [92]. In addition a solid "skin" of polymer has been observed surrounding the scaffold matrix [93, 94].

Microsphere sintering avoids the limitations of TIPS and CO_2 foaming. The technique involves thermally fusing microspheres of polymer together inside a mold [95]. The average pore diameter is controlled by controlling the size of the microspheres. The

resultant interconnectivity of the scaffold is 100%; however, the porosity of the scaffold is significantly lower with the microsphere sintering technique (30-40%) compared to other fabrication techniques (80-95%) [96]. Due to its lower porosity, microsphere sintering yields a scaffold with higher mechanical strength but lower void volume available for tissue ingrowth.

Rapid prototyping (RP) techniques involve the construction of complex 3D scaffolds using a computer-aided design (CAD) data set. These techniques build complex scaffolds one layer at a time to achieve 3D architectures with completely interconnected pores [87, 97, 98]. Because the scaffolds produced with these techniques are very precise, the ability to exactly reproduce them is increased over other scaffold fabrication techniques. One of these RP techniques uses fibers extruded through a nozzle to construct the 3D architecture. However, because the fiber size (and therefore the pore size) is determined by the diameter of the nozzle used to extrude the polymer, this technique is limited by the resolution of available nozzles. In addition, the filaments are frequently smaller than the nozzle diameter and can be hard to control due to variations in polymer melt rheology and the dispening speed of the melt [97]. The porosities of the resulting scaffolds, ranging from 65 – 72%, are slightly lower than those achieved via compression molding/particulate leaching techniques but much higher than seen with the microsphere sintering techniques. Another RP technique uses deflected laser beams (infrared laser or CO_2 laser) to selectively scan over a powder surface and heat the powder particles to melting temperature, effectively sintering the particles together and forming a solid [87, 99]. Then a new layer of powder is deposited on top of the sintered layer and the process repeats itself. However, the dimension of the structures used to construct the scaffold are limited by the laser-beam diameter, roughly 400 microns, and the powder particle size limits [87]. In addition, loose powder can become trapped in the scaffolds [87].

1.7 Perfusion Bioreactor

The role of the bioreactor in our tissue engineering strategy is to facilitate the development of large tissue substitutes *in vitro.* Perfusion bioreactors both supply oxygen

and nutrients to the cells seeded within the biomaterial scaffold, and also expose the cells to physical stimuli in the form of shear stress. Both the increased chemotransport and the applied mechanical stimulation have been shown to facilitate proliferation and differentiation of BMSCs.

Convective transport of oxygen and nutrients is vital for maintenance of cell viability in large 3D scaffolds. Under static conditions, cell viability drops significantly at a distance greater than 1 mm from the surface into the scaffold [100]. Perfusion bioreactors have been shown to solve this problem and maintain a more uniform cell distribution in porous scaffolds [100-102]. Data also suggests that mineralization is limited to the surface of the scaffold, with a maximum penetration depth of roughly 250 microns from the surface [103].

Cells cultured under perfusion conditions are not only more evenly distributed within scaffolds, but also produce more mature bone-like ECM as evidenced by increased levels of ALP and OC [54, 100, 102]. One explanation for the increased expression of osteoblastic markers is that the mechanical shear stress imparted on the cells by fluid flow stimulates osteoblastic differentiation. The benefits of both increased chemotransport and mechanical stimulation have caused continuous perfusion flow strategies to be adopted by many researchers [101, 104-109].

Perfusion strategies *in vitro* seek to emulate the primary source of physiologic fluid shear stress, interstitial fluid flow. *In vivo*, interstitial fluid flow is driven by two sources: the pressure differential of the circulatory system and external loading. As the bone is compressed the fluid is forced out of the areas of high compressive strain and then returns when the compressive force is removed [14]. This suggests that dynamic flow conditions are more physiologically relevant than continuous shearing flow.

1.7.1 Dynamic Flow

Osteoblastic cells in monolayer culture have been shown to respond differently to dynamic flow conditions such as oscillatory flow or pulsatile flow than to steady flow. Studies show that cells respond to oscillatory and pulsatile flow with increased VEGF-A gene expression, prostaglandin (PGE_2) production, OPN gene expression, and activation of

mitogen-activated protein kinases (ERK and p38) relative to steady flow [16, 109-111]. PGE_2 production and MAPK activity have both been linked to increased proliferation and osteoblastic differentiation [112-115]. One explanation for increased response to dynamic flow regimes over steady flow is that steady flow does not stimulate the cells as efficiently because the mechanotransductive signaling pathways involves a refractory period, the amount of time it takes the cell be ready for a second stimulus once it returns to its resting state following an initial stimulation [116]. Several studies show that pulsatile flow frequency enhances cell response in a frequency dependent manner although some of the data and subsequent interpretations conflict with each other. Jacobs *et al.* measured intracellular calcium transients and showed an increase with pulsatile flow over oscillatory flow; however, with both pulsatile and oscillatory flow as frequency increased from 0.5 Hz to 2 Hz, calcium transients decreased [110]. In contrast, both Mullander *et al.* and Nauman *et al.* found that cell response, NO release and PGE_2 synthesis, increased with increasing frequency [117, 118].

As evidence presented in this chapter clearly show, many different external factors such as soluble factors (e.g. glucocorticoids, growth factors, etc), intercellular contact through connexins, integrin mediated adhesion to the biomaterial substrate, and physical stimulation (i.e. perfusion) affect the osteoblastic differentiation of BMSCs (Figure 1.3). Two specific stimuli, the biomaterial substrate and physical stimulation, are the focus of this project.

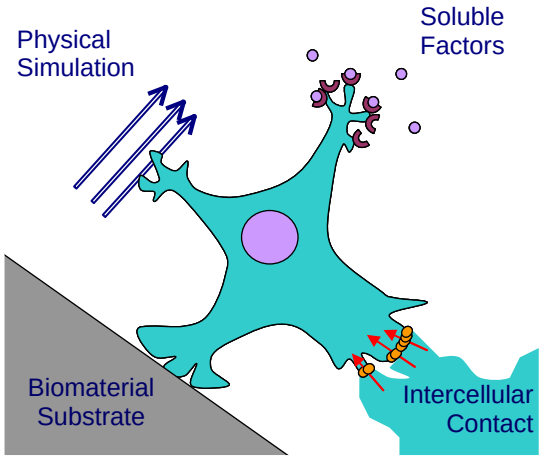

Figure 1.4: Stimuli acting on an osteoprogenitor cell

1.8 Experimental Plan

The over arching goal of this research is to develop an attractive alternative to current bone graft materials using a combination of MSCs, degradable biomaterial scaffolds, and perfusion culture. The central hypothesis of this project is that both substrate compliance and physical stimulation affect bone formation *in vitro*. In turn, modulating the osteoblastic differentiation and secretion of growth factors is anticipated to affect the rate of bone healing *in vivo*. The objective of this proposed research is to evaluate the capacity of two stimuli to modulate the differentiation and secretion of bioactive factors by bone marrow stromal cells (BMSCs): 1) the stiffness of the scaffold and 2) perfusion flow culture.

1.8.1 Aim 1

The goal of the first two studies was to determine the effect of scaffold compliance on the level of osteoblastic differentiation and other bioactive factors. To accomplish this, a family of segmented poly(esterurethane urea) (PEUUR) elastomers were synthesized with varying PCL contents to systematically vary the modulus. Polymer films were seeded with BMSCs and cultured under osteogenic conditions for up to 21 days. Cell proliferation, ALP activity, OPN and OC expression were found to be similar among PEUURs and comparable to poly($_{D,L}$-lactic-co-glycolic acid) (PLGA). This study demonstrated the suitability of this family of PEUURs for determining the effect of biomaterial modulus on bone tissue development.

In the second study the PEUUR elastomers were processed into porous foam scaffolds via a compression molding/particulate leaching technique. BMSCs were seeded into the porous scaffolds and cultured under osteogenic conditions for up to 21 days. Cell proliferation, levels of PGE_2, ALP activity, OPN and VEGF were all significantly different on the PCL 2700 material compared to the PLGA control and the other PEUUR materials. These effects cannot be attributed to differences in material modulus but may be an effect of crystallinity. Therefore, in future studies, the effects of modulus and crystallinity must be de-coupled to more fully investigate the effect of scaffold mechanical properties on osteoblastic differentiation.

1.8.2 Aim 2

The goal of the third study was to determine the effect of frequency of pulsatile perfusion on the development of a bone-like extracellular matrix. To accomplish this, our existing perfusion apparatus was modified with the addition of a micro-processor controlled actuator that can be programmed to alter the pressure drop across the flow system at different frequencies. BMSCs were seeded into porous PLGA foam scaffolds and cultured under osteogenic conditions and exposed to 4 different flow conditions, continuous flow and pulsatile flow (0.083 Hz, 0.05 Hz, and 0.017 Hz). All flow conditions were compared to statically cultured (no flow) control scaffolds grown in 12-well culture plates. Cell proliferation was decreased in the pulsatile conditions compared to the no flow and continuous flow controls. ALP activity was significantly increased with the application of 0.05 Hz pulsatile flow compared to the no flow and continuous flow controls although all flow conditions enhanced ALP activity, OPN gene expression, and OPN protein accumulation. Pulsatile flow clearly induces osteoblastic differentiation at least as well as continuous perfusion and enhances ALP activity above continuous flow. However, a larger range of frequencies must be investigated in the future to discern whether frequency modulates osteoblastic differentiation.

Reprinted from Kavlock, K.D., Pechar, T.W., Hollinger, J.O., Guelcher, S.A., and Goldstein, A.S. *Acta Biomaterialia* 3: 475-484 (2007), with permission from Elsevier Ltd.

Chapter 2: Synthesis and characterization of segmented poly(esterurethane urea) elastomers for bone tissue engineering

Katherine D. Kavlock [a], Todd W. Pechar [b], Jeffrey O. Hollinger [c],
Scott A. Guelcher [d], Aaron S. Goldstein [a,b,*]

[a] School of Biomedical Engineering and Sciences, and
[b] Department of Chemical Engineering,
Virginia Polytechnic Institute and State University, Blacksburg, VA 24061-0211
[c] Bone Tissue Engineering Center, Carnegie Mellon University, Pittsburgh, PA 15213
[d] Department of Chemical Engineering, Vanderbilt University, Nashville, TN 37235

2.1 Abstract

Segmented polyurethanes have been used extensively in implantable medical devices, but their tunable mechanical properties make them attractive for examining the effect of biomaterial modulus on engineered musculoskeletal tissue development. In this study, a family of segmented degradable poly(esterurethane urea)s (PEUURs) were synthesized from 1,4-diisocyanatobutane, a poly(e-caprolactone) (PCL) macrodiol soft segment and a tyramine-1,4-diisocyanatobutane-tyramine chain extender. By systematically increasing the PCL macrodiol molecular weight from 1100 to 2700 Da, the storage modulus, crystallinity and melting point of the PCL segment were systematically varied. In particular, the melting temperature, Tm, increased from 21 to 61°C and the storage modulus at 37°C increased from 52 to 278 MPa with increasing PCL macrodiol molecular weight, suggesting that the crystallinity of the PCL macrodiol contributed significantly to the mechanical properties of the polymers. Bone marrow stromal cells were cultured on rigid polymer films under osteogenic conditions for up to 21 days. Cell density, alkaline phosphatase activity, and osteopontin and osteocalcin expression were similar among PEUURs and comparable to poly($_{D,L}$-lactic-co-glycolic acid). This study demonstrates the suitability of this family of

PEUURs for tissue engineering applications, and establishes a foundation for determining the effect of biomaterial modulus on bone tissue development.

2.2 Introduction

A primary limitation with allogeneic and synthetic materials as replacements for bone tissue function is that they eventually undergo mechanical failure. Tissue engineered bone is envisioned to circumvent this limitation by being degradable and – like autologous bone graft – capable of stimulating the natural tissue remodeling process [29, 30]. Consequently, a variety of approaches have been undertaken that combine resorbable biomaterial scaffolds, bioactive factors and osteoprogenitor cells to produce engineered tissues that are capable of stimulating integration, vascular infiltration and tissue remodeling. Within this family of strategies, the biomaterial scaffold acts as a mechanically robust substratum to support osteoprogenitor cell adhesion, proliferation and differentiation. Importantly, evidence with skeletal muscle suggests that the modulus of the scaffold is critical for achievement of the target phenotype [19]. However, the effect of the mechanical properties of the biomaterial on bone tissue development has not been addressed.

Segmented polyurethanes are an ideal class of materials with which to characterize the effect of mechanical properties on tissue development. These polymers often are prepared via a two-step process that involves reacting a diisocyanate with a 1–5 kDa macrodiol to form an isocyanate-terminated prepolymer, and then chain-extending this prepolymer with a short-chain (<1 kDa) diamine or diol. By careful selection of the diisocyanate, chain extender and macrodiol components, a broad range of physical properties can be achieved. In general, polyurethanes are biocompatible and have been used in a variety of biomedical applications, including ligament and meniscus reconstruction [119, 120], blood-contacting materials [121-123], infusion pumps [124], heart valves [125], insulators for pacemaker leads [126], and nerve guidance channels [127]. For tissue engineering applications a degradable polymer is desirable, and can be achieved by incorporating labile ester linkages into the polymer backbone [128, 129]. Biodegradation to non-cytotoxic components may be promoted by the use of lysine ethyl ester diisocyanate

(LDI) [130] or 1,4-diisocyanatobutane (BDI) [131] in place of methylene bisdiphenylisocyanate (MDI), which has been suggested to degrade into carcinogenic and mutagenic compounds [132].

In this study, a family of degradable poly(esterurethane urea)s (PEUURs) were formed by reacting BDI with poly(ε-caprolactone) (PCL) macrodiols followed by chain-extension of the prepolymer with a tyramine (TyA).BDI.TyA adduct [72]. In the solid state – or service window – the resultant polymer is expected to microphase separate into a soft, PCL-rich phase stabilized by van der Waals forces and a hard, BDI- and TyA-containing phase stabilized by hydrogen bonds. For this study, the molecular weight of the PCL macrodiol was varied from 1100 to 2700 Da to produce a family of chemically similar polymers with hard segment contents of 20–40 wt.%. Increasing the PCL macrodiol molecular weight is also expected to increase the crystallinity of the soft segment. The resultant polymers were characterized by dynamic mechanical analysis (DMA), differential scanning calorimetry (DSC), wide-angle X-ray scattering (WAXS), and contact angle goniometry to determine how the physical properties of these PEUURs depend on the hard segment content.

To verify that these PEUURs are suitable for testing our hypothesis that bone tissue development is sensitive to biomaterial scaffold modulus, cell culture studies were performed on rigid polymer films. Bone marrow stromal cells (BMSCs) – a clinically attractive progenitor cell type [42] – were cultured under osteogenic conditions to verify that the polyurethanes support proliferation and osteoblastic differentiation, and to determine if cell behavior is sensitive to subtle differences in the chemistry of the PEUURs. Cell density, alkaline phosphatase (ALP) activity, and expression of osteopontin (OPN) and osteocalcin (OCN) were measured.

2.3 Materials and Methods

2.3.1 Materials

All chemicals, including BDI, TyA, ε-caprolactone, poly(ε-caprolactone) diol (PCL diol, average molecular weight 2000 Da), 1,4-butanediol (BDO), diethyl ether and dibutyltin

dilaurate (DBTDL), were obtained from Sigma–Aldrich (St. Louis, MO) unless otherwise specified. Anhydrous (<50 ppm water) dimethyl formamide (DMF) was obtained from Acros Organics (Morris Plains, NJ). All chemical reagents were used as received except for PCL2000 and butanediol, which were dried for 24 h at 80°C under vacuum (10 mm Hg), and ε-caprolactone, which was dried over anhydrous $MgSO_4$ prior to use. All cell culture materials were obtained from Fisher Scientific (Pittsburgh, PA) unless otherwise specified.

2.3.2 Synthesis of segmented poly(esterurethane urea) PEUUR elastomers

2.3.2.1 Chain extender synthesis

The diurea diol chain extender TyA.BDI.TyA (Figure 2.1) was synthesized from TyA and BDI as described previously [72]. Briefly, tyramine was dissolved in DMF and placed in a round-bottom reaction flask, and the resultant solution was stirred with a magnetic stirring apparatus and heated to 50°C. The air space of the vessel was purged with argon, the diisocyanate added slowly and the vessel then purged again with argon. The reaction proceeded at 50°C with no catalyst for 24 h and the solids content in the reactor was controlled at 10 wt.%. Complete conversion of diisocyanate was verified by the disappearance of the NCO peak (2250–2270 cm^{-1}) in the IR spectrum. The TyA.BDI.TyA chain extender was precipitated using diethyl ether and dried in a vacuum oven for 24 h at 80°C and 10 mm Hg absolute pressure to yield a fine powder. Because the reactivity of the amine is 1000–2000 times higher than that of phenol at 25°C [124], the 2:1 adduct is the sole reaction product in the absence of catalyst [72].

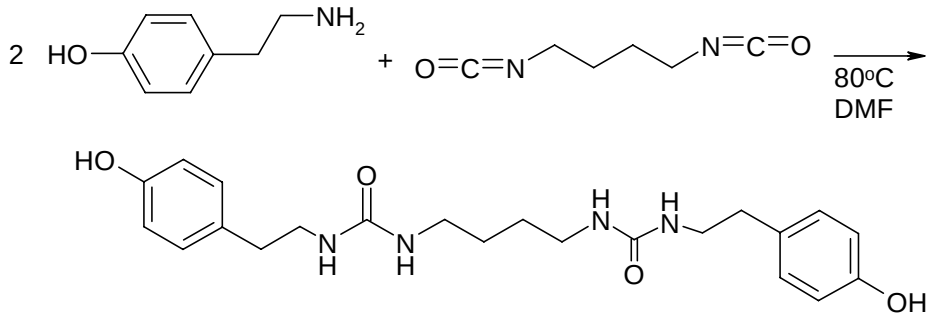

Figure 2.1: Synthesis scheme for forming TyA.BDI.TyA chain extender.

2.3.2.2 Polyester macrodiol synthesis

Three PCL macrodiols (1100, 1425 and 2700 Da) were synthesized from a BDO initiator and ε-caprolactone monomer using previously published techniques [133]. The molecular weight was controlled by varying the ratio of monomer to initiator. Briefly, the appropriate amounts of dried BDO, dried ε-caprolactone and stannous octoate catalyst (1000 ppm) were mixed in a 100 ml flask and heated under an argon atmosphere with mechanical stirring to 135°C. After a reaction time of 24 h, the mixture was removed from the oil bath. Nuclear magnetic resonance (NMR) spectroscopy was performed with a Bruker 300 MHz NMR (Bruker-Biospin, Billerica, MA) to verify the structure of the PCL macrodiol using deuterated dichloromethane as the solvent.

2.3.2.3 Prepolymer synthesis

Anhydrous DMF was charged to a round-bottom flask fitted with a condenser. BDI was added to the flask, which was then immersed in an oil bath at 70°C, purged with argon, and stirred with a Teflon blade stirrer turned by an electric motor. A solution of dried PCL macrodiol – synthesized with a molecular weight of 1100, 1425 or 2700 Da or purchased with a molecular weight of 2000 Da – was charged into the reactor by means of an addition funnel. The NCO:OH equivalent ratio of the prepolymer was equal to 2.0:1.0. (Note that the NCO:OH equivalent ratio is equal to the BDI:PCL macrodiol molar ratio because the BDI and PCL macrodiol each has a functionality of two.) The prepolymer content in the reactor was controlled at 6 wt.%. DBTDL was added to the flask at 1000 ppm and the reaction was allowed to proceed for 24 h. The reaction scheme is summarized in Figure 2.2a.

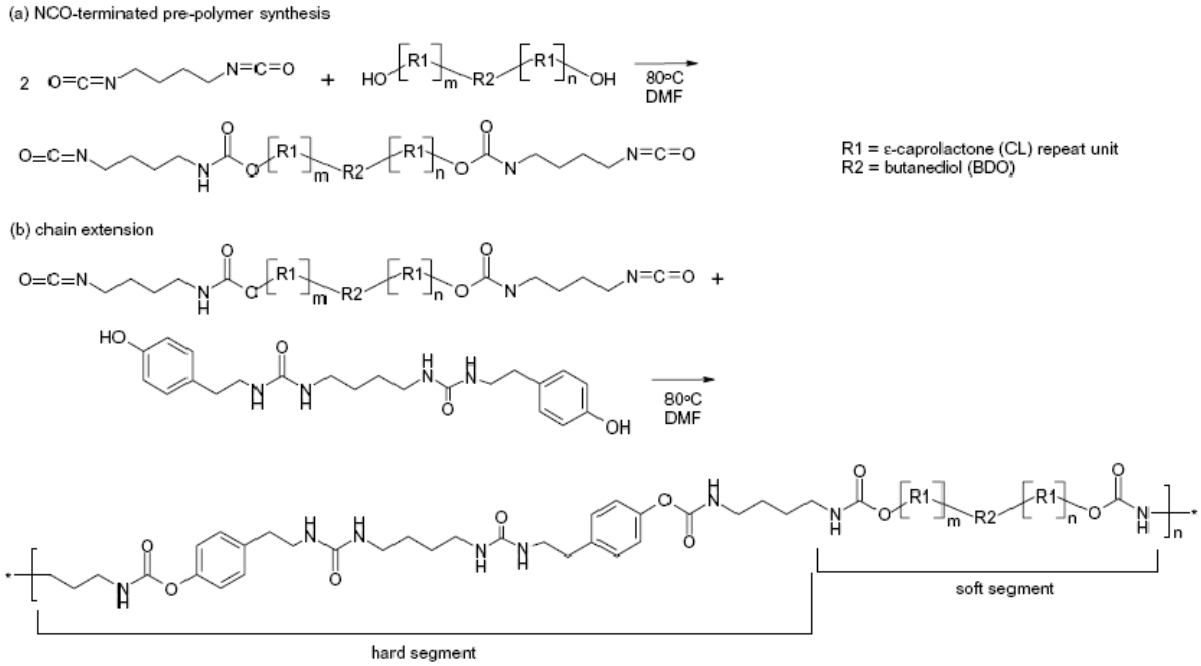

Figure 2.2: Synthesis scheme for forming segmented poly(esterurethane urea) elastomers. (a) Formation of PCL diisocyanate prepolymer. (b) Formation of PEUU by chain extending prepolymer.

2.3.2.4 Segmented PEUUR elastomer synthesis

A solution of chain extender in DMF was prepared at 50°C and added to the prepolymer in the reaction vessel. The NCO:OH equivalent ratio of the polyurethane was controlled at 1.03:1.0 and the polymer concentration was 3–6 wt.%. DBTDL was added to a concentration of 1000 ppm. The reaction was allowed to proceed at 70°C for 4 days. The polymer was then precipitated in diethyl ether and dried in a vacuum oven for 24 h at 80°C under 10 mm Hg vacuum. The reaction scheme is summarized in Figure 2.2b. The hard segment content was calculated from the reaction stoichiometry as the weight fraction of BDI and chain extender in the polymer.

2.3.3 Characterization of segmented PEUUR elastomers

2.3.3.1 Composition and molecular weight

NMR spectroscopy was performed using deuterated dimethylsulfoxide as the solvent to verify the structure of the chain extender and polymers. Number- and weight- average

molecular weight of the polymers were measured by gel permeation chromatography (GPC) with a Waters Alliance GPC 2000 (Waters Corporation, Milford, MA) using DMF as the continuous phase, toluene as an internal standard and monodispersed polystyrene as the calibration standard.

2.3.3.2 Solvent-casting of PEUUR films

For the polymers synthesized from 1100, 1425 and 2000 weight-averaged molecular weight (Mw) PCL macrodiols, 3.0 wt.% solutions were prepared by dissolving the polymer in DMF at 60°C until the solution turned clear. A 2.1 wt.% solution was prepared for the PEUUR synthesized from 2700 Mw PCL. (This was the concentration at which the solution became clear.) The polymer solutions were then filtered and poured into teflon casting dishes. Films were dried at 30 kPa absolute pressure and 60°C for 4 days, then annealed for 24 h at 80°C (above the T_m for all of the PEUURs). The resultant films were analyzed by DSC, DMA and WAXS.

2.3.3.3 Differential scanning calorimetry

Experiments were conducted on a Seiko DSC 220C (Seiko Instruments, Japan) with an attached auto-cooler for precise temperature control. Solvent-cast samples (10–12.5 mg) were heated in a nitrogen atmosphere from -100 to 180°C at 20°C min^{-1}, held at 180°C for 5 min and then cooled to -100°C at 20°C min^{-1}. Samples were held at -100°C for 5 min and then heated again to 180°C at 20°C min^{-1}.

2.3.3.4 Thermal DMA

DMA was performed on a Seiko DMS 210 tensile module with an attached auto-cooler for precise temperature control. Rectangular samples measuring 10 mm in length, approximately 0.5 mm in thickness and 6.3–6.7 mm in width were cut from annealed films. In a nitrogen atmosphere films were cooled to -100°C and then uniaxially deformed in the linear viscoelastic region in tension mode at 1 Hz oscillating frequency. Temperature was increased from -100 to 180°C at a rate of 2°C min^{-1}.

2.3.3.5 Wide-angle X-ray scattering

Photographic flat wide-angle X-ray scattering studies were performed using a Philips PW 1720 X-ray diffractometer (Phillips Electronics, Eindhoven, The Netherlands) emitting Cu K_α radiation with a wavelength of 1.54 Å operating at 40 kV and 20 mA. The sample to film distance was set at 47.3 mm for all samples. Direct exposures were made using Kodak Biomax MS film in an evacuated sample chamber. X-ray exposures lasted 30 min.

2.3.4 Cell Culture

2.3.4.1 Substrate preparation

PEUUR films – for cell culture studies and contact angle measurements – were prepared by spin-coating polymer solutions from DMF followed by annealing in order to achieve polymer morphologies similar to the cast films. Briefly, 18 mm diameter coverslips were sonicated in ethanol for 10 min and dried [134]. Next, 270 µl volumes of 3 wt.% PEUUR in DMF were deposited onto the coverslips and then spun at 2500 rpm for 30 s using a Model 1-EC101D-R485 spin-coater (Headway Research, Garland,TX) under ambient conditions. Control films were prepared by spin-coating 3 wt.% solutions of 75/25 poly($_{D,L}$-lactic-co-glycolic acid) (PLGA; Lactel Biodegradable Polymers, Birmingham, AL) in dichloromethane under the same conditions. PEUUR films were dried in a vacuum oven at 60°C for 72 h and then annealed at 80°C for 24 h. Advancing contact angles for spin-coated films were measured with a Rame´–Hart goniometer (Mountain Lakes, NJ). For each PEUUR, contact angles were measured using 3 µl drops of deionized water at four different locations on each of three films, as previously described [134]. For cell culture studies, substrates were placed in 12-well culture plates, sterilized under ultraviolet light for 12 h and incubated with 2 µg ml^{-1} human fibronectin (Sigma) in phosphate buffered saline (PBS) for 1 h prior to cell seeding.

2.3.4.2 BMSC culture

BMSCs were cultured from bone marrow explants taken from the tibias and femurs of 125–150 g male Sprague–Dawley rats (Harlan, Dublin, VA) in accordance with the Animal Care Committee at Virginia Tech [135, 136]. Explants were dispersed in growth medium (α-MEM (Invitrogen, Gaithersburg, MD), 10% fetal bovine serum (Gemini, Calabasas, CA) and 1% antibiotic/antimycotic (Invitrogen)), and expanded for 14 days with medium changes every 3 or 4 days. After 14 days of primary expansion, cells were rinsed twice with PBS, lifted with trypsin/EDTA (Invitrogen) and seeded at 10^5 cells per well (corresponding to 6.7 x 10^4 cells per coverslip). On the following day, denoted as day 1, the medium was replaced with 2 ml differentiation medium (growth medium containing 0.13 mM ascorbate-2- phosphate, 2 mM β-glycerophosphate and 10 nM dexamethasone). Culture medium was changed every 3 or 4 days and cell layers were collected for analysis at days 7, 14, and 21.

2.3.4.3 Cell number and ALP activity

Cell number was determined at days 7 and 14 by fluorometric measurement of total DNA using Hoechst 33258 dye [103, 137]. ALP activity of cell layers was determined at day 14 using a commercially available kit (Biotron Diagnostics, Hemet, CA). Enzyme activity, defined as the rate of conversion of *p*-nitrophenol phosphate to *p*-nitrophenol, was determined colorimetrically and normalized by cell number [137].

2.3.4.4 OPN synthesis

Accumulation of OPN in cell layers was determined at day 14 by western blot analysis using rabbit anti-rat OPN antibody (Assay Designs, Ann Arbor, MI) followed by horseradish peroxidase (HRP)-conjugated goat antirabbit antibody (Zymed, San Francisco, CA) and visualized by chemiluminescence [135]. Band densities were determined using Scion Image (Scion Corporation), and normalized by band densities for HRP-conjugated glyceraldehyde-3-phosphate dehydrogenase (GAPDH; Santa Cruz Biotechnology, Santa Cruz, CA).

2.3.4.5 mRNA expression

RNA was isolated from cell layers using the RNeasy mini kit (Qiagen, Valencia, CA) according to the manufacturer's instructions. Next, 1 lg of RNA was reverse transcribed to cDNA using the Superscript kit (Invitrogen, Carlsbad, CA) with random hexamers as primers. Real time PCR amplification was performed using an ABI 7300 sequence detection system (Applied Biosciences, Foster, CA), SYBR green Master Mix (Applied Biosciences) and specific primers for β-actin (βA), OPN and OCN (Integrated Technologies, Coralville, IA) with previously published sequences [135]. Quantification of OPN and OCN gene expression was performed using the $2^{-\Delta\Delta Ct}$ method, with βA as the internal reference [138].

2.3.4.6 Statistics

Data were analyzed using a one-way analysis of variance and a 95% confidence criterion to test for differences between treatment groups. An asterisk denotes statistically significant differences between materials.

2.4 Results

2.4.1 Synthesis and characterization of segmented PEUUR elastomers

GPC analysis of the polymers indicated number-average and weight-average molecular weights of 25–36 and 36–64 kDa, respectively, and polydispersity indices of 1.3–1.8, which are typical for segmented polyurethanes (Table 2.1).

Table 2.1
Physical characteristics of PEUURs

PCL M_n (Da)	HS (wt.%)	T_g (°C)	T_m (°C)	M_n (kDa)	M_w (kDa)	Θ (°)
2700	20	-55	61	35.4	47.0	74 ± 3
2000	26	-52	42	36.4	64.4	83 ± 2
1425	35	-52	34	25.1	36.1	79 ± 5
1100	39	-52	21	34.8	53.3	78 ± 4

The theoretical hard segment content, HS, was predicted from the molecular weight of hard and soft segments. The glass transition temperature, T_g, and melting point, T_m, were determined from DSC curves. Number and weight-average molecular weights, M_n and M_w, respectively, were determined by GPC. Static contact angles, θ, were determined on spin-coated polymer films.

DSC was performed to characterize the melting temperature and the relative crystallinity of the PCL microphase (Figure 2.3). Comparison of the first heating curves (Figure 3a, solid lines) reveal a systematic increase in T_m from 21 to 61°C with increasing PCL macrodiol molecular weight, as expected. In addition, the size of the endothermic peak also systematically increased, suggesting an increase in crystallinity of the PCL phase with increasing soft segment content. This increase in crystallinity with PCL segment molecular weight is also supported by systematic increases in the size of the exothermic crystallization peak in the cooling curves (Figure 2.3b) and the melting peak for the second heating curves (Figure 2.3a, dashed lines).

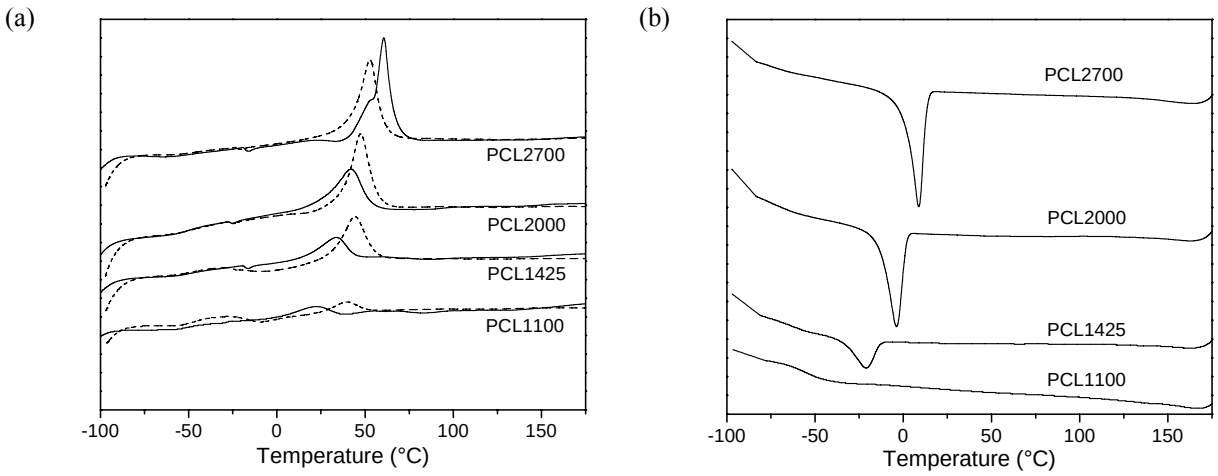

Figure 2.3: DSC analysis of polyurethanes: (a) heating curves; (b) cooling curve. Solid lines and dashed lines correspond to the first and second heating curves, respectively, of annealed polymer samples. A cooling curve was acquired between the first and second heating curves. Curves are offset vertically to permit visual comparison.

Further, the sharper and more intense WAXS pattern for the 2700 Mw PCL relative to the 1100 Mw PCL also indicates an increase in PEUUR crystallinity with increasing macrodiol molecular weight (Figure 2.4).

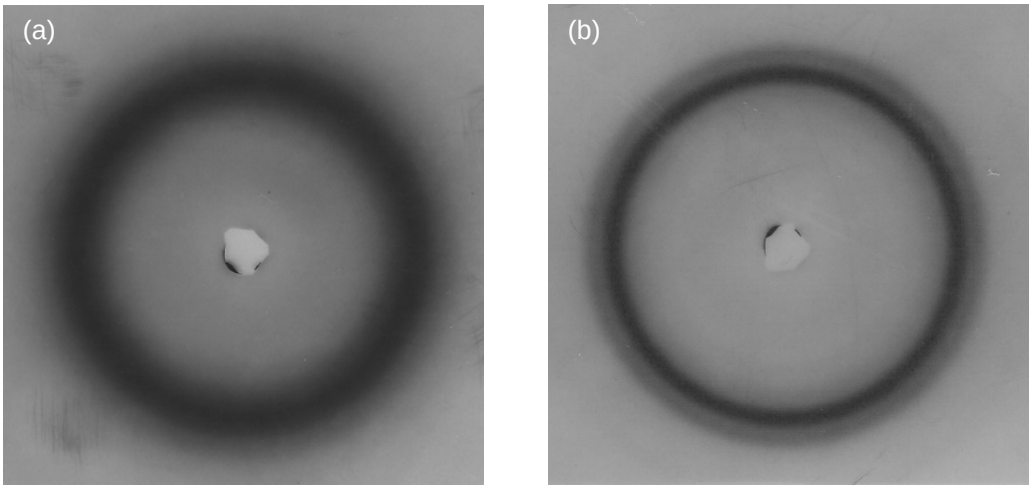

Figure 2.4: WAXS images of PEUURs synthesized from: (a) 100 M_w PCL and (b) 2700 M_w PCL.

DMA was performed on each material in order to monitor changes in the storage modulus (E') and tan δ with temperature (Figure 2.5). A decrease in E' between -75 and -50°C was observed as the material was heated through the glass transition temperature (T_g). The value for T_g was reported as the location of the primary peak in tan δ curve, which fell in the range of -55 to -50°C (Table 2.1) and is comparable to that of pure PCL (-63°C) [133]. A sharper decrease in E' was observed in the temperature range of 0–60°C, and corresponds to melting of the PCL phase. The melting transitions in the DMA curves are consistent with the melting peaks observed by DSC (Figure 2.3a), and the T_m decreases with decreasing PCL segment molecular weight. High molecular weight PCL has a melting temperature of 63°C, but melting point depression has been reported with decreasing PCL molecular weight [133]. The DMA curves also reveal that E' increases systematically with PCL segment molecular weight below T, but decreases with increasing PCL segment molecular weight above T_m. This suggests that the high storage modulus observed at physiologic temperature (37°C) is primarily related to the crystallinity of the PCL segment. At this temperature storage moduli of 52, 49, 110 and 278 MPa were determined for PCL segments of 1100, 1425, 2000, and 2700, respectively (Table 2.1). Above the T_m for the PEUURs, tan δ remains relatively low, indicating that the polymer is not completely melted, and E' increases systematically with

hard segment content, suggesting that the storage modulus is dependent on microphase-separated hard domains.

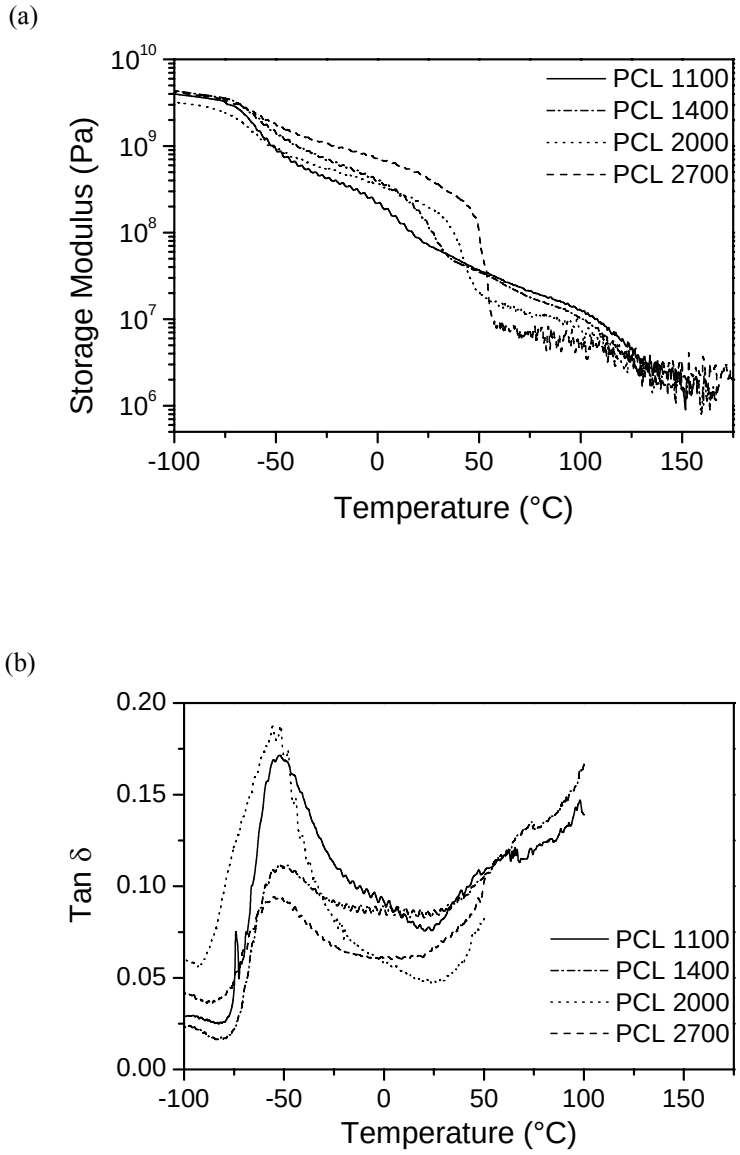

Figure 2.5: DMA analysis of polyurethanes: (a) storage modulus; (b) tan δ.

Measurements of advancing contact angles on spincoated PEUUR films show a small but systematic increase in angle with PCL macrodiol Mw from 1100 to 2000 (Table 2.1), consistent with an increase in the content of the hydrophobic soft segment. However, the

increase in advancing contact angle with PCL macrodiol Mw could also be a consequence of increasing surface roughness [139]. In contrast, the PEUUR with the highest PCL macrodiol Mw demonstrated the lowest contact angle, which suggests that microphase separation and crystallization of PCL segments may partition the hydrophilic TyA.BDI.TyA segments to the surface. By comparison, spin-coated PLGA (control) films exhibited an advancing contact angle of 74 ± 2, which is very similar to the PEUUR synthesized from 2700 M_w PCL.

2.4.2 BMSC proliferation and differentiation on PEUUR films

BMSCs were seeded onto fibronectin-coated PEUUR films and cultured under osteogenic conditions. They were collected at days 7 and 14 to assay for cell number and ALP activity, and at days 14 and 21 to assay for OPN and OCN expression. Cell number increased from 7 to 14 days on all surfaces, indicating that the PEUURs support cell adhesion and proliferation (Figure 2.6), but cell numbers were not statistically different between PEUURs and the PLGA control.

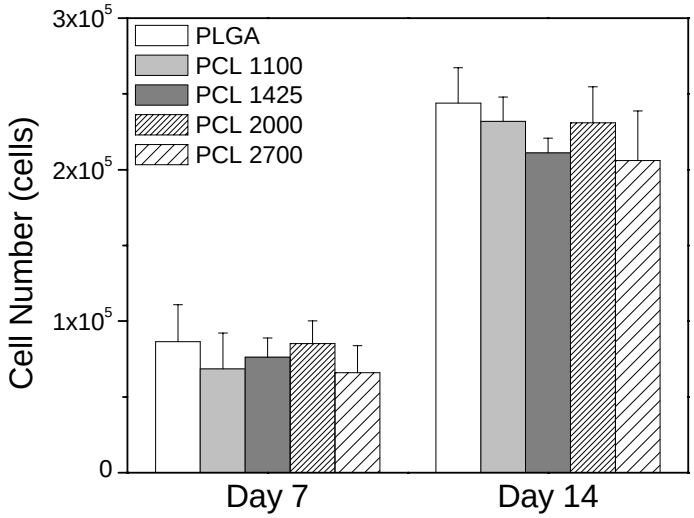

Figure 2.6: Cell number on PEUUR films at 7 and 14 days. PLGA films were used as a reference. Data are mean ± standard error for *n* = 4 samples.

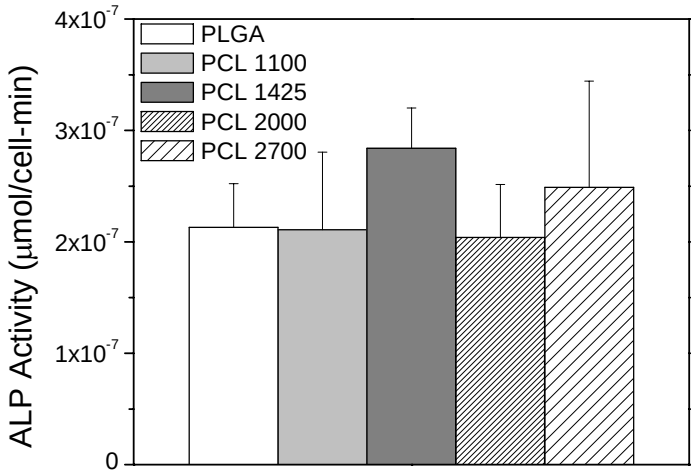

Figure 2.7: ALP activity of BMSCs on PEUUR films at 14 days. PLGA films were used as a reference. Data are mean ± standard error for n = 4 samples. Activity per cell was determined by normalizing activity per cell layer by cell number.

Analysis of OPN accumulation into cell layers – as determined by Western blot analysis at day 14 – indicated that OPN was statistically lower on the PEUUR containing PCL 2700 (Figure 2.8).

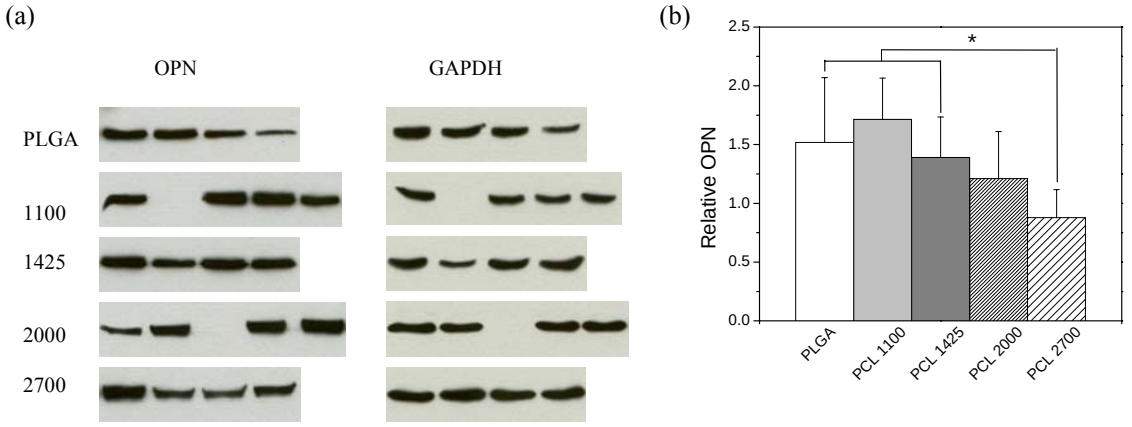

Figure 2.8: OPN protein content of BMSC cell layers on PEUUR films at 14 days. (a) OPN protein bands visualized by chemiluminescence. (b) Density of OPN bands normalized by GAPDH band density. PLGA films were used as a reference. Data are mean ± standard error for n = 8 samples. An asterisk denotes statistically different level of protein content with respect to PLGA ($p < 0.05$).

However, OPN mRNA expression by PCR at days 14 and 21 indicated no statistically significant differences between the polymers (Figure 2.9). Likewise, analysis of OCN, another osteoblastic marker, indicated no differences between the polymers (Figure 2.9b). Together, these data suggest that the PEUURs support osteoblastic differentiation to the same extent as PLGA. However, analysis of OCN synthesis and mineral deposition – definitive markers of osteoblastic maturation – are necessary to demonstrate differentiation.

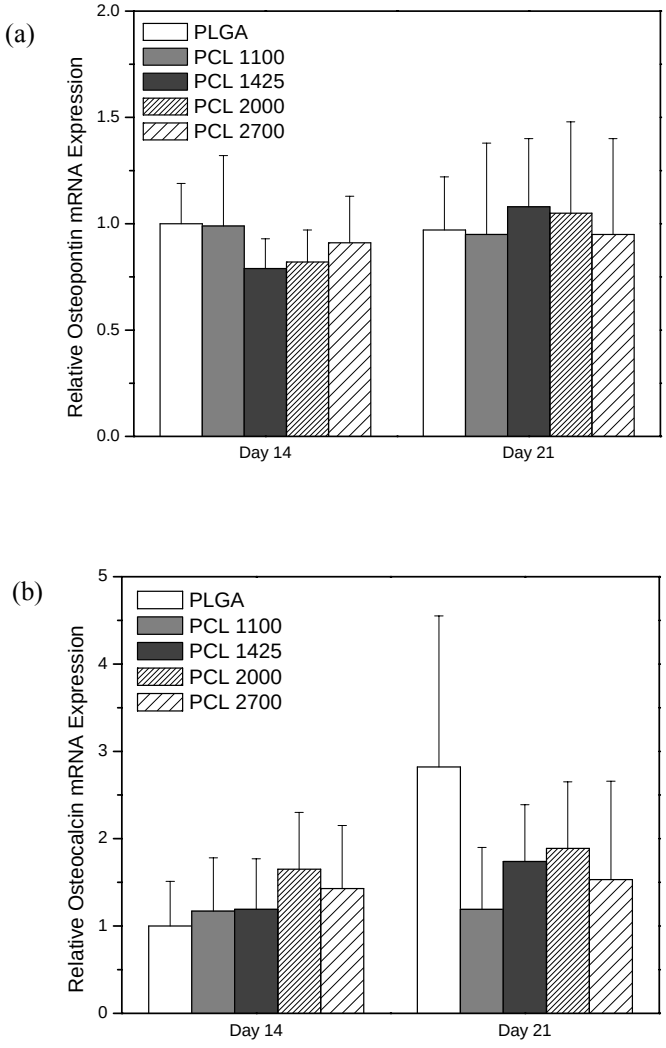

Figure 2.9: (a) OPN and (b) OCN mRNA expression of BMSCs on PEUUR films at 14 and 21 days. Expression was normalized to PLGA films at day 14. Data are mean ± standard error for $n = 4$ samples.

2.5 Discussion

In this study a family of segmented PEUURs was synthesized using PCL macrodiols and a novel TyA.BDI.TyA chain extender. By systematically varying the molecular weight of the PCL segment, the storage modulus, the soft segment T_m and the degree of crystallinity were systematically varied. In particular, the modulus at 37°C increased from 49 to 278 MPa with increasing PCL macrodiol M_w. Cell culture studies using BMSCs showed that all PEUURs supported cell viability, proliferation and osteoblastic differentiation.

One of the underlying motivations for this study was the development of segmented polyurethanes that degrade to non-toxic decomposition products. Polyurethanes and polyureas synthesized from aromatic diisocyanates, such as MDI, exhibit microphase-separated morphologies, ordered hard domains and useful mechanical properties [122]. In recent studies, polyureas synthesized from MDI, a diamine chain extender, and a PCL530 soft segment have been reported to degrade to non-cytotoxic decomposition products *in vivo* [119, 140, 141]. However, other studies have suggested that polyurethanes based on such aromatic polyisocyanates degrade in vivo to carcinogenic and mutagenic compounds [142-144]. Therefore, due to the potentially cytotoxic degradation products associated with MDI, we and others have sought to synthesize biodegradable segmented PEUUR elastomers from aliphatic polyisocyanates such as hexamethylene diisocyanate (HDI), BDI and LDI [72, 129, 131] [73, 145-150]. To date, segmented PEUUR elastomers incorporating a PCL soft segment and aliphatic diisocyanates have been synthesized from a variety of chain extenders, including an adduct of BDO and BDI [73, 131, 145], putrescine (BDA) [129, 146, 151], lysine ethyl ester (Lys) [129], and an adduct of phenylalanine (Phe) and cyclohexanedimethanol [147, 148, 150]. In a previous study, we described the synthesis and characterization of a segmented PEUUR elastomer incorporating a hard segment comprising an adduct of tyramine and BDI [72]. This chain extender was designed with specific structural features to promote ordering of microphase-separated hard domains, including phenyl groups to induce p bond stacking and urea groups to establish bidentate hydrogen bonding [122].

However, thermal phase transitions of the hard segment – definitive evidence of microphase separation – were not detected by DSC (Figure 2.3) in this study. We conjecture that the phase transitions for the hard segment lie above the decomposition temperature, which is consistent with observations for polyureas [122, 152]. However, we note two indirect signs of phase separation of the hard segment. First, at temperatures greater than the T_m of the PCL segment the materials have moduli ranging from 10 to 40 MPa (Figure 2.5), the moduli increase with increasing hard segment content and tan δ is relatively low. In the absence of hard segment ordering, the materials would be anticipated to have mechanical properties resembling a polymer melt (e.g. a storage modulus several orders of magnitude lower).

Second, for microphase-separated materials, each phase exhibits its own T_g. For phase-mixed systems, the value of T_g is related to the T_g of the individual components by the Fox equation [153]:

$$\frac{1}{T_g} = \frac{M_1}{T_{g1}} + \frac{M_2}{T_{g2}}$$

where subscripts 1 and 2 represent the individual segments, and M_i represents the mass fraction of segment *i*. Thus, a systematic shift in T_g with soft segment content would be consistent with the existence of a phase mixed system. However, the T_g for the PCL segment is similar to that for pure PCL (-63°C [133]) and does not vary with PCL content (Table 2.2), suggesting that the system is microphase-separated.

The thermal and mechanical properties of a broad variety of segmented PEUUR elastomers, which incorporate a PCL soft segment, are summarized in Table 2.2. We note that materials previously formed from a 2000 Mw PCL macrodiol exhibit glass transition temperatures ranging from -51 to -54°C, which is quite close to the value of -52°C measured in this study. However, materials incorporating a 1250 M_w PCL soft segment are reported to exhibit T_g values in the range from -34 to -40°C, suggesting a greater degree of phase mixing in these materials relative to the 2000 M_w PCL materials. It is interesting to note that the PEUURs in this study formed from 1100 and 1425 M_w PCL exhibited T_g values of -52°C. These data imply that the extent of microphase separation is not as sensitive to PCL

molecular weight when tyramine-based hard segments are employed. In particular, we conjecture that the relatively large and hydrophilic TyA.BDI.TyA chain extender used in this study may drive microphase separation even when the PCL M_w is relatively low.

Table 2.2
Glass transition temperatures, melting temperatures, and Young's modulus reported for PCL-based segmented PEUUR elastomers

Polymer	T_g (°C)	T_m (°C)	Modulus (MPa)
BDI/BDA/PCL1250 [146]	-37	A	54
BDI/BDA/PCL2000 [146]	-53	40	78
BDI/Lys/PCL1250 [146]	-40	A	14
BDI/Lys/PCL2000 [146]	-54	45	38
LDI/Phe/PCL530 [148]	-6	A	6.6
LDI/Phe/PCL1250 [148]	-34	43	54
LDI/Phe/PCL2000 [148]	-52	45	82
BDI/BDA/PCL2000 [145]	-57	20	52
HDI/BDA/PCL2000 [145]	-51	22	38
LDI/BDA/PCL2000 [145]	-52	41	40
BDI/BDO.BDI.BDO/PCL2000 [131]	-54	18	70

An 'A' denotes amorphous polymers that did not exhibit a PCL melting temperature.

All four of the tyramine-based materials exhibit melting transitions ranging from 21 to 61°C (see Table 2.1), associated with the melting of the PCL diol soft segment. As predicted by the theory of melting point depression [153], the melting temperature decreases with decreasing PCL molecular weight. The 2000 M_w PCL PEUUR examined in this study had a T_m of 42°C, which falls within the narrow range of values (40–45°C) reported for other 2000 M_w PCL PEUUR elastomers (Table 2.2). In contrast, PEUURs synthesized from lower M_w PCL exhibit a broad range of properties: LDI/Phe/PCL1250 material melts at 43°C [148], while the BDI/BDA/PCL1250 and BDI/Lys/PCL1250 materials are amorphous [146]. Although, we did not examine a material with 1250 M_w PCL, we note that our material formed from 1425 and 1100 M_w PCL fall within this range of properties, with melting temperatures of 34 and 21°C, respectively.

The storage moduli (at 37°C) of the materials prepared from 1100, 1425 and 2000 M_w PCL were in the range from 49 to 110 MPa, which is comparable to the values of Young's modulus ranging from 14 to 82 MPa reported for other PCL-based segmented PEUUR elastomers (Table 2.2). The significantly higher modulus of the 2700 M_w PCL based PEUUR (278 MPa) is attributed to the higher crystallinity of this PCL soft segment. At 37°C, the soft segment of this material is substantially below its melting temperature (61°C) and therefore semi-crystalline. This observation is also supported by the WAXS data. The significant change in the modulus observed over the temperaturerange of 20–60°C implies that over this temperature range the mechanical properties are dominated by the PCL soft segment.

Concurrent with the physical analysis of the PEUURs, biochemical analysis of BMSC was undertaken to verify biocompatibility of the polymers and to determine how systematic changes in soft segment content altered proliferation and development of the osteoblastic phenotype. It has been demonstrated that proliferation and phenotypic behavior of osteoblasts is sensitive to both interfacial chemistry and surface roughness. Gross changes in the chemistry at the biomaterial interface have been shown to alter surface hydrophilicity, protein adsorption curves and adsorbed protein conformation [154, 155], and these factors likely act in concert to alter cell morphology, adhesion, proliferation and mineralization [156, 157]. Concurrently, surface roughness, which can be introduced by annealing of polymer blends has been shown to affect cell morphology, cell density and alkaline phosphatase activity [139, 158]. Contact angle measurements (Table 2.1), which are sensitive to surface hydrophobicity, roughness and chemical heterogeneity, indicated only modest differences in the interfacial properties of the annealed polymer films. Although such differences may have influenced OPN deposition (Figure 2.8), we note that cell proliferation, as well as other biochemical markers of osteoblastic differentiation, were not affected.

This research project establishes that a series of segmented PEUURs can be synthesized from PCL (soft) and TyA.BDI.TyA (hard) segments, exhibit a broad range of storage moduli at 37°C, and support proliferation and osteoblastic differentiation of bone marrow stromal cells. Our next step will be to use these PEUURs to form porous foam

scaffolds with similar architectures but differing compressive moduli. Because, we have shown here that BMSC density, ALP activity and mRNA expression of OPN and OCN are insensitive to variations in PEUUR hard segment content, we will use these foam scaffolds to determine how BMSC properties vary with scaffold modulus.

2.6 Conclusions

A series of poly(esterurethane urea)s were synthesizedfrom TyA.BDI.TyA and PCL macrodiols of molecular weights ranging from 1100 to 2700 with hard segment contents of 20–40 wt.%. DMA showed the materials had storage moduli ranging from 49 to 278 MPa at 37°C, and DSC and WAXS showed that storage modulus correlated with crystallinity of the soft (PCL) phase. BMSCs cultured on the different films exhibited similar cell densities, ALP activities, and mRNA expression of OCN and OPN to conventional PLGA, indicating the suitability of these materials for bone tissue engineering applications.

Chapter 3: Effect of poly(ε-caprolactone) content on the proliferation and osteogenic differentiation of bone marrow stromal cells

Katherine D. Kavlock[1], Scott A. Guelcher[3], Aaron S. Goldstein[1,2*]

[1]School of Biomedical Engineering and Sciences and
[2]Department of Chemical Engineering
Virginia Polytechnic Institute and State University
Blacksburg, VA 24061-0211

[3]Department of Chemical Engineering, Vanderbilt University
Nashville, TN 37235

3.1 Abstract

Tunable physical properties make segmented polyurethanes an ideal platform for examining the effects of scaffold modulus on engineered tissue development. In this study, a family of poly(esterurethane urea)s (PEUURs) were synthesized with a poly(ε-caprolactone) (PCL) soft segment. By systematically varying the molecular weight of the PCL segment from 1425 to 2700 Da, the crystallinity and compressive modulus of the scaffolds was systematically increased. Polymers were processed into scaffolds with similar porosities and pore diameters. When bone marrow stromal cells were cultured in these scaffolds, cell number decreased with increasing PEUUR stiffness while prostaglandin E_2 (PGE_2) production and alkaline phosphatase (ALP) activity were similar on all scaffold materials except the PCL 2700 where they were highly elevated. Osteopontin, osteocalcin, bone morphogenetic protein-2, and vascular endothelial growth factor gene expression were all similar among the PEUURs. The increases in PGE_2 production and ALP activity cannot be attributed to changes in scaffold modulus but may be due to varying crystallinity.

3.2 Introduction

An engineered bone tissue consisting of a bone-like extracellular matrix (ECM) deposited on the internal pores of a resorbable biomaterial is postulated to stimulate integration, infiltration, and bone remodeling when implanted *in vivo*. Bone marrow stromal cells (BMSCs) may be an important ingredient in this strategy because with the appropriate cues from the cellular microenvironment, BMSCs have been shown to synthesize the necessary bone-like ECM *in vitro*. Numerous aspects of the microenvironment (e.g. growth factors, mechanical stimulus, and biomaterial substrates) are being actively investigated. One particularly important factor that has not previously been evaluated is the effect of the mechanical properties of the biomaterial scaffold on bone-like tissue development.

Substrate properties, including chemistry, roughness, and compliance, have a significant effect on osteoblast behavior, and therefore may play a role in the development of an engineered bone tissue. Surface chemistry, in regards to the capacity of a material to adsorb ECM proteins, regulates cell adhesion [159]. For example, cell adhesion has been shown to be greater on hydrophilic surfaces relative to hydrophobic surfaces [159]. Osteoblasts on hydrophobic surfaces exhibit low cell attachment efficiency and require a longer induction period prior to entering the exponential growth phase [160]. Additionally studies on well defined model surfaces have shown that terminal amine (NH_2) and carboxylic acid (COOH) groups result in greater cell adhesion than methyl (CH_3) terminated surfaces [161].

Surface roughness or topography of a material surface also influences cell behavior. For example, well-ordered topographies such as oriented fibers or grooves dictate the orientation and spread of adherent cells through a phenomenon known as contact guidance [162, 163]. Additionally, random topographies, such as acid-etched or sand-blasted surfaces, have been shown to decrease osteoblast proliferation while increasing phenotypic markers of osteoblastic maturation such as alkaline phosphatase (ALP) activity and osteocalcin. The size of topographical features has also been examined and features as small as 0.2 μm have been shown to have a positive effect on osteoblastic phenotype [164-166].

Substrate compliance may be a critical facet of cell microenvironment that contributes to achieving an intended phenotype [167]. Engler *et al*. tested the influence of substrate elasticity on osteoblastic differentiation of human mesenchymal stem cells (MSCs) and found that MSCs expressed increased levels of bone ECM proteins such as osteocalcin and osteopontin on the stiffest substrates [167]. Similarly, the pre-osteoblastic cell line, MC3T3-E1 cells, has shown increased alkaline phosphatase activity, mRNA expression of osteocalcin, and mineralization with increasing stiffness [168, 169]. Although these results clearly indicate that substrate mechanics influence cell growth and bone tissue development, studies to investigate the effects of substrate stiffness on cell behavior have largely been carried out in soft 2D gel systems, such as polyacrylamide, where the degree of crosslinking can be used to modulate the mechanical properties. Model systems such as the 2D gel systems are useful for gaining insights about what aspects of the surface characteristics are most influential; however, the gel systems are many orders of magnitude softer than mineralized bone tissue and for the creation of engineered bone tissue grafts, 3D architectures must employed. Therefore, additional studies involving 3D porous scaffolds made of stiffer materials are necessary to determine how the mechanical properties of a biomaterial scaffold may be tuned to achieve engineered bone tissue.

The goal of this study is to determine the effects of scaffold modulus on the osteoblastic differentiation of BMSCs. Segmented polyurethanes are a class of synthetic polymer composed of alternating soft polyol segments and hard urethane segments. The synthesis method is a two-step process where a macrodiol and an excess of diisocyanate are reacted first to form a prepolymer. The prepolymer is then chain-extended with a short diamine or diol. Segmented polyurethanes are an excellent model system for probing the effect of scaffold mechanical properties on cell behavior because the two-step synthesis process makes tuning mechanical properties to a desired range very easy through careful choice or macrodiol, diisocyanate, and chain-extender [71, 74-76].

To isolate the contribution of substrate chemistry, a family of poly(esterurethane urea) (PEUUR) elastomers were previously synthesized, spun onto glass coverslips, and the proliferation and differentiation of BMSCs was evaluated. Cell density, alkaline phosphatase

activity (ALP), and osteopontin and osteocalcin gene expression were similar among PEUURs and comparable to poly($_{D,L}$-lactic-co-glycolic acid) (PLGA) [170]. For the purposes of this study, the PEUUR elastomers were fabricated into porous foams by solvent casting/particulate leaching to achieve a series of scaffolds with similar architectures but different moduli to isolate and characterize the effect of biomaterial modulus. The porosity, pore size distribution, crystallinity, and compressive modulus of the polymer scaffolds were determined. Finally, BMSCs were cultured on porous PEUUR foams under osteoblastic conditions to determine if cell behavior is sensitive to differences in modulus and crystallinity of the PEUURs. Cell density, prostaglandin E_2 (PGE_2) production, ALP activity, and gene expression were measured to determine the effect of PEUUR modulus on osteoblastic differentiation.

3.3 Materials and Methods

3.3.1 Materials

All chemicals were obtained from Sigma-Aldrich (St. Louis, MO) and all cell culture materials were obtained from Fisher Scientific (Pittsburgh, PA) unless otherwise specified.

3.3.2 Scaffold fabrication

Poly (esterurethane urea) (PEUUR) elastomers with varying PCL molecular weights (1425, 2000, and 2700 Da) were synthesized using a tyramine-1,4-diisocyanatobutane-tyramine (TyA.BDI.TyA) chain extender and poly(ε-caprolactone) microdiol as previously described [170]. Dynamic mechanical analysis indicated moduli of 39, 119, and 278 MPa for PCL segments of 1425, 2000, and 2700 Da respectively [170]. Next, PEUUR elastomers were formed into foam scaffolds using an established solvent casting/particulate leaching method [100]. Approximately 5% (w/v) PEUUR solutions in DMF were prepared and cast over NaCl crystals (sieved 300-500 μm). The DMF was evaporated to create a 15 wt% PEUUR/85 wt% NaCl composite, which was cut into small 3-5 mm pieces and loaded into a cylindrical teflon-lined mold (12.7 mm internal diameter). The mold was then heated with a band heater to 140°C and compressed axially under 1.2 MPa of pressure for 10 min. The

composite material was dried in an oven for 72 h at 60°C, and then annealed under vacuum at 80°C for 24 h. The composite material was then cut into 2.5 mm thick discs for cell seeding and 25 mm rods for mechanical testing. The NaCl particulates were leached out of the discs by immersion in deionized water for 72 h and the resulting porous foams were then soaked in ethanol for 48 h to remove any residual DMF before being dried and stored in a desiccator.

Control scaffolds for these studies were prepared from 75:25 poly($_{D,L}$-lactic-co-glycolic acid) (PLGA; Lactel Biodegradable Polymers, Birmingham, AL) as previously published [100]. Briefly, approximately 5% solutions of PLGA in dichloromethane cast over NaCl crystals sieved 300-500 μm at a ratio of 15 wt% PLGA/85 wt% NaCl. PLGA scaffolds were heated to 100°C for 30 min under 1.2 MPa of pressure. The material was cut into 2.5 mm discs for cell studies and 25 mm rods for mechanical testing with a low speed diamond wheel saw (South Bay Technology, San Clemente, CA) and leached for 72 h in deionized water to remove the NaCl particulates. The resulting foams were dried and stored in a desiccator until sterilization by γ-irradiation. Scaffolds were incubated in a 2 μg/mL solution of fibronectin (Invitrogen) for one hour prior to seeding.

3.3.3 Scaffold characterization

Porosity and pore size distribution were measured using a mercury intrusion porosimeter (Autopore III; Micromeritics Instrument Corp., Norcross, GA). Mercury intrusion porosimetry was conducted for 3 samples of approximately 0.1 g of each PEUUR with a mercury-filling pressure of 0.16 psi, a maximum intrusion pressure of 500 psi. Pore sizes were calculated from intrusion data by assuming a mercury contact angle of 137 degrees.

The pore shape, interconnectivity, and surface roughness were visually inspected for differences in topography by scanning electron microscopy (SEM). Briefly, porous scaffolds were mounted and sputtercoated with a 5 nm thick layer of palladium as previously described [171]. Images were captured at 100, 2K, and 20K × magnification using a LEO 1550 Field Emission SEM (Carl Zeiss SMT, Thornwood, NY).

The compressive moduli of PEUUR scaffolds were measured using 25 mm thick rods, cut to allow for a 2:1 length to diameter ratio. All foams were soaked in phosphate buffered saline (PBS) overnight prior to compressive testing. Foams were tested wet at 37°C with a hydraulic MTS 810 material testing system (MTS Systems Corporation, Eden Prairie, MN) and compressed with a crosshead speed of 1.0 mm/min. Each sample was compressed to approximately 10% strain and then released at the same rate. The compressive modulus was measured as the slope of the linear elastic region of deformation for n = 3 samples per polymer.

Degradation of the PEUURs was measured after determination of the compressive modulus. Samples were dried, cut into pieces averaging approximately 30 mg, weighed, and re-wet in PBS. Foam pieces were incubated in PBS at 37ºC for up to 6 months with 3 pieces removed every 2 weeks. Each piece was dried completely and re-weighed to determine the fraction of foam remaining. In addition, both number- and weight- average molecular weights were determined by gel permeation chromatography (GPC) with a Waters Alliance GPC 2000 (Waters Corporation, Milford, MA) using DMF as the continuous phase, toluene as an internal standard, and monodispersed polystyrene as the calibration standard.

Differential scanning calorimety (DSC) was performed to evaluate the level of crystallinity of the processed PEUUR scaffolds. DSC analysis was conducted on a Q2000 (TA Instruments, New Castle, DE). Porous foam samples (3.5 – 5.7 mg) were heated in a nitrogen atmosphere from slightly below room temperature (20°C) to 120°C at 10°C min^{-1}, held at 120°C for 2 min, and then cooled to -50°C at 10°C min^{-1}. Foams were not cooled prior to the first heating curve so that the crystallinity calculated was from the scaffold fabrication process and not induced by the DSC analysis.

3.3.4 Bone marrow stromal cell culture

BMSCs were developed from bone marrow explants harvested from the tibias and femurs of 125 – 150 g male Sprague-Dawley rats (Harlan, Dublin, VA) in accordance with the Institutional Animal Care and Use Committee at Virginia Tech [135, 136]. Briefly, explants were dispersed in growth medium (α-MEM (Invitrogen, Carlsbad, CA)

supplemented with 10% fetal bovine serum (Gemini, Calabasas, CA) and 1% antibiotic/antimycotic (Invitrogen) and expanded for approximately 10 days with medium changes every 3 or 4 days. After 10 days the cells were rinsed twice with PBS, lifted with trypsin/EDTA (Invitrogen), split 1:2, and defined as passage 1. After the cells reached approximately 90% confluence the passaging process was repeated twice until the cells were approximately 90% confluent at passage 3. At this point cells were lifted and suspended in growth medium at a density of 2×10^6 cells/mL. Cells were seeded into scaffolds were seeded by dropwise addition of approximately 1 mL of cell suspension to each scaffold. (Here, the estimated void volume of the scaffolds is only 300 μL; however, the excess volume of cell suspension has been shown to provide uniform seeding [100].) The seeded scaffolds were placed into 12 well plates and allowed to sit in the sterile cabinet for 1 hour to permit cell attachment prior to the addition of 2 mL growth media and placement into the CO_2 incubator. On the following day, denoted as day 0, growth medium was replaced with osteogenic differentiation medium (growth medium supplemented with 0.13 mM ascorbate-2-phosphate, 2 mM β-glycerophosphate, and 10 nM dexamethasone). Thereafter, the culture medium was changed twice weekly.

Scaffolds as well as samples of conditioned culture medium were collected at days 14 and 21. Scaffolds were rinsed twice with PBS, cut into quarters and weighed. To facilitate the extraction of cellular materials, scaffolds were frozen in liquid nitrogen before being crushed and homogenized in the appropriate collection buffer for analysis of cell number, ALP activity, and gene expression.

3.3.5 Cell number

Cell number was determined after 14 and 21 days using PicoGreen reagent (Invitrogen). Two quarters of each sample were collected in 1 mL TE buffer (10 mM Tris-HCl, 1 mM EDTA, pH 7.5) and sonicated on ice for 10 min to release the DNA. DNA standards of 0.016 to 1 μg/mL were prepared in TE buffer according to manufacturer's instructions. A volume of 100 μL of samples and standards were added to a 96-well plate in duplicate. PicoGreen reagent was diluted 1:200 in TE buffer and then 100 μL of the diluted

PicoGreen reagent was added to each well. Fluorescence was measured with a SpectraMax fluorescent plate reader (Molecular Devices, Sunnyvale, CA) using excitation and emission frequencies of 488 and 525 nm, respectively, and a linear standard curve was plotted correlating fluorescence to μg/mL DNA. Cell number was calculated from the standard curve using a constant of 8.1 pg DNA/cell and normalized by the mass of the scaffold. This constant was experimentally determined with a series of BMSC suspensions with known concentrations.

3.3.6 Prostaglandin E_2 production

Accumulation of prostaglandin E_2 (PGE_2) in conditioned medium was determined at days 14 and 21 by an enzyme immunometric assay (EIA) kit (Assay Designs, Ann Arbor, MI) according to the manufacturer's instructions. The PGE_2 ELISA kit is a competitive immunoassay that uses a monoclonal antibody to bind the PGE_2 in samples of conditioned medium. Absorption at a wavelength 405 nm was measured with a Labsystems Multiskan RC ELISA plate reader (Labsystems, Frankfurt, Germany). All measurements were performed in duplicate and protein content was calculated from curves generated using standards provided with the kits.

3.3.7 ALP activity

After 14 and 21 days of osteoblastic culture, ALP activity was determined using a commercially available kit (Biotron Diagnostics, Hemet, CA). Scaffold quarters for analysis of ALP activity were homogenized in 500 μL TGT solution (50 mM Trizma HCL, 100 mM glycine, 0.1 % Triton X100, pH 10.5) containing 1% protease inhibitors (aprotinin, bestatin, leupeptin, E-64, and pepstatin A). A volume of 100 μL of homogenized sample was combined with 500 μL ALP reagent and incubated at 37°C for 15 minutes as previously described [137]. After 15 minutes the reaction was stopped with 500 μL of 0.3 M NaOH and the absorbance of the reaction mixture was measured at 405 nm using a Spectronic Genesys 5 spectrophotometer (Spectronic Analytical Instruments, Leeds, UK). Enzyme activity,

defined as the rate of conversion of *p*-nitrophenol phosphate to *p*-nitrophenol, was calculated and normalized by the mass of the scaffold and then by cell number to yield activity per cell.

3.3.8 mRNA expression

Expression of mRNA for osteopontin (OPN), osteocalcin (OC), vascular endothelial growth factor A (VEGF-A), and bone morphogenic protein 2 (BMP-2) was determined by quantitative RT-PCR as described previously [170]. Briefly, RNA was isolated from the samples using the RNeasy mini kit (Qiagen, Valencia, CA) according to manufacturer's instructions. Next, 9 μL of isolated RNA was reverse transcribed to cDNA using the Superscript kit (Invitrogen) and random hexamers as primers. Quantitative RT-PCR was performed using an ABI 7300 sequence detection system (Applied Biosciences, Foster, CA), SYBR green master mix (Applied Biosciences), and specific primers for β-actin (βA), OPN, OC, and BMP-2 (Integrated Technologies, Coralville, IA) [135, 172]. A primer pair for detection of VEGF-A was designed using Primer Express software (ABI) and the NCBI database (Accession number: NM_031836) where the forward and reverse primers are GCT GCA CCC ACG ACA GAA and GGC AAT AGC TGC GCT GGT A respectively. The $2^{-\Delta\Delta Ct}$ method was used to quantify the gene expression of OPN, OC, BMP-2, and VEGF-A using βA as the internal reference [138].

3.3.9 Statistics

Data were analyzed using a student's paired t-test and a 95% confidence criterion to test for differences between polymer groups. All data is presented as mean ± standard error of the mean (SEM) and an asterisk denotes a statistically significant difference between a PEUUR group and the PLGA control.

3.4 Results

3.4.1 Physical characterization of PEUUR foams

PEUUR elastomers were processed into porous foam scaffolds as previously described and visual inspection indicated similar pore architectures for the four different

scaffolds (Figure 3.1). The jaggedness of the pore edges is probably due to the process of cutting the scaffolds to fit on the SEM mounts. The holes inside the pores indicate a high level of pore interconnectivity.

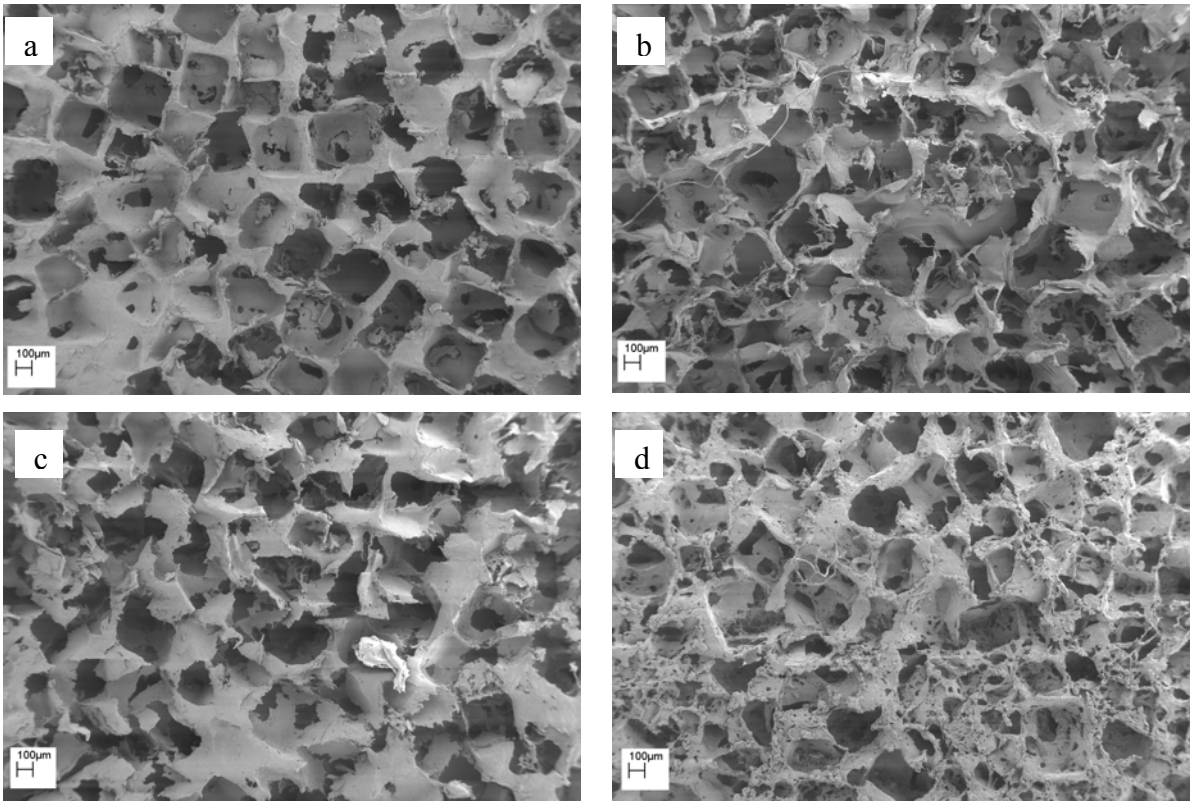

Figure 3.1: SEM images of scaffolds at 100x magnification (a) PCL 1425, (b) PCL 2000, (c) PCL 2700, and (d) PLGA

In addition, SEM analysis of the pore surfaces at higher magnification (Figure 3.2) did not reveal any obvious differences in surface topography between the PEUURs. The PLGA control was imaged at a lower magnification due to the high energy beam causing cracking and destruction of the sample.

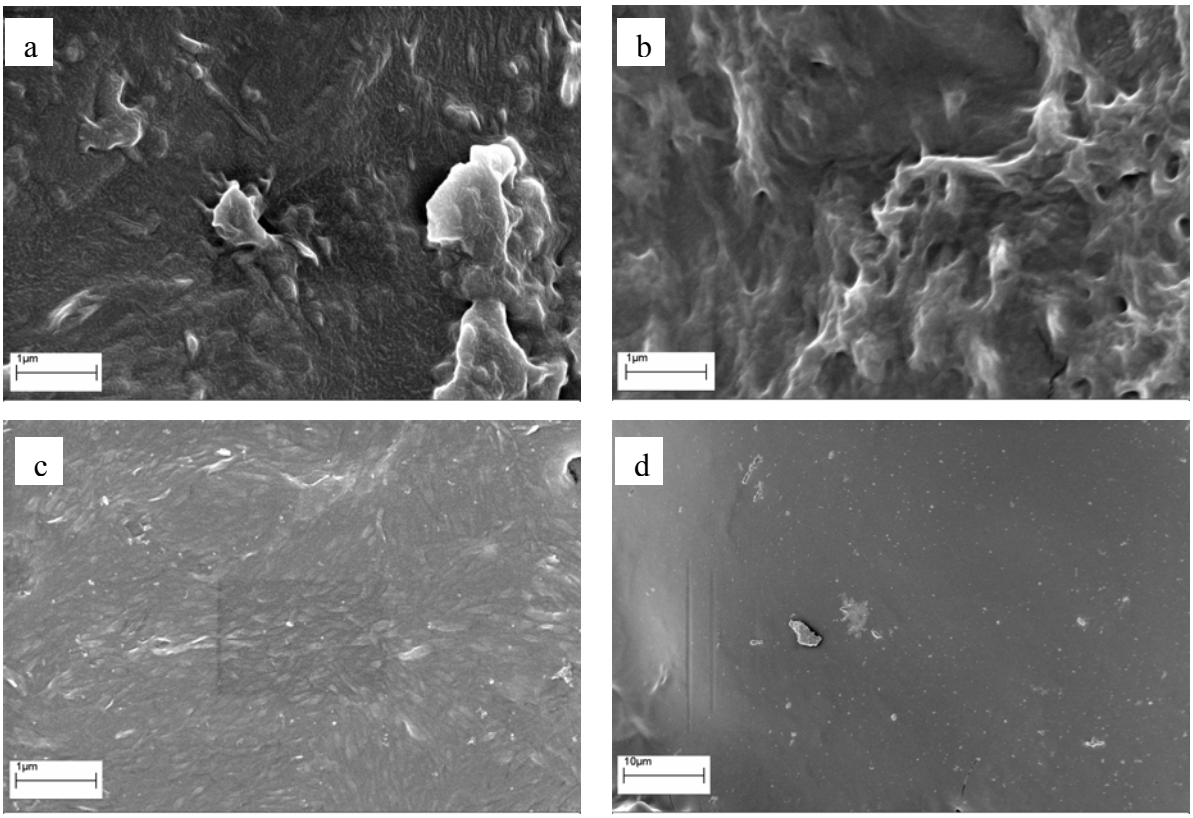

Figure 3.2: SEM images of pore surfaces within foam scaffolds at 20Kx magnification (a) PCL 1425, (b) PCL 2000, (c) PCL 2700, and (d) PLGA (2Kx magnification).

Mercury intrusion porosimetry analysis of the PEUUR foams confirmed that the PEUUR foams have similar porosities and average pore sizes ranging from 78% to 86% and from 63 to 78 μm in diameter respectively (Table 3.1). The porosities and pore sizes of the PEUUR foams are comparable to the porosity of 78.8% and pore size of 70 μm previously reported for PLGA [100]. Contact angle (θ), a measure of surface hydrophilicity and to some extent surface roughness, was measured on spin-coated coverslips and previously published [170]. The PCL 2700 material has a slightly lower contact angle than the other two PEUUR materials, indicating minor differences in the wettability of the PCL 2700 material and could be affected by small differences in surface roughness.

Compressive testing, performed under physiologically relevant conditions (at 37°C and in saline solution), indicated that the compressive moduli of the PEUUR foams systematically increase from 0.18 MPa to 0.80 MPa with increasing PCL content (Table 3.1). These moduli – for hydrated 80% porous PEUUR foams – is two and a half orders of

magnitude lower than the moduli of dry cast films, differences that are attributable to the addition of water and the porous architecture of the scaffolds. [170]. However, both dry and wet PEUUR materials exhibit a similar trend of increasing modulus with increasing PCL content. By comparison, the PLGA controls were found to have a compressive modulus of 6.33 MPa.

Table 3.1

Properties of PEUUR foams. Percent porosity and average pore size were determined by mercury porosimetry. Compressive modulus was determined from stress strain curves.

Polymer	θ (°)	Porosity (%)	Average Pore Size (μm)	Modulus (MPa)	Degree Crystallinity (%)
PCL 1425	79 ± 5	78.8 ± 3.8	77.6 ± 11.6	0.18 ± 0.07	16.0
PCL 2000	83 ± 2	86.0 ± 2.4	70.2 ± 7.0	0.38 ± 0.11	25.2
PCL 2700	74 ± 3	77.6 ± 3.1	63.2 ± 0.5	0.80 ± 0.40	45.3
PLGA		78.8 *	70 *	6.33 ± 2.88	

DSC analysis of processed polyurethane foams (Figure 3.3) revealed systematic increases in the degree of crystallinity with increasing PCL content. Degree of crystallinity was calculated from the size of the endothermic melting peak (Figure 3.3a) and summarized in Table 3.1:

$$\%\ Crystallinity = \frac{\frac{\Delta H}{g}_{PEUUR} \times \%\ PCL\ content}{\frac{\Delta H}{g}_{100\%\ PCL}}$$

Our calculations are supported by the systematic increases observed in the size of the exothermic crystallization peak in the cooling curves (Figure 3.3b).

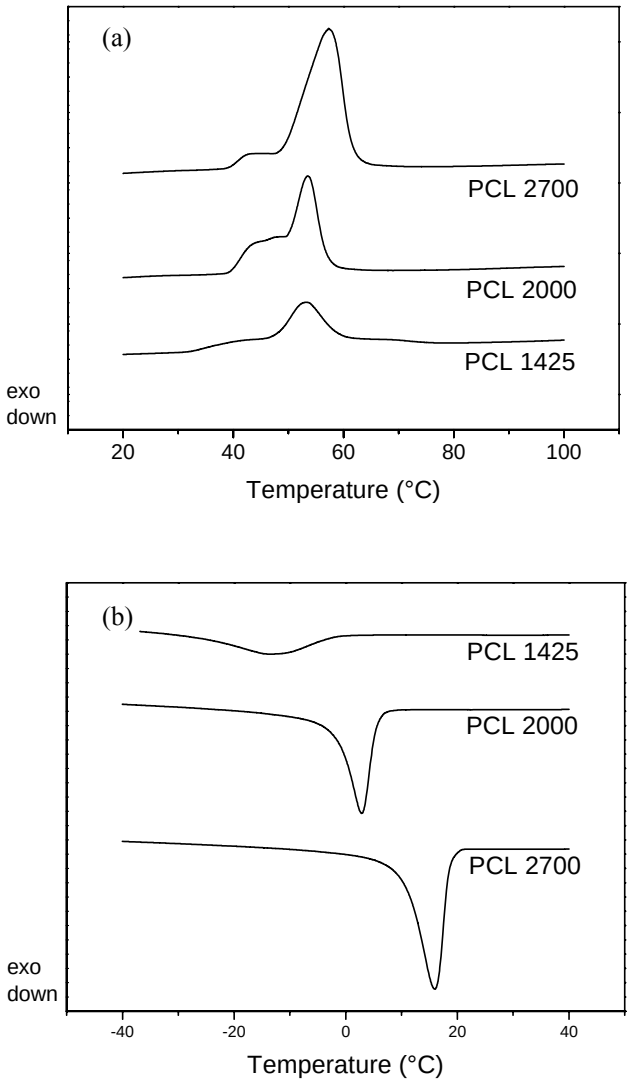

Figure 3.3: DSC analysis of processed PEUUR foams, (a) first heating curve and (b) cooling curve. Curves are offset vertically to permit visual comparison.

Degradation of the foams was characterized by both percent mass loss and change in molecular weight with time. Measurement of dry weight of PCL 1425, 2000, and 2700 indicated that they lost approximately 20%, 21%, and 40%, respectively, of their total mass over at 24 week time period (Figure 3.4a). Change in molecular weight with time was measured by gel permeation chromatography (GPC). GPC analysis shows the loss of weight-average molecular weight as a function of time for PEUUR foams (Figure 3.4b).

GPC analysis indicated that PCL 1425, PCL 2000, and PCL 2700 lost approximately 30%, 39%, and 29% of their molecular weight, respectively, over a 24 week time period showing that degradation rates are relatively similar between PEUURs.

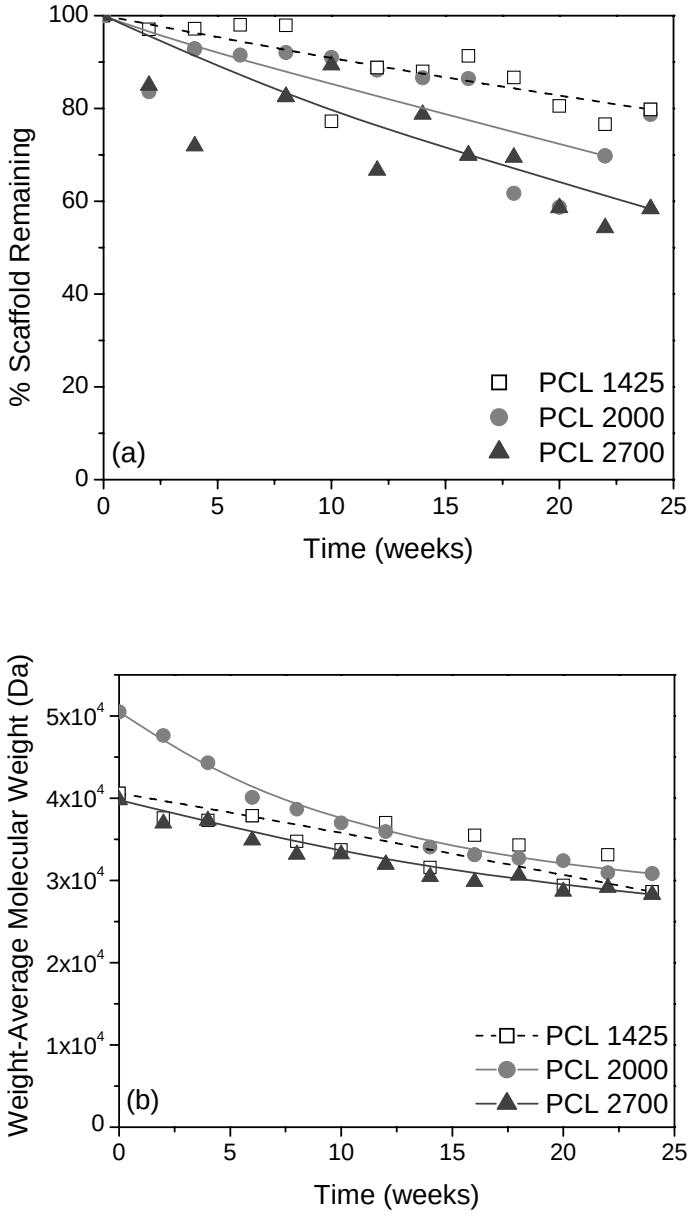

Figure 3.4: Degradation profile of PEUURs reported as weight-average molecular weight determined by GPC analysis. The lines are intended to lead the eye.

3.4.2 BMSC proliferation and differentiation on PEUUR foams

The cell numbers at days 14 and 21 indicated proliferation of cells from an estimated initial seeding density of 6×10^5 (Figure 3.5). A trend among the PEUUR scaffolds was noted in which one with the lowest PCL exhibited the highest cell density whereas the one with the highest PCL content had the lowest cell density. Cell number in the PLGA scaffold was similar to that in the PEUUR with the intermediate PCL content. Finally, increases in cell density were not observed from 14 to 21 days on any polymer. Based on calculations of surface area within the scaffold, cells were not confluent, indicating that the cells were not contact inhibited but rather made the transition from the proliferation phase to differentiation.

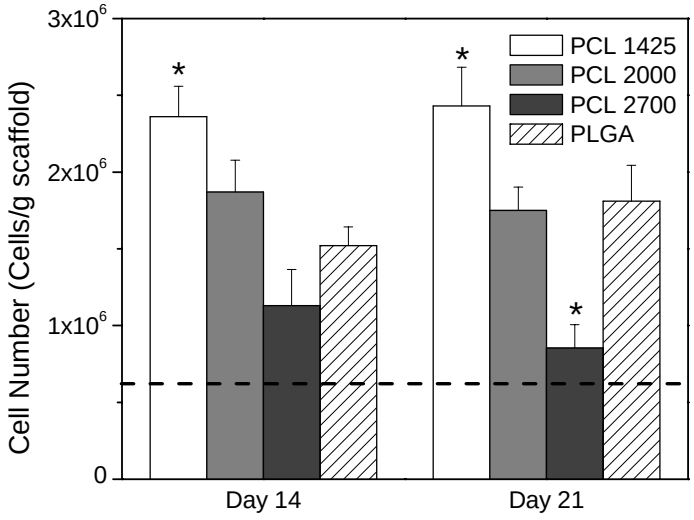

Figure 3.5: Cell number in PEUUR porous foams at 14 and 21 days. Data are mean ± SEM for n = 6 samples. The dashed line indicates the seeding density (approximately 6 x 10^5 cells). An asterisk denotes a significant difference with respect to PLGA at the same time point ($p<0.05$).

PGE_2 is a stress-related lipid hormone synthesized from arachidonic acid by the cyclooxygenase (COX) enzymes. PGE_2 is elevated when cells are cultured on rough surfaces [164, 165, 173]. Increases in PGE_2 synthesis have also been linked to increases in alkaline phosphatase activity and bone formation [114]. Analysis of levels of PGE_2 (Figure 3.6) indicated a statistically significant increase in the level of production of PGE_2 by BMSCs on the PCL 2700 scaffolds.

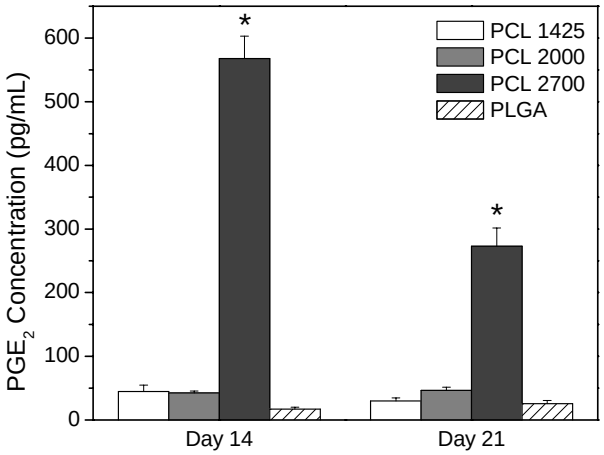

Figure 3.6: PGE_2 concentration in conditioned media at 14 and 21 days. Data are mean ± SEM for n = 6 samples. An asterisk denotes a significant difference with respect to PLGA at the same time point ($p<0.05$).

Analysis of ALP activity indicated very similar enzyme levels (on a per cell basis) for the PCL 1425, PCL 2000, and PLGA scaffolds at days 14 and 21 (Figure 3.7) despite significant differences in cell number. However, ALP activity in the PCL 2700 foams was significantly elevated compared to all other experimental groups at both time points.

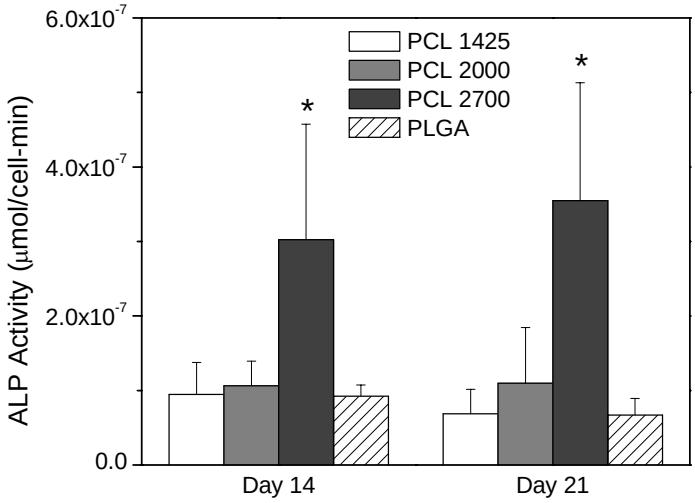

Figure 3.7: ALP activity of BMSCs in PEUUR foam scaffolds at 14 and 21 days. Data are mean ± SEM for n = 6 samples. An asterisk denotes a significant difference with respect to PLGA at the same time point ($p<0.05$).

Analysis of gene expression by quantitative RT-PCR showed that differences between materials were not statistically significant for all genes at all time points (Figure 3.8), although OPN expression appears elevated for BMSCs in PCL 2700 scaffolds. Higher levels of BMP-2 and OC at day 14 suggest BMSCs differentiate a little faster on softer surfaces. Expression of these genes did not change significantly from day 14 to day 21.

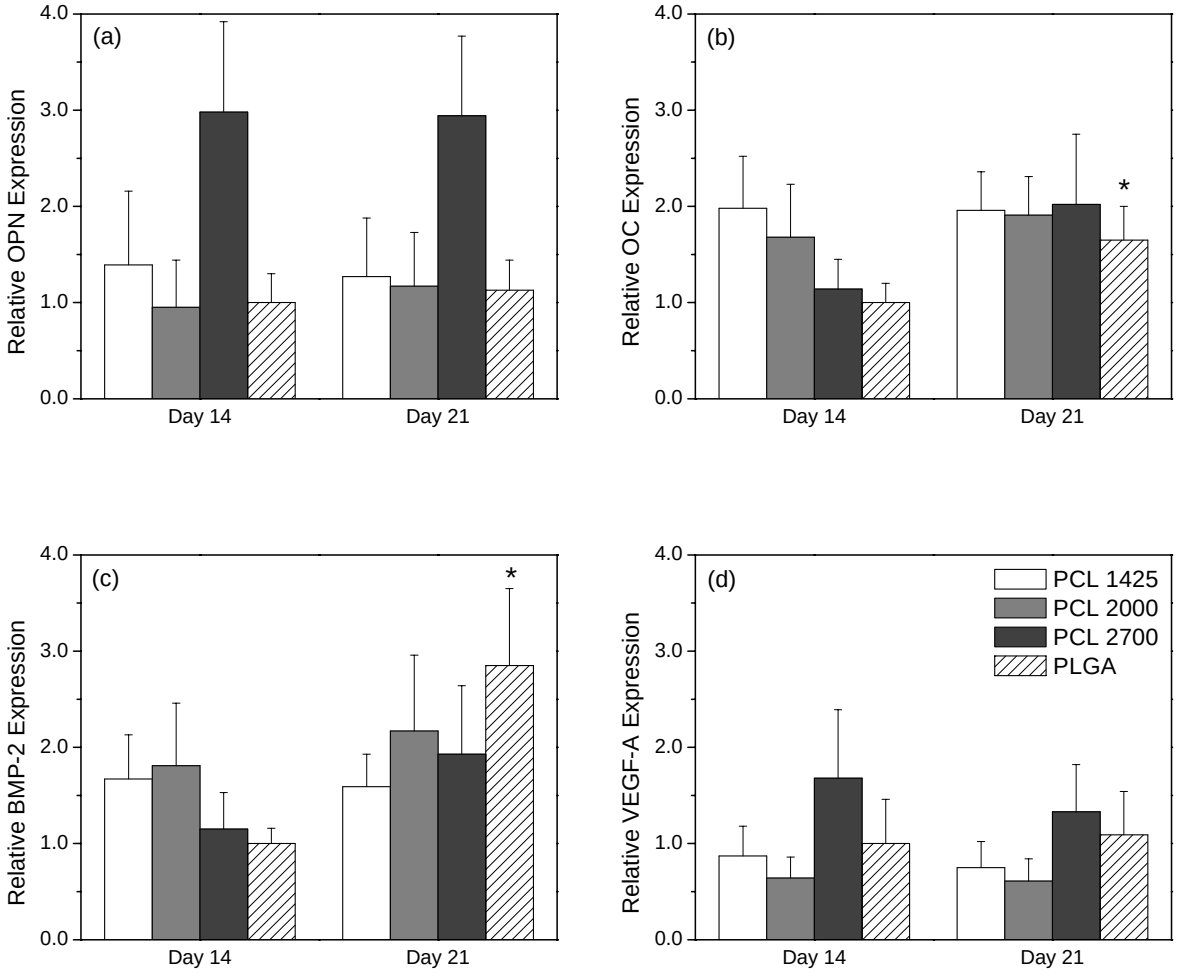

Figure 3.8: (a) OPN mRNA expression, (b) OC mRNA expression, (c) BMP-2 mRNA expression, and (d) VEGF-A mRNA expression of BMSCs in PEUUR foams at 14 and 21 days. β-Actin was used as the housekeeping gene and data are normalized to PLGA foams at day 14. Data are ± SEM for n = 6 samples.

3.5 Discussion

The goal of this study was to determine the effect of scaffold modulus on the osteoblastic differentiation of BMSCs. A family of PEUURs with different mechanical properties were synthesized and formed into scaffolds with similar architectures. The porosity, surface texture, compressive modulus, crystallinity, and degradation rate of the PEUUR foams were all evaluated in order to characterize the effect of modulus and crystallinity on cell behavior. Porosities, average pore size, and degradation rates of the PEUUR foams were determined to be similar for PCL contents. Compressive modulus and crystallinity were shown to increase systematically with increasing PCL content as expected. The PCL 2700 material supported significantly fewer cells compared to the PLGA control while PGE_2 secretion and ALP activity were significantly elevated on the PCL 2700 material compared to all other experimental groups. Finally, gene expression was not significantly different for any gene on any PEUUR compared to the PLGA controls. While the mRNA expression profiles of VEGF-A and OPN showed no significant difference between the PCL 2700 and the other materials, the profiles exhibited the same trends as ALP activity and PGE_2.

Previous investigations into the effect of substrate mechanical properties on the osteogenic potential of preosteoblasts (MC3T3-E1s) or MSCs were conducted on hydrogels such as polyacrylamide, or poly(ethylene glycol) (PEG). Stiffness of the stubstrate was controlled by manipulating the degree of crosslinking. This processing technique resulted in very low modulus substrates. The polyacrylamide substrates ranged in modulus from 0.1 – 39 kPa [167, 169] and the PEG substrate ranged from 14 – 424 kPa [168]. In comparison, our materials have moduli ranging from 1 to 3 orders of magnitude greater. On the stiffer PEG substrates ALP activity was increased as stiffness increased. These results are in agreement with our results in PEUUR foams. Similarly, on both PEG and polyacrylamide substrates, late markers of osteoblastic differentiation including OPN and OC were upregulated as substrate stiffness was increased [77, 78]. However, our OC and OPN results show no trend with regard to PEUUR scaffold stiffness. Only Engler *et al.* has investigated the effect of scaffold modulus on the osteogenic growth factor BMP-2 and similarly to our

results, Engler and colleagues found no trend in BMP-2 expression due to substrate stiffness [77].

The differences between PCL 2700 and the other materials cannot be attributed to differences in scaffold stiffness because while PLGA is stiffer than the PEUURs, the PLGA scaffolds did not prove to be more osteoinductive than the PCL 1425 and PCL 2000 materials. PLGA is stiffer than the PEUUR materials, but it is also amorphous, suggesting that the differences in cellular response on the PCL 2700 materials may be due to variations in crystallinity rather than modulus. Recently, the effect of crystallinity on osteoblasts was studied using four different graphitic and carbonaceous matrices. Czarnecki *et al.* found that the number of cells adhered to the carbon substrate decreased as crystallinity of the material increased [174]. Our results are in excellent agreement with the results published by Czarnecki because our cell number was significantly less on our most crystalline PEUUR material, the PCL 2700.

Changes in crystallinity can also affect surface properties, including interfacial chemistry and surface roughness. These surface properties have been shown to alter the proliferation and phenotypic behavior of osteoblasts. Variations in chemistry at the biomaterial interface can alter surface hydrophilicity, protein adsorption, and conformation of adsorbed protein [154, 175]. Surface roughness, generated by annealing of polymer blends, has been shown to affect osteoblast morphology, cell density, and ALP activity [139, 158]. Recent evidence with human mesenchymal stem cells shows an inverse correlation between surface roughness and cell number but a positive correlation between roughness and ALP activity [176]. In principle, effects of surface chemistry and topography can be varied independently; however, in practice the separation is difficult to achieve and it is even more difficult to prove that these two parameters are indeed independent. Contact angle measurements are sensitive to surface hydrophobicity, surface roughness, and heterogeneity of the surface chemistry. Previous results, summarized in Table 3.1, indicate a modest difference in contact angle between the PCL 2700 material and the other PEUUR materials. While SEM images (Figure 3.2) do not reveal differences in surface topography within the

pores of the PEUUR scaffolds, differences in surface roughness of less than 1 μm have been shown to increase PGE_2 production [164].

PGE_2 production, ALP activity, and OPN gene expression data suggests cells are responding to differences in surface roughness. These early markers predict increased mineral deposition. For these studies mineral deposition could not be measured because the alizarin red s stain for calcium was non-specifically absorbed into scaffold, staining the whole scaffold red

Biodegradation of our materials is theorized to progress by hydrolysis of ester linkages yielding α-hydroxy acid by-products and urethane and urea fragments [177]. Hydrolytic scission of the molecular chains starts on contact with water as reflected by an initial drop in molecular weight. However, the chains are not small enough to diffuse out as oligomers so significant mass reductions are not observed initially. Additionally, there may be different rates of degradation for the crystalline and amorphous phases, resulting in residues of crystals. These crystals are undesirable because they may cause foreign body reactions analogous to ultrahigh molecular weight polyethylene wear particles in total joints [178].

3.6 Conclusions

A series of poly(esterurethane urea)s were processed into porous foam scaffolds with varying mechanical properties and the capacity of each material to induce osteoblastic differentiation of bone marrow stromal cells was measured. BMSCs exhibited increased ALP activity and PGE_2 synthesis on the PCL 2700 material compared with the less stiff, less crystalline PEUURs. While gene expression was not significantly affected, analysis of BMP-2 and OC gene expression at day 14 suggests that BMSCs differentiate faster on softer surfaces.

Chapter 4: Effect of pulse frequency on the proliferation and osteogenic differentiation of bone marrow stromal cells seeded in porous scaffolds and cultured in a perfusion bioreactor

Katherine D. Kavlock[1] and Aaron S. Goldstein[1,2*]

[1]School of Biomedical Engineering and Sciences and
[2]Department of Chemical Engineering
Virginia Polytechnic Institute and State University
Blacksburg, VA 24061-0211

4.1 Abstract

Engineered bone substitutes are an attractive alternative to autologous bone grafts. However, strategies are needed to facilitate the development of engineered bone graft substitutes *in vitro*. Perfusion bioreactors have been investigated as a component of engineered bone strategies because they both supply oxygen and nutrients (needed to expand cells) and apply an osteoblastic stimulus in the form of fluid shear stress (needed to differentiate the cells). In addition to steady flow cultures, evidence with planar cell cultures has shown that dynamic flow regimens elicit an enhanced osteoblastic response over steady flow regimens. However, dynamic perfusion strategies have only been investigated in short term cultures (<48 hours) and have not yet been testing in clinically relevant scaffold architectures. The objective of this research is to investigate whether pulsatile flow patterns enhance osteogenic differentiation of bone marrow stromal cells seeded in porous scaffolds over a continuous flow pattern. To accomplish this bone marrow stromal cells were seeded in porous poly(lactic-co-glycolic acid) scaffolds, and cultured for 15 days. No flow and continuous flow control conditions were compared to 3 frequencies of pulsatile flow: 0.083, 0.050, and .018 Hz. Scaffolds were analyzed for markers of osteoblastic differentiation as indicated by levels of alkaline phosphatase activity and the bone extracellular matrix proteins, osteopontin and osteocalcin. Our results indicate that pulsatile flow suppresses cell

number while all flow conditions enhanced alkaline phosphatase activity and osteopontin expression. Additionally, these markers are preferentially enhanced by 0.05 Hz pulsatile flow over continuous flow. However, no trends were observed in expression of markers of osteoblastic differentiation with respect to flow frequency. These results indicate that dynamic perfusion may be a useful component of the engineered bone tissue strategy, and the effect of pulsatile frequency warrants further investigation.

4.2 Introduction

An engineered bone tissue consisting of a bone-like extracellular matrix deposited on the internal pores of a resorbable biomaterial scaffold is postulated to stimulate integration, vascular infiltration, and normal bone remodeling when implanted in vivo. Bone marrow stromal cells (BMSCs) have the potential to synthesize the necessary bone-like matrix under the appropriate conditions, and consequently the identification of osteogenic stimuli is of great importance. One such osteogenic stimulus is hydrodynamic shear stress that is exerted on cells under perfusion culture.

Perfusion culture is important for maintenance of cell viability in large scaffolds. Perfusion supplies oxygen and nutrients to cells in the interior of scaffolds and beyond the limits of diffusive transport. Under static conditions, cell viability drops significantly at a distance greater than 1 mm from the surface of the scaffold [100]. Perfusion bioreactors have been shown to mitigate this problem and maintain a more uniform cell distribution in porous scaffolds [100-102].

Fluid flow has been shown to induce signaling molecules associated with osteoblastic gene regulation including prostaglandin E_2 (PGE_2), nitric oxide (NO), cyclooxygenase 2 (COX-2), and mRNA expression of transforming growth factor β1 (TGF-β1) via stretch and voltage-activated calcium ion channels [113, 179, 180]. In addition, steady perfusion has been shown to enhance later markers of osteoblastic phenotype including alkaline phosphatase (ALP) activity, synthesis of type I collagen, and synthesis of the non-collagenous extracellular matrix proteins, osteopontin (OPN)) and osteocalcin (OC) [54, 100, 102, 106, 181].

Model studies involving osteoblastic cells in monolayer cultures have shown that dynamic flow conditions such as oscillatory or pulsatile flow enhance mRNA expression of OPN and vascular endothelial growth factor (VEGF-A), synthesis of prostaglandin (PGE_2), and activation of mitogen-activated protein kinases (ERK and p38) [16, 109, 110, 182]. In addition, several studies have reported that cell response to pulsatile flow is frequency-dependent [110, 117, 118]. Jacobs *et al.* measured intracellular calcium release in response to both oscillatory and pulsatile flow at three different frequencies, 0.5, 1, and 2 Hz. They reported that pulsatile flow resulted in greater calcium transients than oscillatory flow and that the response dropped off as the frequency of dynamic flow increased [110]. A lack of consensus exists in the literature about the effect of dynamic flow frequency on PGE_2 synthesis. Nauman *et al.* reported that PGE_2 production increased with increasing frequency while Mullander *et al.* reported no change in PGE_2 with respect to frequency although Mullander did report an increase in NO release as frequency increased from 1 to 9 Hz [117, 118].

Only two studies examining the effect of dynamic flow regimens on cells seeded in 3D porous scaffolds were found in the literature. However, these experiments both focused on early time points, 0-48 h, and early osteoblastic signaling molecules, PGE_2 and COX-2 [109, 183]. In addition, neither of the investigations of dynamic flow involving 3D cultures have examined the effect of frequency. Therefore, based on the aforementioned results reported by Jacobs *et al.,* pulsatile flow at low frequencies was selected as the appropriate flow strategy for examining the effect of dynamic perfusion. Specifically, our objective is to examine the effect of frequency on the level of later markers of osteogenic differentiation, ALP activity and gene expression of non-collagenous bone matrix proteins, of BMSCs seeded in porous foam scaffolds.

To test the effect of pulsatile flow on osteogenic differentiation we have cultured BMSCs in 75/25 poly(D,L-lactic-co-glycolic acid) (PLGA) foam scaffolds. PLGA is a well characterized material used for many biomedical applications. The cells seeded within the PLGA scaffolds were subjected to pulsatile flow at frequencies of 0.083, 0.050, and 0.018 Hz. These frequencies were chosen based both on evidence that lower frequencies have

produced increased cellular response and on the limitations of our current flow system [110]. Control scaffolds were kept under static conditions and under continuous perfusion conditions. Proliferation of BMSCs and levels of ALP activity, osteopontin and osteocalcin mRNA expression, and accumulated OPN protein were measured in addition to the early osteoblastic signaling molecule, PGE_2.

4.3 Materials and Methods

4.3.1 Materials

All chemicals were obtained from Sigma-Aldrich (St. Louis, MO) and all cell culture materials were obtained from Fisher Scientific (Pittsburgh, PA) unless otherwise specified.

4.3.2 Scaffold fabrication

Scaffolds for these studies were prepared from PLGA (Lactel Biodegradable Polymers, Birmingham, AL) using an established solvent casting/particulate leaching method [100]. Briefly, approximately 10% (w/v) PLGA solutions in dichloromethane were cast over NaCl crystals (sieved 300-500 μm) at a ratio of 15 wt% PLGA/85 wt% NaCl. The PLGA/NaCl composite was loaded into a cylindrical teflon-lined mold (12.7 mm internal diameter) and heated to 100°C for 30 min under 1.2 MPa of pressure. The composite material was cut into 2.5 mm discs for cell studies and 25 mm rods for mechanical testing with a low speed diamond wheel saw (South Bay Technology, San Clemente, CA) and leached for 48 h in deionized water to remove the NaCl particulates. The resulting foams were dried, press-fit into acrylic cassettes, and sterilized by gamma irradiation. The acrylic cassettes allows for easy insertion and removal of the scaffold from the perfusion bioreactor.

Prior to seeding, the scaffolds were immersed in 70% ethanol and a vacuum was drawn to release air bubbles trapped within the pores of the scaffolds. Mechanical agitation to further facilitate the escape of air bubbles was applied and the ethanol was removed. The scaffolds were rinsed three times with phosphate buffered saline (PBS) and the foams were soaked in PBS overnight to remove any additional ethanol. Scaffolds were incubated in a 2 μg/mL solution of fibronectin (Invitrogen) for one hour prior to cell seeding.

4.3.3 Bone marrow stromal cell culture

BMSCs were developed from bone marrow explants harvested from the tibias and femurs of 125 – 150 g male Sprague-Dawley rats (Harlan, Dublin, VA) in accordance with the Institutional Animal Care and Use Committee at Virginia Tech [135, 136]. Briefly, explants were dispersed in growth medium (α-MEM (Invitrogen, Carlsbad, CA) supplemented with 10% fetal bovine serum (Gemini, Calabasas, CA) and 1% antibiotic/antimycotic (Invitrogen) and expanded for approximately 10 days with medium changes every 3 or 4 days.

After 10 days the cells were rinsed twice with PBS, lifted with trypsin/ ethylenediaminetetraacetic acid (EDTA) (Invitrogen), split 1:2, and defined as passage 1. After the cells reached approximately 90% confluence the passaging process was repeated until the cells were approximately 90% confluent at passage 3 or 4. Cells were then lifted and suspended in growth medium at a density of 2×10^6 cells/mL. Cells were seeded by dropwise addition of approximately 750 - 1000 μL of cell suspension to each scaffold. (Here, the estimated void volume of the scaffolds is only 300 μL based on the porosity and size of the scaffold; however, the excess volume of cell suspension has been shown to provide uniform seeding [100].) The seeded scaffolds were placed into 12 well plates and allowed to sit in the sterile cabinet for 1 hour to permit cell attachment prior to the addition of 2 mL growth media and placement into the CO_2 incubator.

4.3.4 Perfusion bioreactor

Cellularized scaffolds were incubated in growth medium overnight to allow for further cell attachment. On the following day, denoted as day 0, the acrylic inserts containing cellularized scaffolds were placed into the perfusion bioreactor chambers. An acrylic block containing 6 perfusion chambers with scaffolds was then connected to medium reservoirs (one reservoir per experimental group), peristaltic pump (Cole Parmer, Vernon Hills, IL) and a flow meter as previously described (Figure 4.1a) [100, 184]. Pinch valves were used to regulate flow rate and a programmable microprocessor-driven actuator was used

to create pulses, square wave flow patterns of varying frequencies (0.083, 0.050, and 0.018 Hz, Figure 4.1b).

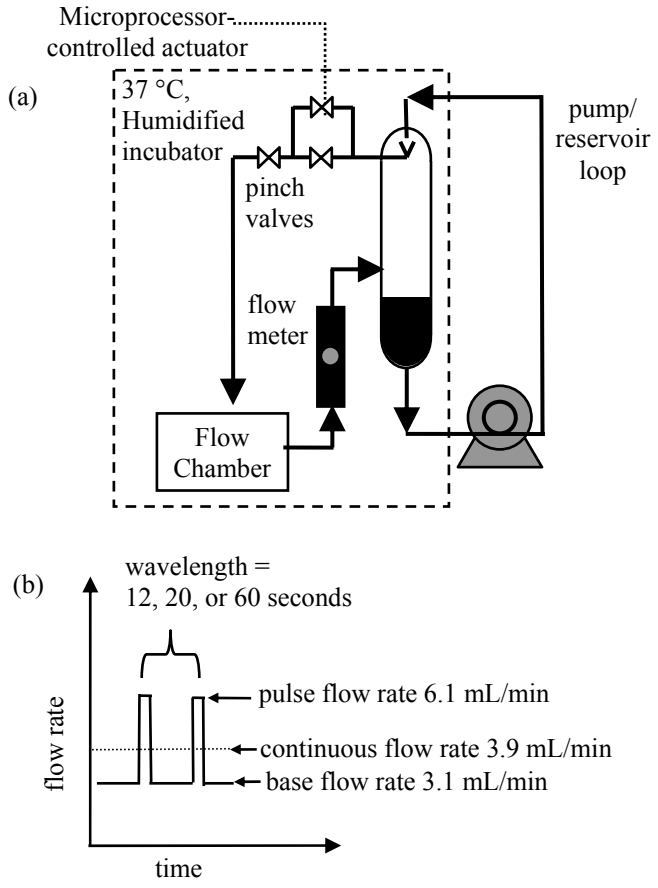

Figure 4.1: (a) Schematic of perfusion flow system, and (b) pulsatile flow pattern.

The base flow rate was 3.1 mL/min and periods of high flow rate, 6.1 mL/min, were superimposed on top of the base flow to create the pulsatile flow patterns. The continuous flow experimental group (no pulses) was maintained at a flow rate of 3.9 mL/min so that the time average flow rate of all experimental conditions was the same. Static controls were prepared identically but maintained in 12 well culture plates with 2 mL of medium per well.

Growth medium was replaced with osteogenic differentiation medium (growth medium supplemented with 25mM HEPES, 2 mM β-glycerophosphate, 0.13 mM ascorbate-2-phosphate and 10nM dexamethasone). The total volume of osteoblastic differentiation

medium in the flow system was 60 mL and half of this volume was changed every 3 days. The bioreactor was operated within a 5% CO_2 incubator at 37°C. Samples of conditioned media were collected at the time of each media change. Scaffolds were collected for analysis after 15 days of perfusion. The scaffolds were removed from the flow system, rinsed twice with PBS, cut into quarters and weighed. To facilitate the extraction of cellular materials, the scaffolds were frozen in liquid nitrogen before being crushed in the appropriate collection buffer for analysis of cell number, ALP activity, and osteoblastic gene expression.

4.3.5 Cell number

Cell number was determined at day 15 using PicoGreen reagent (Invitrogen). One quarter of each sample was crushed and collected in 300 µL digestion buffer containing proteinase K. The DNA was isolated and recovered using a phenol chloroform extraction process and the DNA was resuspended 0.5 mL TE buffer (10 mM Tris-HCl, 1 mM EDTA, pH 7.5). DNA standards of 0.016 to 1 µg/mL were prepared in TE buffer according to manufacturer's instructions. A volume of 100 µL of samples and standards were added to a 96-well plate in duplicate. PicoGreen reagent was diluted 1:200 in TE buffer and then 100 µL of the diluted PicoGreen reagent was added to each well. Fluorescence was measured with a SpectraMax fluorescent plate reader (Molecular Devices, Sunnyvale, CA) using excitation and emission frequencies of 488 and 525 nm, respectively, and a linear standard curve was plotted correlating fluorescence to µg/mL DNA. Cell number was calculated from the standard curve using a constant of 8.1 pg DNA/cell and normalized by the mass of the scaffold. This constant was experimentally determined with a series of BMSC suspensions with known concentrations.

4.3.6 ALP activity

After 15 days of flow, ALP activity was determined using a commercially available kit (Biotron Diagnostics, Hemet, CA). Scaffold quarters for analysis of ALP activity were homogenized in 500 µL TGT solution (50 mM Trizma HCL, 100 mM glycine, 0.1 % Triton X100, pH 10.5) containing 1% protease inhibitors (aprotinin, bestatin, leupeptin, E-64, and

pepstatin A). A volume of 100 μL of homogenized sample was combined with 500 μL ALP reagent and incubated at 37°C for 15 minutes as previously described [137]. After 15 minutes the reaction was stopped with 500 μL of 0.3 M NaOH and the absorbance of the reaction mixture was measured at 405 nm using a Spectronic Genesys 5 spectrophotometer (Spectronic Analytical Instruments, Leeds, UK). Enzyme activity, defined as the rate of conversion of *p*-nitrophenol phosphate to *p*-nitrophenol, was calculated and normalized by the mass of the scaffold and then by cell number to yield activity per cell.

4.3.7 mRNA expression

Expression of mRNA for osteopontin and osteocalcin was determined after 15 days of flow by quantitative RT-PCR as described previously [170]. Briefly, RNA was isolated from the samples using the RNeasy mini kit (Qiagen, Valencia, CA) according to manufacturer's instructions. Next, 200 ng or 9 μL of isolated RNA was reverse transcribed to cDNA using the Superscript kit (Invitrogen) and random hexamers as primers. Quantitative RT-PCR was performed using an ABI 7300 sequence detection system (Applied Biosciences, Foster, CA), SYBR green master mix (Applied Biosciences), and specific primers for β-actin (βA), OPN, and OC (Integrated Technologies, Coralville, IA) [135]. The $2^{-\Delta\Delta Ct}$ method was used to quantify the gene expression of OPN and OC using βA as the internal reference [138].

4.3.8 OPN and PGE_2 content

Accumulation of OPN protein and prostaglandin E_2 (PGE_2) in conditioned medium was determined at the time of each media change by enzyme immunometric assay (EIA) kits (Assay Designs, Ann Arbor, MI) according to the manufacturer's instructions. The OPN ELISA kit is a "sandwich" assay; it uses a polyclonal antibody immobilized on a plate to bind the OPN. The PGE_2 ELISA kit is a competitive immunoassay that uses a monoclonal antibody to bind the PGE_2 in samples of conditioned medium. Absorption at a wavelength 450 nm and 405 nm for the OPN and PGE_2 ELISAs respectively, was measured with a Labsystems Multiskan RC ELISA plate reader (Labsystems, Frankfurt, Germany). OPN and

PGE2 protein content was calculated from curves generated using the standards provided with the kits.

4.3.9 Statistics

Data were analyzed using a student's paired t-test and a 95% confidence criterion to test for differences between polymer groups. All data is presented as mean ± standard error of the mean (SEM). An asterisk denotes a statistically significant difference between a flow condition and the no flow control while a pound sign indicates a statistically significant difference between a pulsatile flow condition and the continuous flow control.

4.4 Results

The primary goal of this study was to determine the effect of pulsatile perfusion compared to continuous perfusion on the proliferation and osteoblastic differentiation of BMSCs. A secondary goal of this study was to determine if the response of the BMSCs to pulsatile flow was modulated by the frequency of pulsatile flow. To accomplish these goals, frequencies of 0.017, 0.050, and 0.083 Hz were tested and the continuous flow control was set to the time-average flow rate so that any effect of shear stress magnitude would be equalized. A set of scaffolds were also maintained under static conditions to provide a no-flow control.

To determine the effect of pulsatile flow on the proliferation of BMSCs, cell number was calculated from the total DNA quantified in each scaffold after 15 days of culture. Based on estimates of void volume, the initial seeding density of these scaffolds was approximately 600,000 cells per scaffold. However, since the figure represents the combination of three individual experiments, the data is normalized the no flow control of the respective experiment. Figure 4.2 indicates that cell number was reduced in all pulsatile flow conditions compared to the no flow control.

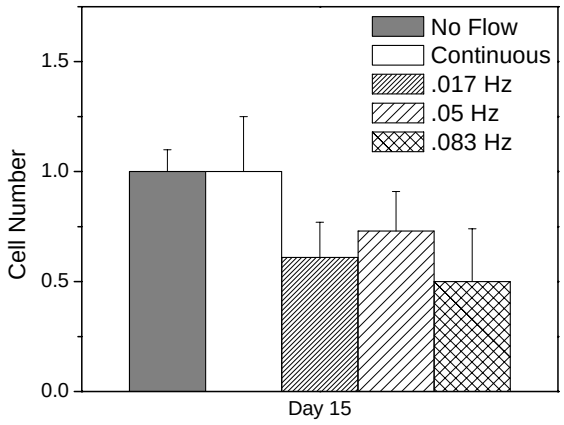

Figure 4.2: Cell number in porous PLGA foams at 15 days, normalized to the no flow control. Data are mean ± SEM for n = 6 to 9 samples.

The effect of pulsatile flow on the osteoblastic differentiation of BMSCs was determined by analyzing ALP activity and gene expression. ALP activity at day 15 was calculated on a per cell basis and then normalized to the no flow control of the respective individual experiment. Analysis revealed that all flow conditions enhance ALP activity over the no flow control. The middle frequency pulsatile flow conditions, 0.050 Hz, also enhanced ALP activity over the continuous flow control (Figure 4.3).

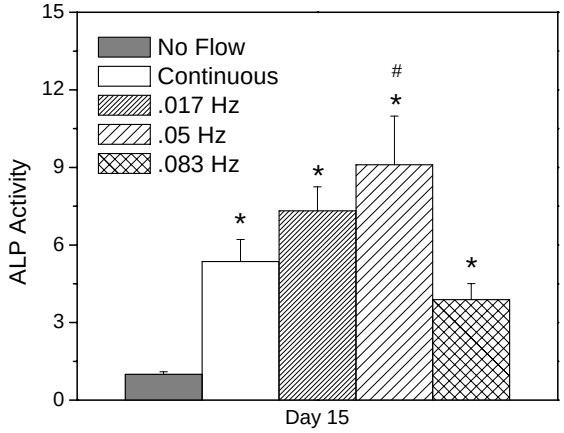

Figure 4.3: ALP activity per cell of BMSCs seeded in PLGA scaffolds at day 15, normalized to the no flow control. Data are mean ± SEM for n = 6 to 9 samples. An asterisk denotes a significant difference from the no flow control while a pound sign denotes a significant different with respect to the continuous flow control ($p<0.05$).

Analysis of OPN and OC gene expression by quantitative RT-PCR indicates that all flow conditions significantly upregulated OPN expression compared to the no flow control (Figure 4.4a). Similar to ALP activity, OPN expression is most enhanced with the 0.05 Hz pulsatile condition. However, OC expression appeared to be down-regulated for all flow conditions compared to the no flow control (Figure 4.4b), and no statistically significant difference exists between any of the experimental conditions.

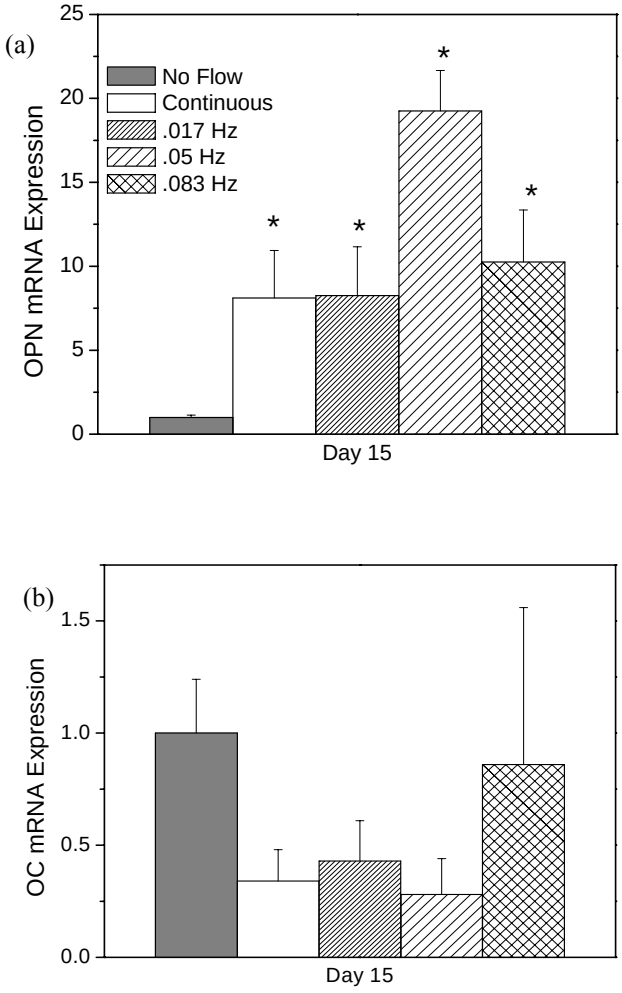

Figure 4.4: (a) OPN mRNA expression and (b) OC mRNA expression of BMSCs in PLGA foams at 15 days. βA was used as the housekeeping gene and data are normalized to the no flow control. Data are mean ± SEM for n = 6 to 9 samples. An asterisk denotes a significant difference with respect to the no flow control.

PGE_2 production was measured with samples of conditioned media collected at the time of each media change. PGE_2 (Figure 4.5) increased in all groups and leveled out after approximately 6 days. All flow conditions were elevated over the no flow control and the slowest frequency pulsatile flow condition had the highest overall PGE_2 production. The differences between the flow conditions and the no flow control were significant at every time point.

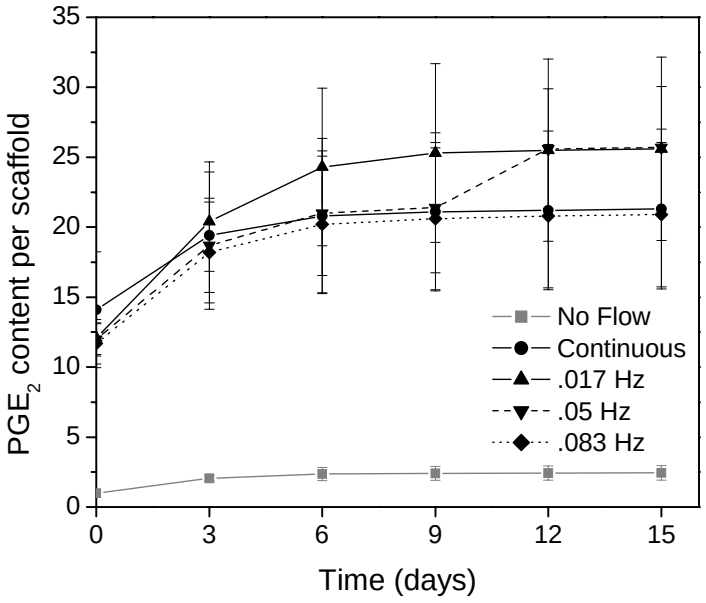

Figure 4.5: PGE_2 concentration per scaffold at 0, 3, 6, 9, 12, and 15 days. Data are normalized by the no flow control at day 0 and plotted as mean ± SEM for n = 3 experiments.

Finally, samples of conditioned media were collected from the flow system and statically cultured constructs at the time of each media change were analyzed for the accumulation of OPN protein over time by ELISA (Figure 4.6). OPN protein accumulation increased most quickly in the two pulsatile flow conditions with highest frequency, 0.050 and 0.083 Hz. All flow regimens significantly enhanced the synthesis of OPN protein over the no flow control at every time point except day 0. Additionally, at day 3 the OPN accumulation was statistically higher in the 0.05 Hz pulsatile flow condition over the continuous flow control. This result suggests that BMSCs differentiate a more quickly when

exposed to the 0.05 Hz frequency flow condition compared to continuous flow. By 15 days the level of OPN protein accumulation mirrors that of mRNA expression, with the 0.05 Hz and 0.083 Hz frequency conditions resulting in the most OPN accumulation.

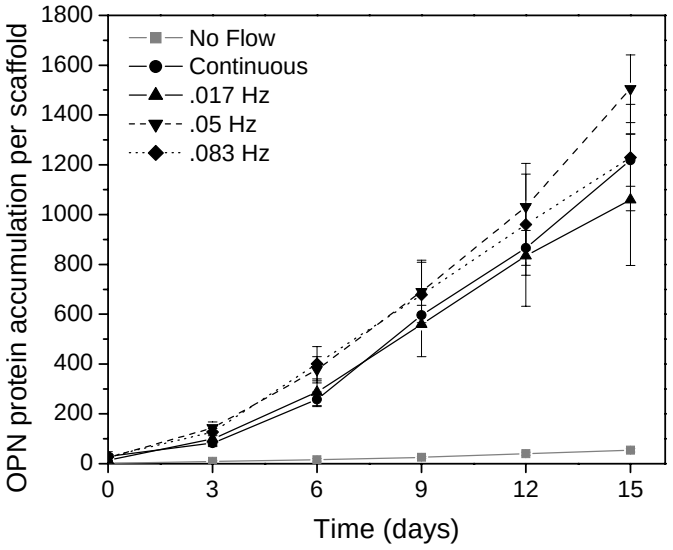

Figure 4.6: OPN protein accumulation per scaffold at 0, 3, 6, 9, 12, and 15 days. Data are normalized by the no flow control at day 0 and plotted as mean ± SEM for n = 3 experiments.

4.5 Discussion

Perfusion bioreactors are widely acknowledged to aid in maintenance of cell viability and to enhance the formation of bone-like extracellular matrix in large scaffolds; however, previous studies have been limited to continuous flow regimens. Recent work involving dynamic flow regimens shows that dynamic flow regimens may be more effective at eliciting a cellular response than continuous flow regimens; however these studies have all been performed in planar culture. The overall goal of this study was twofold: to determine if pulsatile flow enhances the proliferation and differentiation of BMSCs compared to continuous perfusion, and how these responses are modulated by frequency in 3D culture.

BMSCs were cultured in PLGA porous foam scaffolds under static conditions, continuous perfusion, or pulsatile flow with frequencies of 0.017, 0.050, or 0.083 Hz. After 15 days the scaffolds were collected and analyzed for cell number, ALP activity, and mRNA

expression of the non-collagenous bone matrix proteins OPN and OC. While pulsatile flow surpressed BMSC proliferation, the highest frequency pulsatile conditions had a significant stimulatory effect on markers of osteoblastic differentiation including ALP activity and OPN mRNA expression. Conditioned media, taken at the time of each media change and analyzed for OPN protein accumulation, was also shown to contain increased amounts of OPN protein in the highest frequency pulsatile flow conditions. This is in contrast to the synthesis of PGE_2 which was highest with the no flow and lowest frequency pulsatile flow conditions.

Cell number was shown to be reduced with the application of pulsatile flow and it is possible that the cells are detaching under these flow conditions. It has been previously theorized that cells detach under flow conditions, causing a systematic decrease in cell number with increasing duration of flow [135, 185]. Additionally, cell number has been shown to be lower with dynamic flow conditions compared to both steady flow and static conditions [186]. The low cell numbers under pulsatile flow conditions observed both in this experiment and in previously published works could perhaps be due to areas of instability in the flow field where recirculation or separation of flow occurs.

Our data is consistent with previously published studies showing that markers of osteogenic differentiation such as ALP activity, OPN expression, and synthesis of OPN protein are enhanced by perfusion flow over no flow controls [106, 107, 187, 188]. Unfortunately, we saw no trends in the expression of osteogenic markers with respect to frequency. This is in contrast to previously published studies in 2D model systems increases in calcium transients as frequency decreased and increases in PGE_2 production as frequency increased [110, 117, 118]. Future work in this area will investigate a larger range of frequencies.

Several bone related growth factors associated with bone formation and healing *in vivo* – such as transforming growth factor-β1 (TGF-β1), fibroblast growth factor-2 (FGF-2), VEGF and BMP-2 – have recently been enhanced *in vitro* by continuous perfusion flow [61]. We hypothesize that enhanced osteogenic differentiation observed in this study may be a consequence of increased deposition of BMPs and VEGF because flow also stimulates deposition of these bioactive factors. Further, VEGF-A was found to be significantly

enhanced in response to dynamic flow in planar culture [182]. Therefore, we plan to investigate the effect of dynamic flow strategies on the deposition of these bioactive factors.

4.6 Conclusions

Overall, this research shows that osteogenic differentiation is enhanced by both steady and pulsed perfusion flow. However, cell proliferation is unaffected by steady flow but inhibited by pulsed flow. ALP activity and OPN content appear specifically enhanced by pulsed flow over continuous flow which indicates that dynamic perfusion may be a useful component of the engineered bone tissue strategy and warrants further investigation. Future investigations will involve a larger range of frequencies and will also measure levels of bioactive factors such as BMPs and VEGF, growth factors shown to be enhanced by fluid shear stress and stimulate healing of bone defects *in vivo*.

Chapter 5: Conclusions and future work

5.1 Conclusions

The overall goal of this work was to investigate the effect of mechanical environment on the osteoblastic differentiation of bone marrow stromal cells for bone tissue engineering applications. Two studies were conducted to investigate the effect of scaffold compliance on the osteoblastic differentiation of BMSCs. In the first study a family of segmented poly(esterurethane urea)s were synthesized from 1,4-diisocyanatobutane, a poly(ε-caprolactone) soft segment, and a TyA.BDI.TyA chain extender. Segmented polyurethanes make an attractive system for studying the effect of biomaterial modulus because they have tunable mechanical properties. By systematically increasing the PCL molecular weight from 1100 kDa to 2700 kDa, the melting temperature of the materials increased from 21 to 61°C, the storage modulus increased from 52 to 278 MPa, and the crystallinity of the materials increased. In Chapter 2 the PEUURs were spun onto glass coverslips and seeded with BMSCs to see if there were any effects of varying chemistry on osteoblastic differentiation. Cell density, ALP activity, and OPN and OC gene expression were similar on all the surfaces indicating that variations in surface chemistry did not impact the osteoblastic differentiation of BMSCs to any appreciable degree. This study demonstrated that the PEUURs were biocompatible and suitable for isolating the effect of scaffold modulus.

The second study (Chapter 3) involved fabricating the PEUURs into porous foam scaffolds via a compression molding/particulate leaching technique. The scaffolds were analyzed for compressive modulus and crystallinity. As PCL content increased, the scaffold modulus increased from 0.18 to 0.80 MPa and the degree of crystallinity increased from 16 to 45%. PEUUR scaffolds were seeded with BMSCs and compared to PLGA scaffolds which are stiffer but amorphous. Cell number decreased as PCL increased, while PGE_2 and ALP activity were significantly increased on only the PCL 2700 material. Additionally, OPN and VEGF-A gene expression showed similar trends to ALP activity. However, OC and BMP-2 gene expression levels were higher at day 14 on the softer substrates suggesting that BMSCs differentiate faster on softer materials. Differences due to surface chemistry

were effectively eliminated with our experiment seeding BMSCs on 2D PEUUR films. However, while the effects of surface chemistry and topography can be varied independently in theory; in practice the separation is difficult to achieve. The differences between the PCL 2700 material and the other two PEUUR materials are likely due to differences in crystallinity and nano-scale topographical features rather than modulus.

The third study (Chapter 4) focused on the effect of dynamic fluid flow as an osteogenic stimulus. A microprocessor-drive actuator was incorporated into the perfusion flow system and programmed to deliver pulsatile flow at 3 different frequencies: 0.083 Hz, 0.05 Hz, and 0.017 Hz. The pulsatile flow conditions were compared to a continuous flow control and a no flow control. All three pulsatile flow conditions resulted in lower (but not statistically significant) cell densities. All flow conditions stimulated ALP activity, OPN gene expression, and OPN protein accumulation above the no flow control. Additionally, the middle frequency pulsatile flow conditions, 0.05 Hz, enhanced ALP activity above even the continuous flow control. This study confirmed that dynamic flow stimulates expression of osteoblastic differentiation and demonstrated that dynamic flow may be an attractive means to further enhance osteoblastic differentiation *in vitro* over continuous perfusion.

5.2 Future work

The overall goal of this work is to produce an engineered tissue capable of stimulating healing *in vivo*. Natural extensions of the work presented in Chapter 4 would involve 1) analysis of important growth factors, such as bone morphogenic proteins, in response to dynamic perfusion strategies; 2) utilization of a broader range of pulse frequencies closer to physiological range; and 3) investigation of the effect of pulse magnitude once an optimal pulse frequency has been determined.

The third study of this dissertation (Chapter 4) was designed to investigate the effect of low frequencies of pulsatile flow on the osteoblastic differentiation of BMSCs and it successfully demonstrated that pulsatile flow enhances some markers of osteoblastic differentiation over continuous flow. However, the third study does not incorporate analysis of other important markers like bone morphogenic proteins (i.e. BMP-2, 4, and 7) that might

enhance the healing of bone defects *in vivo* better than a scaffold containing a more mature osteogenic ECM. The first future study will be a time course experiment to determine the optimal time point for evaluation evaluate the level of BMPs and other beneficial growth factors such as VEGF-A. These experiments are already underway and preliminary data (Figure 5.1) show that early time points (<7 days) or late time pints (>17 days) are optimal for examining the expression of BMP-2 and VEGF-A as they are up-regulated.

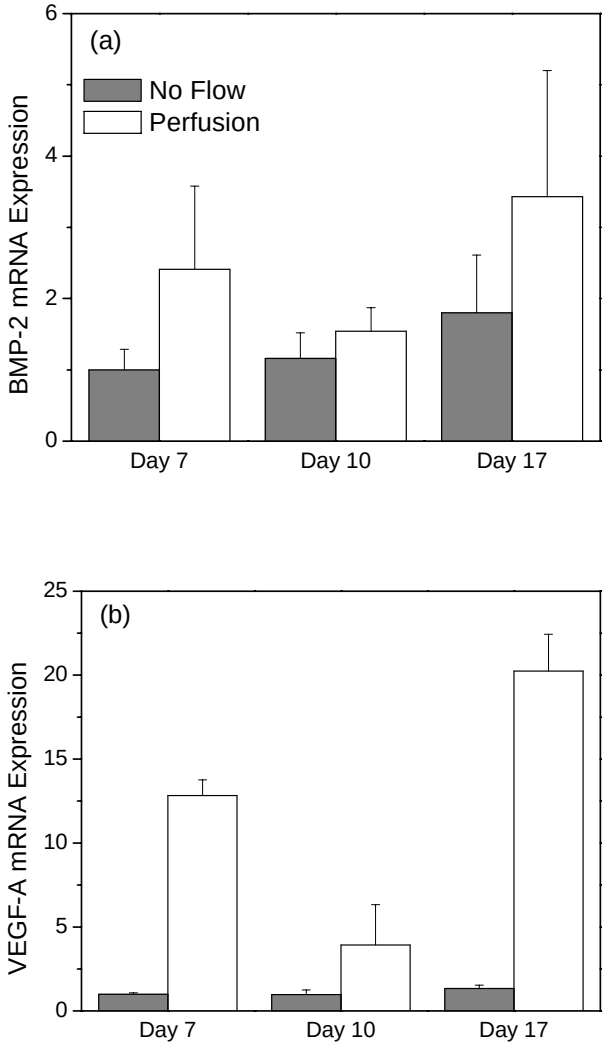

Figure 5.1: Analysis of (a) BMP-2 mRNA expression and (b) VEGF-A mRNA expression during a time course study of continuous flow versus no flow. Data mean ± SEM for n = 3 samples.

The goal of the second future study proposed will be further investigate the effect of frequency of pulsatile flow using a broader range of frequencies that are more physiologically relevant, 0.50 Hz to 2 Hz. Previous studies in planar culture suggest that lower frequencies are more beneficial to bone development because they are more effective at inducing calcium transients. However, this pattern might not be repeated with 3D perfusion flow and so these frequencies should be repeated with cells seeded in a scaffold architecture. Initial results of a 0.5 Hz frequency oscillation (Figure 5.2) show that oscillatory flow at a frequency of 0.5 Hz induces not only OPN gene expression but that of BMP-2 as well.

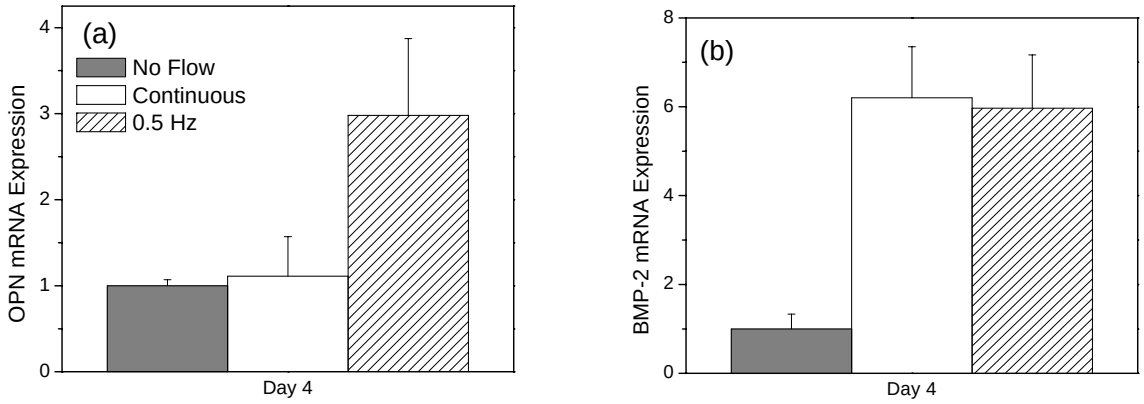

Figure 5.2: Analysis of (a) OPN gene expression and (b) BMP-2 gene expression after 4 days of perfusion flow. Data are mean ± SEM for n = 3 samples.

The third proposed study would evaluate the magnitude of pulses required to stimulate osteoblastic differentiation or an increase in growth factors. The effect of shear stress magnitude has been under debate as conflicting data has been reported. Sikavitsas and colleagues decoupled the main two effects of perfusion flow (increased chemotransport and applied shear stress) by systematically varying the viscosity of the culture medium at a constant flow rate [108]. By changing the viscosity of the medium, Sikavitsas *et al.* were able to change the magnitude of shear stress without significantly affecting convective mass transport rates. Their results indicated that matrix mineralization, but not ALP activity, is sensitive to shear stress magnitude [108]. However, another study found that while ALP

activity and OPN are sensitive to perfusion flow, they are insensitive to flow rate indicating that shear stress magnitude had no effect on osteoblastic differentiation [181].

Ultimately scaffolds seeded with BMSCs and cultured under optimal conditions (duration of flow, pulse frequency, and pulse magnitude) can be tested for healing critical sized bone defects in an animal model. BMSCs can be seeded foam scaffolds, cultured in the perfusion bioreactor, and then implanted into a rat critical sized femoral defect (>6mm). The amount of bone growth in the defect site can be quantified throughout the healing process by μCT. After the animals are sacrificed, the implants can be collected and analyzed to quantitatively determine the extent of new bone growth and vascularization within the defect.

References

[1] T. Neighbour, "The Global Orthobiologics Market: Players, products and technologies driving change," Espicom Business Intelligence 2008.

[2] I. Taylor, "Orthopaedic Market Report 2008," Espicom Business Intelligence 2007.

[3] P. V. Giannoudis, H. Dinopoulos, and E. Tsiridis, "Bone substitutes: an update," *Injury,* vol. 36 Suppl 3, pp. S20-7, Nov 2005.

[4] W. R. Moore, S. E. Graves, and G. I. Bain, "Synthetic bone graft substitutes," *ANZ J Surg,* vol. 71, pp. 354-61, Jun 2001.

[5] V. I. Sikavitsas, J. S. Temenoff, and A. G. Mikos, "Biomaterials and bone mechanotransduction," *Biomaterials,* vol. 22, pp. 2581-93, Oct 2001.

[6] A. S. Greenwald, S. D. Boden, V. M. Goldberg, Y. Khan, C. T. Laurencin, and R. N. Rosier, "Bone-graft substitutes: facts, fictions, and applications," *J Bone Joint Surg Am,* vol. 83-A Suppl 2 Pt 2, pp. 98-103, 2001.

[7] H. Burchardt, "The biology of bone graft repair," *Clin Orthop Relat Res,* pp. 28-42, Apr 1983.

[8] W. F. Enneking, J. L. Eady, and H. Burchardt, "Autogenous cortical bone grafts in the reconstruction of segmental skeletal defects," *J Bone Joint Surg Am,* vol. 62, pp. 1039-58, Oct 1980.

[9] J. L. Young, A. Fritz, G. Liu, K. Thoburn, J. Kres, and S. Roffers, 2000.

[10] H. L. Holtorf, J. A. Jansen, and A. G. Mikos, "Modulation of cell differentiation in bone tissue engineering constructs cultured in a bioreactor," *Adv Exp Med Biol,* vol. 585, pp. 225-41, 2006.

[11] J. P. Bilezikian, L. G. Raisz, and G. A. Rodan, *Principles of bone biology*, 2nd ed. San Diego: Academic Press, 2002.

[12] F. Bronner and M. Farach-Carson, *Bone formation*. London ; New York: Springer, 2004.

[13] A. Scott, K. M. Khan, V. Duronio, and D. A. Hart, "Mechanotransduction in human bone: in vitro cellular physiology that underpins bone changes with exercise," *Sports Med,* vol. 38, pp. 139-60, 2008.

[14] J. Rubin, C. Rubin, and C. R. Jacobs, "Molecular pathways mediating mechanical signaling in bone," *Gene,* vol. 367, pp. 1-16, Feb 15 2006.

[15] N. X. Chen, K. D. Ryder, F. M. Pavalko, C. H. Turner, D. B. Burr, J. Qiu, and R. L. Duncan, "Ca(2+) regulates fluid shear-induced cytoskeletal reorganization and gene expression in osteoblasts," *Am J Physiol Cell Physiol,* vol. 278, pp. C989-97, May 2000.

[16] J. You, G. C. Reilly, X. Zhen, C. E. Yellowley, Q. Chen, H. J. Donahue, and C. R. Jacobs, "Osteopontin gene regulation by oscillatory fluid flow via intracellular calcium mobilization and activation of mitogen-activated protein kinase in MC3T3-E1 osteoblasts," *J Biol Chem,* vol. 276, pp. 13365-71, Apr 20 2001.

[17] H. Pommerenke, C. Schmidt, F. Durr, B. Nebe, F. Luthen, P. Muller, and J. Rychly, "The mode of mechanical integrin stressing controls intracellular signaling in osteoblasts," *J Bone Miner Res,* vol. 17, pp. 603-11, Apr 2002.

[18] H. B. Wang, M. Dembo, S. K. Hanks, and Y. Wang, "Focal adhesion kinase is involved in mechanosensing during fibroblast migration," *Proc Natl Acad Sci U S A,* vol. 98, pp. 11295-300, Sep 25 2001.
[19] D. E. Discher, P. Janmey, and Y. L. Wang, "Tissue cells feel and respond to the stiffness of their substrate," *Science,* vol. 310, pp. 1139-43, Nov 18 2005.
[20] A. D. Bakker, K. Soejima, J. Klein-Nulend, and E. H. Burger, "The production of nitric oxide and prostaglandin E(2) by primary bone cells is shear stress dependent," *J Biomech,* vol. 34, pp. 671-7, May 2001.
[21] T. N. McAllister and J. A. Frangos, "Steady and transient fluid shear stress stimulate NO release in osteoblasts through distinct biochemical pathways," *J Bone Miner Res,* vol. 14, pp. 930-6, Jun 1999.
[22] J. Klein-Nulend, E. H. Burger, C. M. Semeins, L. G. Raisz, and C. C. Pilbeam, "Pulsating fluid flow stimulates prostaglandin release and inducible prostaglandin G/H synthase mRNA expression in primary mouse bone cells," *J Bone Miner Res,* vol. 12, pp. 45-51, Jan 1997.
[23] S. Wadhwa, S. L. Godwin, D. R. Peterson, M. A. Epstein, L. G. Raisz, and C. C. Pilbeam, "Fluid flow induction of cyclo-oxygenase 2 gene expression in osteoblasts is dependent on an extracellular signal-regulated kinase signaling pathway," *J Bone Miner Res,* vol. 17, pp. 266-74, Feb 2002.
[24] H. Fujino, W. Xu, and J. W. Regan, "Prostaglandin E2 induced functional expression of early growth response factor-1 by EP4, but not EP2, prostanoid receptors via the phosphatidylinositol 3-kinase and extracellular signal-regulated kinases," *J Biol Chem,* vol. 278, pp. 12151-6, Apr 4 2003.
[25] S. Katz, R. Boland, and G. Santillan, "Modulation of ERK 1/2 and p38 MAPK signaling pathways by ATP in osteoblasts: involvement of mechanical stress-activated calcium influx, PKC and Src activation," *Int J Biochem Cell Biol,* vol. 38, pp. 2082-91, 2006.
[26] C. Granet, A. G. Vico, C. Alexandre, and M. H. Lafage-Proust, "MAP and src kinases control the induction of AP-1 members in response to changes in mechanical environment in osteoblastic cells," *Cell Signal,* vol. 14, pp. 679-88, Aug 2002.
[27] C. C. Wu, Y. S. Li, J. H. Haga, N. Wang, I. Y. Lian, F. C. Su, S. Usami, and S. Chien, "Roles of MAP kinases in the regulation of bone matrix gene expressions in human osteoblasts by oscillatory fluid flow," *J Cell Biochem,* vol. 98, pp. 632-41, Jun 1 2006.
[28] E. A. Cowles, L. L. Brailey, and G. A. Gronowicz, "Integrin-mediated signaling regulates AP-1 transcription factors and proliferation in osteoblasts," *J Biomed Mater Res,* vol. 52, pp. 725-37, Dec 15 2000.
[29] R. Langer and J. P. Vacanti, "Tissue engineering," *Science,* vol. 260, pp. 920-6, May 14 1993.
[30] G. M. Crane, S. L. Ishaug, and A. G. Mikos, "Bone tissue engineering," *Nat Med,* vol. 1, pp. 1322-4, Dec 1995.
[31] J. R. Mauney, C. Jaquiery, V. Volloch, M. Heberer, I. Martin, and D. L. Kaplan, "In vitro and in vivo evaluation of differentially demineralized cancellous bone scaffolds

combined with human bone marrow stromal cells for tissue engineering," *Biomaterials,* vol. 26, pp. 3173-85, Jun 2005.
[32] H. Hosseinkhani, M. Yamamoto, Y. Inatsugu, Y. Hiraoka, S. Inoue, H. Shimokawa, and Y. Tabata, "Enhanced ectopic bone formation using a combination of plasmid DNA impregnation into 3-D scaffold and bioreactor perfusion culture," *Biomaterials,* vol. 27, pp. 1387-98, Mar 2006.
[33] U. Meyer and H. P. Wiesmann, *Bone and cartilage engineering*. Berlin ; New York: Springer, 2006.
[34] S. P. Bruder and B. S. Fox, "Tissue engineering of bone. Cell based strategies," *Clin Orthop Relat Res,* pp. S68-83, Oct 1999.
[35] H. Declercq, N. Van den Vreken, E. De Maeyer, R. Verbeeck, E. Schacht, L. De Ridder, and M. Cornelissen, "Isolation, proliferation and differentiation of osteoblastic cells to study cell/biomaterial interactions: comparison of different isolation techniques and source," *Biomaterials,* vol. 25, pp. 757-68, Feb 2004.
[36] S. A. Kuznetsov, M. H. Mankani, S. Gronthos, K. Satomura, P. Bianco, and P. G. Robey, "Circulating skeletal stem cells," *J Cell Biol,* vol. 153, pp. 1133-40, May 28 2001.
[37] Y. A. Romanov, V. A. Svintsitskaya, and V. N. Smirnov, "Searching for alternative sources of postnatal human mesenchymal stem cells: candidate MSC-like cells from umbilical cord," *Stem Cells,* vol. 21, pp. 105-10, 2003.
[38] K. Igura, X. Zhang, K. Takahashi, A. Mitsuru, S. Yamaguchi, and T. A. Takashi, "Isolation and characterization of mesenchymal progenitor cells from chorionic villi of human placenta," *Cytotherapy,* vol. 6, pp. 543-53, 2004.
[39] M. S. Tsai, J. L. Lee, Y. J. Chang, and S. M. Hwang, "Isolation of human multipotent mesenchymal stem cells from second-trimester amniotic fluid using a novel two-stage culture protocol," *Hum Reprod,* vol. 19, pp. 1450-6, Jun 2004.
[40] H. E. Young, M. L. Mancini, R. P. Wright, J. C. Smith, A. C. Black, Jr., C. R. Reagan, and P. A. Lucas, "Mesenchymal stem cells reside within the connective tissues of many organs," *Dev Dyn,* vol. 202, pp. 137-44, Feb 1995.
[41] P. A. Zuk, M. Zhu, H. Mizuno, J. Huang, J. W. Futrell, A. J. Katz, P. Benhaim, H. P. Lorenz, and M. H. Hedrick, "Multilineage cells from human adipose tissue: implications for cell-based therapies," *Tissue Eng,* vol. 7, pp. 211-28, Apr 2001.
[42] P. Bianco, M. Riminucci, S. Gronthos, and P. G. Robey, "Bone marrow stromal stem cells: nature, biology, and potential applications," *Stem Cells,* vol. 19, pp. 180-92, 2001.
[43] S. P. Bruder, D. J. Fink, and A. I. Caplan, "Mesenchymal stem cells in bone development, bone repair, and skeletal regeneration therapy," *J Cell Biochem,* vol. 56, pp. 283-94, Nov 1994.
[44] P. H. Krebsbach, S. A. Kuznetsov, P. Bianco, and P. G. Robey, "Bone marrow stromal cells: characterization and clinical application," *Crit Rev Oral Biol Med,* vol. 10, pp. 165-81, 1999.
[45] A. J. Friedenstein, S. Piatetzky, II, and K. V. Petrakova, "Osteogenesis in transplants of bone marrow cells," *J Embryol Exp Morphol,* vol. 16, pp. 381-90, Dec 1966.

[46] N. Jaiswal, S. E. Haynesworth, A. I. Caplan, and S. P. Bruder, "Osteogenic differentiation of purified, culture-expanded human mesenchymal stem cells in vitro," *J Cell Biochem,* vol. 64, pp. 295-312, Feb 1997.
[47] B. Johnstone, T. M. Hering, A. I. Caplan, V. M. Goldberg, and J. U. Yoo, "In vitro chondrogenesis of bone marrow-derived mesenchymal progenitor cells," *Exp Cell Res,* vol. 238, pp. 265-72, Jan 10 1998.
[48] M. K. Majumdar, M. A. Thiede, J. D. Mosca, M. Moorman, and S. L. Gerson, "Phenotypic and functional comparison of cultures of marrow-derived mesenchymal stem cells (MSCs) and stromal cells," *J Cell Physiol,* vol. 176, pp. 57-66, Jul 1998.
[49] M. F. Pittenger, A. M. Mackay, S. C. Beck, R. K. Jaiswal, R. Douglas, J. D. Mosca, M. A. Moorman, D. W. Simonetti, S. Craig, and D. R. Marshak, "Multilineage potential of adult human mesenchymal stem cells," *Science,* vol. 284, pp. 143-7, Apr 2 1999.
[50] S. A. Kuznetsov, P. H. Krebsbach, K. Satomura, J. Kerr, M. Riminucci, D. Benayahu, and P. G. Robey, "Single-colony derived strains of human marrow stromal fibroblasts form bone after transplantation in vivo," *J Bone Miner Res,* vol. 12, pp. 1335-47, Sep 1997.
[51] J. B. Lian and G. S. Stein, "Concepts of osteoblast growth and differentiation: basis for modulation of bone cell development and tissue formation," *Crit Rev Oral Biol Med,* vol. 3, pp. 269-305, 1992.
[52] H. Siggelkow, K. Rebenstorff, W. Kurre, C. Niedhart, I. Engel, H. Schulz, M. J. Atkinson, and M. Hufner, "Development of the osteoblast phenotype in primary human osteoblasts in culture: comparison with rat calvarial cells in osteoblast differentiation," *J Cell Biochem,* vol. 75, pp. 22-35, Oct 1 1999.
[53] S. P. Bruder, N. Jaiswal, N. S. Ricalton, J. D. Mosca, K. H. Kraus, and S. Kadiyala, "Mesenchymal stem cells in osteobiology and applied bone regeneration," *Clin Orthop Relat Res,* pp. S247-56, Oct 1998.
[54] J. van den Dolder, G. N. Bancroft, V. I. Sikavitsas, P. H. Spauwen, J. A. Jansen, and A. G. Mikos, "Flow perfusion culture of marrow stromal osteoblasts in titanium fiber mesh," *J Biomed Mater Res A,* vol. 64, pp. 235-41, Feb 1 2003.
[55] N. Price, S. P. Bendall, C. Frondoza, R. H. Jinnah, and D. S. Hungerford, "Human osteoblast-like cells (MG63) proliferate on a bioactive glass surface," *Journal of Biomedical Materials Research,* vol. 37, pp. 394-400, Dec 5 1997.
[56] J. Toquet, R. Rohanizadeh, J. Guicheux, S. Couillard, N. Passuti, G. Daculsi, and D. Heymann, "Osteogenic potential in vitro of human bone marrow cells cultured on macroporous biphasic calcium phosphate ceramic," *Journal of Biomedical Materials Research,* vol. 44, pp. 98-108, Jan 1999.
[57] T. Yoshikawa, H. Ohgushi, and S. Tamai, "Immediate bone forming capability of prefabricated osteogenic hydroxyapatite," *Journal of Biomedical Materials Research,* vol. 32, pp. 481-492, Nov 1996.
[58] W. Bensaid, J. T. Triffitt, C. Blanchat, K. Oudina, L. Sedel, and H. Petite, "A biodegradable fibrin scaffold for mesenchymal stem cell transplantation," *Biomaterials,* vol. 24, pp. 2497-502, Jun 2003.

[59] J. George, Y. Kuboki, and T. Miyata, "Differentiation of mesenchymal stem cells into osteoblasts on honeycomb collagen scaffolds," *Biotechnol Bioeng,* vol. 95, pp. 404-11, Oct 20 2006.
[60] L. Meinel, O. Betz, R. Fajardo, S. Hofmann, A. Nazarian, E. Cory, M. Hilbe, J. McCool, R. Langer, G. Vunjak-Novakovic, H. P. Merkle, B. Rechenberg, D. L. Kaplan, and C. Kirker-Head, "Silk based biomaterials to heal critical sized femur defects," *Bone,* vol. 39, pp. 922-31, Oct 2006.
[61] M. E. Gomes, C. M. Bossano, C. M. Johnston, R. L. Reis, and A. G. Mikos, "In vitro localization of bone growth factors in constructs of biodegradable scaffolds seeded with marrow stromal cells and cultured in a flow perfusion bioreactor," *Tissue Eng,* vol. 12, pp. 177-88, Jan 2006.
[62] Z. Li, H. R. Ramay, K. D. Hauch, D. Xiao, and M. Zhang, "Chitosan-alginate hybrid scaffolds for bone tissue engineering," *Biomaterials,* vol. 26, pp. 3919-28, Jun 2005.
[63] G. Lisignoli, N. Zini, G. Remiddi, A. Piacentini, A. Puggioli, C. Trimarchi, M. Fini, N. M. Maraldi, and A. Facchini, "Basic fibroblast growth factor enhances in vitro mineralization of rat bone marrow stromal cells grown on non-woven hyaluronic acid based polymer scaffold," *Biomaterials,* vol. 22, pp. 2095-105, Aug 2001.
[64] J. C. Middleton and A. J. Tipton, "Synthetic biodegradable polymers as orthopedic devices," *Biomaterials,* vol. 21, pp. 2335-46, Dec 2000.
[65] G. Q. Chen and Q. Wu, "The application of polyhydroxyalkanoates as tissue engineering materials," *Biomaterials,* vol. 26, pp. 6565-78, Nov 2005.
[66] J. Zhang, B. A. Doll, E. J. Beckman, and J. O. Hollinger, "A biodegradable polyurethane-ascorbic acid scaffold for bone tissue engineering," *J Biomed Mater Res A,* vol. 67, pp. 389-400, Nov 1 2003.
[67] K. Rezwan, Q. Z. Chen, J. J. Blaker, and A. R. Boccaccini, "Biodegradable and bioactive porous polymer/inorganic composite scaffolds for bone tissue engineering," *Biomaterials,* vol. 27, pp. 3413-3431, Jun 2006.
[68] B. L. Seal, T. C. Otero, and A. Panitch, "Polymeric biomaterials for tissue and organ regeneration," *Materials Science & Engineering R-Reports,* vol. 34, pp. 147-230, Oct 10 2001.
[69] A. Burke and N. Hasirci, "Polyurethanes in biomedical applications," *Adv Exp Med Biol,* vol. 553, pp. 83-101, 2004.
[70] R. J. Zdrahala and I. J. Zdrahala, "Biomedical applications of polyurethanes: a review of past promises, present realities, and a vibrant future," *J Biomater Appl,* vol. 14, pp. 67-90, Jul 1999.
[71] N. M. K. Lamba, K. A. Woodhouse, S. L. Cooper, and M. D. Lelah, *Polyurethanes in biomedical applications*. Boca Raton: CRC Press, 1998.
[72] S. A. Guelcher, K. M. Gallagher, J. E. Didier, D. B. Klinedinst, J. S. Doctor, A. S. Goldstein, G. L. Wilkes, E. J. Beckman, and J. O. Hollinger, "Synthesis of biocompatible segmented polyurethanes from aliphatic diisocyanates and diurea diol chain extenders," *Acta Biomater,* vol. 1, pp. 471-84, Jul 2005.
[73] C. J. Spaans, J. H. De Groot, V. W. Belgraver, and A. J. Pennings, "A new biomedical polyurethane with a high modulus based on 1,4-butanediisocyanate and epsilon-caprolactone," *J Mater Sci Mater Med,* vol. 9, pp. 675-8, Dec 1998.

[74] D. J. Martin, G. F. Meijs, G. M. Renwick, P. A. Gunatillake, and S. J. McCarthy, "Effect of soft-segment CH2/O ratio on morphology and properties of a series of polyurethane elastomers," *Journal of Applied Polymer Science,* vol. 60, pp. 557-571, Apr 25 1996.
[75] D. J. Martin, G. F. Meijs, G. M. Renwick, S. J. McCarthy, and P. A. Gunatillake, "The effect of average soft segment length on morphology and properties of a series of polyurethane elastomers .1. Characterization of the series," *Journal of Applied Polymer Science,* vol. 62, pp. 1377-1386, Nov 28 1996.
[76] E. J. Woo, G. Farber, R. J. Farris, C. P. Lillya, and J. C. W. Chien, "Structure-Property Relationships in Thermoplastic Elastomers .1. Segmented Polyether-Polyurethanes," *Polymer Engineering and Science,* vol. 25, pp. 834-840, 1985.
[77] A. J. Engler, S. Sen, H. L. Sweeney, and D. E. Discher, "Matrix elasticity directs stem cell lineage specification," *Cell,* vol. 126, pp. 677-89, Aug 25 2006.
[78] C. B. Khatiwala, S. R. Peyton, M. Metzke, and A. J. Putnam, "The regulation of osteogenesis by ECM rigidity in MC3T3-E1 cells requires MAPK activation," *J Cell Physiol,* Mar 8 2007.
[79] C. B. Khatiwala, S. R. Peyton, and A. J. Putnam, "Intrinsic mechanical properties of the extracellular matrix affect the behavior of pre-osteoblastic MC3T3-E1 cells," *Am J Physiol Cell Physiol,* vol. 290, pp. C1640-50, Jun 2006.
[80] S. Taqvi and K. Roy, "Influence of scaffold physical properties and stromal cell coculture on hematopoietic differentiation of mouse embryonic stem cells," *Biomaterials,* vol. 27, pp. 6024-31, Dec 2006.
[81] T. W. Thomas and P. A. DiMilla, "Spreading and motility of human glioblastoma cells on sheets of silicone rubber depend on substratum compliance," *Med Biol Eng Comput,* vol. 38, pp. 360-70, May 2000.
[82] S. Even-Ram, V. Artym, and K. M. Yamada, "Matrix control of stem cell fate," *Cell,* vol. 126, pp. 645-7, Aug 25 2006.
[83] J. C. Zhang, H. Zhang, L. B. Wu, and J. D. Ding, "Fabrication of three dimensional polymeric scaffolds with spherical pores," *Journal of Materials Science,* vol. 41, pp. 1725-1731, Mar 2006.
[84] J. S. Capes, H. Y. Ando, and R. E. Cameron, "Fabrication of polymeric scaffolds with a controlled distribution of pores," *J Mater Sci Mater Med,* vol. 16, pp. 1069-75, Dec 2005.
[85] L. Draghi, S. Resta, M. G. Pirozzolo, and M. C. Tanzi, "Microspheres leaching for scaffold porosity control," *J Mater Sci Mater Med,* vol. 16, pp. 1093-7, Dec 2005.
[86] M. Hacker, M. Ringhofer, B. Appel, M. Neubauer, T. Vogel, S. Young, A. G. Mikos, T. Blunk, A. Gopferich, and M. B. Schulz, "Solid lipid templating of macroporous tissue engineering scaffolds," *Biomaterials,* vol. 28, pp. 3497-507, Aug 2007.
[87] T. Weigel, G. Schinkel, and A. Lendlein, "Design and preparation of polymeric scaffolds for tissue engineering," *Expert Rev Med Devices,* vol. 3, pp. 835-51, Nov 2006.
[88] R. Zhang and P. X. Ma, "Poly(alpha-hydroxyl acids)/hydroxyapatite porous composites for bone-tissue engineering. I. Preparation and morphology," *J Biomed Mater Res,* vol. 44, pp. 446-55, Mar 15 1999.

[89] A. G. Coombes and J. D. Heckman, "Gel casting of resorbable polymers. 1. Processing and applications," *Biomaterials,* vol. 13, pp. 217-24, 1992.
[90] Y. H. Gong, Z. W. Ma, C. Y. Gao, W. Wang, and J. C. Shen, "Specially elaborated thermally induced phase separation to fabricate poly(L-lactic acid) scaffolds with ultra large pores and good interconnectivity," *Journal of Applied Polymer Science,* vol. 101, pp. 3336-3342, Sep 5 2006.
[91] L. D. Harris, B. S. Kim, and D. J. Mooney, "Open pore biodegradable matrices formed with gas foaming," *J Biomed Mater Res,* vol. 42, pp. 396-402, Dec 5 1998.
[92] X. H. Liu and P. X. Ma, "Polymeric scaffolds for bone tissue engineering," *Annals of Biomedical Engineering,* vol. 32, pp. 477-486, Mar 2004.
[93] L. D. Harris, B. S. Kim, and D. J. Mooney, "Open pore biodegradable matrices formed with gas foaming," *Journal of Biomedical Materials Research,* vol. 42, pp. 396-402, Dec 5 1998.
[94] D. J. Mooney, D. F. Baldwin, N. P. Suh, L. P. Vacanti, and R. Langer, "Novel approach to fabricate porous sponges of poly(D,L-lactic-co-glycolic acid) without the use of organic solvents," *Biomaterials,* vol. 17, pp. 1417-1422, Jul 1996.
[95] M. Borden, M. Attawia, Y. Khan, and C. T. Laurencin, "Tissue engineered microsphere-based matrices for bone repair: design and evaluation," *Biomaterials,* vol. 23, pp. 551-559, Jan 2002.
[96] M. Borden, S. F. El-Amin, M. Attawia, and C. T. Laurencin, "Structural and human cellular assessment of a novel microsphere-based tissue engineered scaffold for bone repair," *Biomaterials,* vol. 24, pp. 597-609, Feb 2003.
[97] M. E. Hoque, D. W. Hutmacher, W. Feng, S. Li, M. H. Huang, M. Vert, and Y. S. Wong, "Fabrication using a rapid prototyping system and in vitro characterization of PEG-PCL-PLA scaffolds for tissue engineering," *J Biomater Sci Polym Ed,* vol. 16, pp. 1595-610, 2005.
[98] J. J. Sun, C. J. Bae, Y. H. Koh, H. E. Kim, and H. W. Kim, "Fabrication of hydroxyapatite-poly(epsilon-caprolactone) scaffolds by a combination of the extrusion and bi-axial lamination processes," *Journal of Materials Science-Materials in Medicine,* vol. 18, pp. 1017-1023, Jun 2007.
[99] K. H. Tan, C. K. Chua, K. F. Leong, C. M. Cheah, P. Cheang, M. S. Abu Bakar, and S. W. Cha, "Scaffold development using selective laser sintering of polyetheretherketone-hydroxyapatite biocomposite blends," *Biomaterials,* vol. 24, pp. 3115-23, Aug 2003.
[100] A. S. Goldstein, T. M. Juarez, C. D. Helmke, M. C. Gustin, and A. G. Mikos, "Effect of convection on osteoblastic cell growth and function in biodegradable polymer foam scaffolds," *Biomaterials,* vol. 22, pp. 1279-88, Jun 2001.
[101] J. F. Alvarez-Barreto, S. M. Linehan, R. L. Shambaugh, and V. I. Sikavitsas, "Flow perfusion improves seeding of tissue engineering scaffolds with different architectures," *Ann Biomed Eng,* vol. 35, pp. 429-42, Mar 2007.
[102] L. Meinel, V. Karageorgiou, R. Fajardo, B. Snyder, V. Shinde-Patil, L. Zichner, D. Kaplan, R. Langer, and G. Vunjak-Novakovic, "Bone tissue engineering using human mesenchymal stem cells: effects of scaffold material and medium flow," *Ann Biomed Eng,* vol. 32, pp. 112-22, Jan 2004.

[103] S. L. Ishaug, G. M. Crane, M. J. Miller, A. W. Yasko, M. J. Yaszemski, and A. G. Mikos, "Bone formation by three-dimensional stromal osteoblast culture in biodegradable polymer scaffolds," *J Biomed Mater Res,* vol. 36, pp. 17-28, Jul 1997.
[104] S. H. Cartmell, B. D. Porter, A. J. Garcia, and R. E. Guldberg, "Effects of medium perfusion rate on cell-seeded three-dimensional bone constructs in vitro," *Tissue Eng,* vol. 9, pp. 1197-203, Dec 2003.
[105] N. Datta, Q. P. Pham, U. Sharma, V. I. Sikavitsas, J. A. Jansen, and A. G. Mikos, "In vitro generated extracellular matrix and fluid shear stress synergistically enhance 3D osteoblastic differentiation," *Proc Natl Acad Sci U S A,* vol. 103, pp. 2488-93, Feb 21 2006.
[106] L. Fassina, L. Visai, L. Asti, F. Benazzo, P. Speziale, M. C. Tanzi, and G. Magenes, "Calcified matrix production by SAOS-2 cells inside a polyurethane porous scaffold, using a perfusion bioreactor," *Tissue Eng,* vol. 11, pp. 685-700, May-Jun 2005.
[107] H. Hosseinkhani, Y. Inatsugu, Y. Hiraoka, S. Inoue, and Y. Tabata, "Perfusion culture enhances osteogenic differentiation of rat mesenchymal stem cells in collagen sponge reinforced with poly(glycolic Acid) fiber," *Tissue Eng,* vol. 11, pp. 1476-88, Sep-Oct 2005.
[108] V. I. Sikavitsas, G. N. Bancroft, H. L. Holtorf, J. A. Jansen, and A. G. Mikos, "Mineralized matrix deposition by marrow stromal osteoblasts in 3D perfusion culture increases with increasing fluid shear forces," *Proc Natl Acad Sci U S A,* vol. 100, pp. 14683-8, Dec 9 2003.
[109] J. Vance, S. Galley, D. F. Liu, and S. W. Donahue, "Mechanical stimulation of MC3T3 osteoblastic cells in a bone tissue-engineering bioreactor enhances prostaglandin E2 release," *Tissue Eng,* vol. 11, pp. 1832-9, Nov-Dec 2005.
[110] C. R. Jacobs, C. E. Yellowley, B. R. Davis, Z. Zhou, J. M. Cimbala, and H. J. Donahue, "Differential effect of steady versus oscillating flow on bone cells," *J Biomech,* vol. 31, pp. 969-76, Nov 1998.
[111] M. M. Thi, D. A. Iacobas, S. Iacobas, and D. C. Spray, "Fluid Shear Stress Up-regulates Vascular Endothelial Growth Factor Gene Expression in Osteoblasts," *Ann N Y Acad Sci,* Jul 23 2007.
[112] C. Chen, A. J. Koh, N. S. Datta, J. Zhang, E. T. Keller, G. Z. Xiao, R. T. Franceschi, N. J. D'Silva, and L. K. McCauley, "Impact of the mitogen-activated protein kinase pathway on parathyroid hormone-related protein actions in osteoblasts," *Journal of Biological Chemistry,* vol. 279, pp. 29121-29129, Jul 9 2004.
[113] S. Kapur, D. J. Baylink, and K. H. W. Lau, "Fluid flow shear stress stimulates human osteoblast proliferation and differentiation through multiple interacting and competing signal transduction pathways," *Bone,* vol. 32, pp. 241-251, Mar 2003.
[114] D. Shamir, S. Keila, and M. Weinreb, "A selective EP4 receptor antagonist abrogates the stimulation of osteoblast recruitment from bone marrow stromal cells by prostaglandin E-2 in vivo and in vitro," *Bone,* vol. 34, pp. 157-162, Jan 2004.
[115] G. Z. Xiao, R. Gopalakrishnan, D. Jiang, E. Reith, M. D. Benson, and R. T. Franceschi, "Bone morphogenetic proteins, extracellular matrix, and mitogen-activated protein kinase signaling pathways are required for osteoblast-specific gene

expression and differentiation in MC3T3-E1 cells," *Journal of Bone and Mineral Research,* vol. 17, pp. 101-110, Jan 2002.
[116] S. W. Donahue, H. J. Donahue, and C. R. Jacobs, "Osteoblastic cells have refractory periods for fluid-flow-induced intracellular calcium oscillations for short bouts of flow and display multiple low-magnitude oscillations during long-term flow," *J Biomech,* vol. 36, pp. 35-43, Jan 2003.
[117] M. G. Mullender, S. J. Dijcks, R. G. Bacabac, C. M. Semeins, J. J. Van Loon, and J. Klein-Nulend, "Release of nitric oxide, but not prostaglandin E2, by bone cells depends on fluid flow frequency," *J Orthop Res,* vol. 24, pp. 1170-7, Jun 2006.
[118] E. A. Nauman, R. L. Satcher, T. M. Keaveny, B. P. Halloran, and D. D. Bikle, "Osteoblasts respond to pulsatile fluid flow with short-term increases in PGE(2) but no change in mineralization," *J Appl Physiol,* vol. 90, pp. 1849-54, May 2001.
[119] K. Gisselfalt, B. Edberg, and P. Flodin, "Synthesis and properties of degradable poly(urethane urea)s to be used for ligament reconstructions," *Biomacromolecules,* vol. 3, pp. 951-8, Sep-Oct 2002.
[120] C. J. Spaans, V. W. Belgraver, O. Rienstra, J. H. de Groot, R. P. Veth, and A. J. Pennings, "Solvent-free fabrication of micro-porous polyurethane amide and polyurethane-urea scaffolds for repair and replacement of the knee-joint meniscus," *Biomaterials,* vol. 21, pp. 2453-60, Dec 2000.
[121] M. D. Lelah and S. L. Cooper, *Polyurethanes in medicine*. Boca Raton, Fla.: CRC Press, 1986.
[122] G. Oertel and L. Abele, *Polyurethane handbook : chemistry, raw materials, processing, application, properties*, 2nd ed. Munich ; New York
Cincinnati: Hanser ;
Hanser/Gardner [distributor], 1994.
[123] V. Thomas, T. V. Kumari, and M. Jayabalan, "In vitro studies on the effect of physical cross-linking on the biological performance of aliphatic poly(urethane urea) for blood contact applications," *Biomacromolecules,* vol. 2, pp. 588-96, Summer 2001.
[124] M. Szycher, *Szycher's handbook of polyurethanes*. Boca Raton: CRC Press, 1999.
[125] D. Hoffman, G. Gong, L. Pinchuk, and D. Sisto, "Safety and intracardiac function of a silicone-polyurethane elastomer designed for vascular use," *Clin Mater,* vol. 13, pp. 95-100, 1993.
[126] C. D. Capone, "Biostability of a non-ether polyurethane," *J Biomater Appl,* vol. 7, pp. 108-29, Oct 1992.
[127] M. Borkenhagen, R. C. Stoll, P. Neuenschwander, U. W. Suter, and P. Aebischer, "In vivo performance of a new biodegradable polyester urethane system used as a nerve guidance channel," *Biomaterials,* vol. 19, pp. 2155-65, Dec 1998.
[128] J. H. de Groot, F. M. Zijlstra, H. W. Kuipers, A. J. Pennings, J. Klompmaker, R. P. Veth, and H. W. Jansen, "Meniscal tissue regeneration in porous 50/50 copoly(L-lactide/epsilon-caprolactone) implants," *Biomaterials,* vol. 18, pp. 613-22, Apr 1997.
[129] J. Guan, M. S. Sacks, E. J. Beckman, and W. R. Wagner, "Synthesis, characterization, and cytocompatibility of elastomeric, biodegradable poly(ester-urethane)ureas based

on poly(caprolactone) and putrescine," *J Biomed Mater Res,* vol. 61, pp. 493-503, Sep 5 2002.
[130] J. Y. Zhang, E. J. Beckman, J. Hu, G. G. Yang, S. Agarwal, and J. O. Hollinger, "Synthesis, biodegradability, and biocompatibility of lysine diisocyanate-glucose polymers," *Tissue Eng,* vol. 8, pp. 771-85, Oct 2002.
[131] C. J. Spaans, J. H. De Groot, F. G. Dekens, and A. J. Pennings, "High molecular weight polyurethanes and a polyurethane urea based on 1,4-butate diisocyanate," *Polymer Bulletin,* vol. 41, pp. 131-8, 1998.
[132] M. Szycher, "Biostability of polyurethane elastomers: a critical review," *J Biomater Appl,* vol. 3, pp. 297-402, Oct 1988.
[133] A. S. Sawhney and J. A. Hubbell, "Rapidly degraded terpolymers of dl-lactide, glycolide, and epsilon-caprolactone with increased hydrophilicity by copolymerization with polyethers," *J Biomed Mater Res,* vol. 24, pp. 1397-411, Oct 1990.
[134] A. S. Badami, M. R. Kreke, M. S. Thompson, J. S. Riffle, and A. S. Goldstein, "Effect of fiber diameter on spreading, proliferation, and differentiation of osteoblastic cells on electrospun poly(lactic acid) substrates," *Biomaterials,* vol. 27, pp. 596-606, Feb 2006.
[135] M. R. Kreke, W. R. Huckle, and A. S. Goldstein, "Fluid flow stimulates expression of osteopontin and bone sialoprotein by bone marrow stromal cells in a temporally dependent manner," *Bone,* vol. 36, pp. 1047-55, Jun 2005.
[136] R. M. Porter, W. R. Huckle, and A. S. Goldstein, "Effect of dexamethasone withdrawal on osteoblastic differentiation of bone marrow stromal cells," *J Cell Biochem,* vol. 90, pp. 13-22, Sep 1 2003.
[137] A. S. Goldstein, "Effect of seeding osteoprogenitor cells as dense clusters on cell growth and differentiation," *Tissue Eng,* vol. 7, pp. 817-27, Dec 2001.
[138] K. J. Livak and T. D. Schmittgen, "Analysis of relative gene expression data using real-time quantitative PCR and the 2(-Delta Delta C(T)) Method," *Methods,* vol. 25, pp. 402-8, Dec 2001.
[139] J. Y. Lim, J. C. Hansen, C. A. Siedlecki, J. Runt, and H. J. Donahue, "Human foetal osteoblastic cell response to polymer-demixed nanotopographic interfaces," *J R Soc Interface,* vol. 2, pp. 97-108, Mar 22 2005.
[140] E. Liljensten, K. Gisselfalt, B. Edberg, H. Bertilsson, P. Flodin, A. Nilsson, A. Lindahl, and L. Peterson, "Studies of polyurethane urea bands for ACL reconstruction," *J Mater Sci Mater Med,* vol. 13, pp. 351-9, Apr 2002.
[141] K. Gisselfalt, *Structure dependent chemical and biological interactions of poly(urethane urea)s*: Goteborg: Chalmers University of Technology, 2002.
[142] P. Blais, "Letter to the editor," *Journal of Applied Biomaterials,* vol. 1, p. 197, 1990.
[143] A. Coury, "Biomaterials science: an introduction to materials in medicine.," B. Ratner, A. Hoffman, F. Schoen, and J. Lemons, Eds. Boston, MA: Academic Press, 2004, pp. 411-30.
[144] M. Szycher and A. A. Siciliano, "An assessment of 2,4 TDA formation from Surgitek polyurethane foam under simulated physiological conditions," *J Biomater Appl,* vol. 5, pp. 323-36, Apr 1991.

[145] J. H. de Groot, R. de Vrijer, B. S. Wildeboer, C. J. Spaans, and A. J. Pennings, "New biomedical polyurethane ureas with high tear strengths," *Polymer Bulletin,* vol. 38, pp. 211-8, 1997.
[146] J. Guan, M. S. Sacks, E. J. Beckman, and W. R. Wagner, "Biodegradable poly(ether ester urethane)urea elastomers based on poly(ether ester) triblock copolymers and putrescine: synthesis, characterization and cytocompatibility," *Biomaterials,* vol. 25, pp. 85-96, Jan 2004.
[147] G. A. Skarja and K. A. Woodhouse, "Synthesis and characterization of degradable polyurethane elastomers containing and amino acid-based chain extender," *J Biomater Sci Polym Ed,* vol. 9, pp. 271-95, 1998.
[148] G. A. Skarja and K. A. Woodhouse, "Structure-property relationshios of degradable polyurethane elastomers containing an amino acid-based chain extender," *Journal of Applied Polymer Science,* vol. 75, pp. 1522-34, 2000.
[149] P. Bruin, G. J. Veenstra, A. J. Nijenhuis, and A. J. Pennings, "Design and synthesis of biodegradable poly(esterurethane) elastomer networks composed of non-toxic building blocks," *Makromolekular Chemie, Rapid Communications,* vol. 9, pp. 589-94, 1988.
[150] J. D. Fromstein and K. A. Woodhouse, "Elastomeric biodegradable polyurethane blends for soft tissue applications," *J Biomater Sci Polym Ed,* vol. 13, pp. 391-406, 2002.
[151] J. J. Stankus, J. Guan, and W. R. Wagner, "Fabrication of biodegradable elastomeric scaffolds with sub-micron morphologies," *J Biomed Mater Res A,* vol. 70, pp. 603-14, Sep 15 2004.
[152] R. Herrington, K. Hock, and R. Autenrieth, *Flexible polyurethane foams*, 2nd ed. Midland, MI: Dow Chemical Co., 1997.
[153] L. H. Sperling, *Introduction to physical polymer science*, 4th ed. Hoboken, N.J.: Wiley, 2006.
[154] B. G. Keselowsky, D. M. Collard, and A. J. Garcia, "Surface chemistry modulates fibronectin conformation and directs integrin binding and specificity to control cell adhesion," *J Biomed Mater Res A,* vol. 66, pp. 247-59, Aug 1 2003.
[155] K. E. Michael, V. N. Vernekar, B. G. Keselowsky, J. C. Meredith, R. A. Latour, and A. J. Garcia, "Adsorption-induced conformational changes in fibronectin due to interactions with well-defined surface chemistries," *Langmuir,* vol. 19, pp. 8033-40, 2003.
[156] C. A. Scotchford, E. Cooper, G. J. Leggett, and S. Downes, "Growth of human osteoblast-like cells on alkanethiol on gold self-assembled monolayers: the effect of surface chemistry," *J Biomed Mater Res,* vol. 41, pp. 431-42, Sep 5 1998.
[157] B. G. Keselowsky, D. M. Collard, and A. J. Garcia, "Surface chemistry modulates focal adhesion composition and signaling through changes in integrin binding," *Biomaterials,* vol. 25, pp. 5947-54, Dec 2004.
[158] J. C. Meredith, J. L. Sormana, B. G. Keselowsky, A. J. Garcia, A. Tona, A. Karim, and E. J. Amis, "Combinatorial characterization of cell interactions with polymer surfaces," *J Biomed Mater Res A,* vol. 66, pp. 483-90, Sep 1 2003.

[159] J. M. Schakenraad, H. J. Busscher, C. R. Wildevuur, and J. Arends, "The influence of substratum surface free energy on growth and spreading of human fibroblasts in the presence and absence of serum proteins," *J Biomed Mater Res,* vol. 20, pp. 773-84, Jul-Aug 1986.
[160] X. Liu, J. Y. Lim, H. J. Donahue, R. Dhurjati, A. M. Mastro, and E. A. Vogler, "Influence of substratum surface chemistry/energy and topography on the human fetal osteoblastic cell line hFOB 1.19: Phenotypic and genotypic responses observed in vitro," *Biomaterials,* vol. 28, pp. 4535-50, Nov 2007.
[161] J. D. Bronzino, *The biomedical engineering handbook*, 3rd ed. Boca Raton: CRC/Taylor & Francis, 2006.
[162] R. G. Flemming, C. J. Murphy, G. A. Abrams, S. L. Goodman, and P. F. Nealey, "Effects of synthetic micro- and nano-structured surfaces on cell behavior," *Biomaterials,* vol. 20, pp. 573-88, Mar 1999.
[163] R. Singhvi, G. Stephanopoulos, and D. I. Wang, "Effects of substratum morphology on cell physiology," *Biotechnol Bioeng,* vol. 43, pp. 764-71, Apr 5 1994.
[164] B. D. Boyan, R. Batzer, K. Kieswetter, Y. Liu, D. L. Cochran, S. Szmuckler-Moncler, D. D. Dean, and Z. Schwartz, "Titanium surface roughness alters responsiveness of MG63 osteoblast-like cells to 1 alpha,25-(OH)2D3," *J Biomed Mater Res,* vol. 39, pp. 77-85, Jan 1998.
[165] C. H. Lohmann, L. F. Bonewald, M. A. Sisk, V. L. Sylvia, D. L. Cochran, D. D. Dean, B. D. Boyan, and Z. Schwartz, "Maturation state determines the response of osteogenic cells to surface roughness and 1,25-dihydroxyvitamin D3," *J Bone Miner Res,* vol. 15, pp. 1169-80, Jun 2000.
[166] J. Y. Martin, Z. Schwartz, T. W. Hummert, D. M. Schraub, J. Simpson, J. Lankford, Jr., D. D. Dean, D. L. Cochran, and B. D. Boyan, "Effect of titanium surface roughness on proliferation, differentiation, and protein synthesis of human osteoblast-like cells (MG63)," *J Biomed Mater Res,* vol. 29, pp. 389-401, Mar 1995.
[167] A. J. Engler, S. Sen, H. L. Sweeney, and D. E. Discher, "Matrix elasticity directs stem cell lineage specification," *Cell,* vol. 126, pp. 677-689, Aug 25 2006.
[168] C. B. Khatiwala, S. R. Peyton, M. Metzke, and A. J. Putnam, "The regulation of osteogenesis by ECM rigidity in MC3T3-E1 cells requires MAPK activation," *Journal of Cellular Physiology,* vol. 211, pp. 661-672, Jun 2007.
[169] C. B. Khatiwala, S. R. Peyton, and A. J. Putnam, "Intrinsic mechanical properties of the extracellular matrix affect the behavior of pre-osteoblastic MC3T3-E1 cells," *American Journal of Physiology-Cell Physiology,* vol. 290, pp. C1640-C1650, Jun 2006.
[170] K. D. Kavlock, T. W. Pechar, J. O. Hollinger, S. A. Guelcher, and A. S. Goldstein, "Synthesis and characterization of segmented poly(esterurethane urea) elastomers for bone tissue engineering," *Acta Biomater,* vol. 3, pp. 475-84, Jul 2007.
[171] C. A. Bashur, L. A. Dahlgren, and A. S. Goldstein, "Effect of fiber diameter and orientation on fibroblast morphology and proliferation on electrospun poly(D,L-lactic-co-glycolic acid) meshes," *Biomaterials,* vol. 27, pp. 5681-8, Nov 2006.

[172] T. Q. Ngo, M. A. Scherer, F. H. Zhou, B. K. Foster, and C. J. Xian, "Expression of bone morphogenic proteins and receptors at the injured growth plate cartilage in young rats," *J Histochem Cytochem,* vol. 54, pp. 945-54, Aug 2006.
[173] J. Lincks, B. D. Boyan, C. R. Blanchard, C. H. Lohmann, Y. Liu, D. L. Cochran, D. D. Dean, and Z. Schwartz, "Response of MG63 osteoblast-like cells to titanium and titanium alloy is dependent on surface roughness and composition," *Biomaterials,* vol. 19, pp. 2219-32, Dec 1998.
[174] J. S. Czarnecki, K. Lafdi, and P. A. Tsonis, "A novel approach to control growth, orientation, and shape of human osteoblasts," *Tissue Eng Part A,* vol. 14, pp. 255-65, Feb 2008.
[175] K. E. Michael, V. N. Vernekar, B. G. Keselowsky, J. C. Meredith, R. A. Latour, and A. J. Garcia, "Adsorption-induced conformational changes in fibronectin due to interactions with well-defined surface chemistries," *Langmuir,* vol. 19, pp. 8033-8040, Sep 16 2003.
[176] Z. Schwartz, R. Olivares-Navarrete, S. Hyzy, C. Erdman, D. L. Cochran, M. Weiland, and B. D. Boyan, "Surface microtopographies regulate human mesenchymal cells both directly and indirectly," in *55th Annual Meeting of the Orthopaedic Research Society*, Las Vegas, NV, 2009.
[177] S. A. Guelcher, "Biodegradable polyurethanes: synthesis and applications in regenerative medicine," *Tissue Eng Part B Rev,* vol. 14, pp. 3-17, Mar 2008.
[178] K. A. Athanasiou, C. M. Agrawal, F. A. Barber, and S. S. Burkhart, "Orthopaedic applications for PLA-PGA biodegradable polymers," *Arthroscopy,* vol. 14, pp. 726-37, Oct 1998.
[179] S. R. Bannister, C. H. Lohmann, Y. Liu, V. L. Sylvia, D. L. Cochran, D. D. Dean, B. D. Boyan, and Z. Schwartz, "Shear force modulates osteoblast response to surface roughness," *J Biomed Mater Res,* vol. 60, pp. 167-74, Apr 2002.
[180] K. Sakai, M. Mohtai, and Y. Iwamoto, "Fluid shear stress increases transforming growth factor beta 1 expression in human osteoblast-like cells: modulation by cation channel blockades," *Calcif Tissue Int,* vol. 63, pp. 515-20, Dec 1998.
[181] G. N. Bancroft, V. I. Sikavitsas, J. van den Dolder, T. L. Sheffield, C. G. Ambrose, J. A. Jansen, and A. G. Mikos, "Fluid flow increases mineralized matrix deposition in 3D perfusion culture of marrow stromal osteoblasts in a dose-dependent manner," *Proc Natl Acad Sci U S A,* vol. 99, pp. 12600-5, Oct 1 2002.
[182] M. M. Thi, D. A. Iacobas, S. Iacobas, and D. C. Spray, "Fluid shear stress upregulates vascular endothelial growth factor gene expression in osteoblasts," *Ann N Y Acad Sci,* vol. 1117, pp. 73-81, Nov 2007.
[183] M. J. Jaasma and F. J. O'Brien, "Mechanical stimulation of osteoblasts using steady and dynamic fluid flow," *Tissue Eng Part A,* vol. 14, pp. 1213-23, Jul 2008.
[184] G. N. Bancroft, V. I. Sikavitsas, and A. G. Mikos, "Design of a flow perfusion bioreactor system for bone tissue-engineering applications," *Tissue Eng,* vol. 9, pp. 549-54, Jun 2003.
[185] T. G. van Kooten, J. M. Schakenraad, H. C. van der Mei, A. Dekker, C. J. Kirkpatrick, M. Walter, D. Korzec, J. Engemann, and H. J. Busscher, "Fluid shear

induced endothelial cell detachment from modified polystyrene substrata," *Colloids and Surfaces B: Biointerfaces,* vol. 3, pp. 147-158, 1994.
[186] M. J. Jaasma, N. A. Plunkett, and F. J. O'Brien, "Design and validation of a dynamic flow perfusion bioreactor for use with compliant tissue engineering scaffolds," *J Biotechnol,* vol. 133, pp. 490-6, Feb 29 2008.
[187] H. L. Holtorf, J. A. Jansen, and A. G. Mikos, "Flow perfusion culture induces the osteoblastic differentiation of marrow stroma cell-scaffold constructs in the absence of dexamethasone," *J Biomed Mater Res A,* vol. 72, pp. 326-34, Mar 1 2005.
[188] H. L. Holtorf, T. L. Sheffield, C. G. Ambrose, J. A. Jansen, and A. G. Mikos, "Flow perfusion culture of marrow stromal cells seeded on porous biphasic calcium phosphate ceramics," *Ann Biomed Eng,* vol. 33, pp. 1238-48, Sep 2005.

Appendix A: Basic Stamp Program to Control Pulsatile Flow

```
'================================================================================

' File .... Quad_VALVE-control.BS2
' version .... 0.9
' Purpose .... VALVEs Controller
' Author .... riley chan (Copyright 2005, All Rights Reserved)
' Started .... riley, August 2005
' Updated ....
' modified .... 6/12/06
' pulses 3/12 (valve 1), 5/20 (valve 2), 15/60 (valve 3)

'================================================================================

'-----<USER'S PARAMETERS ENTRY>-----------------------------------------------------------
' ..... MINUTE = 5                              ' Time of VALVE FLOW, in minutes
'-----</USER'S PARAMETERS ENTRY>----------------------------------------------------------

'-----<NOTES>-----------------------------------------------------------------------------------------------
' program written for Goldstein.
' PAUSE = about 1 millisecond, 1 to 65535 counts
'-----</NOTES>----------------------------------------------------------------------------------------------

'-----<APPENDs>---------------------------------------------------------------------------------------------

'-----</APPENDs>--------------------------------------------------------------------------------------------

'-----<Program Description>---------------------------------------------------------------------------------
' Program to control FOUR (4) SOLENOID VALVES to switch ON and OFF as defined by a
' Time_Base, "MINUTE", as defined above. The four VALVEs are switched in a 1-2-4-8
' sequence.

' A switch is used to START and STOP the control sequence. Restart is effected by the
' RESET switch.

' PAUSE 1000 command is used establish a 1 SECOND interval which is counted by 60,
' [ FOR-NEXT ] to get a one (1) MINUTE basis. The SECOND interval is also used to drive
' a HeartBeat LED display, connected to PIN 11.

' The 1-2-4-8 interval is generated by four (4) "A = A + 1" loops counting in 1, 2, 4, 8 reset
' rates, respectively. At the end of the count rates, the OUTPUT pins associated with a
' VALVE is TOGGLED.
```

```
' A switch, connected to PIN 9, is used to START/STOP the sequence using the BUTTON
' command.
' -----</Program Description>----------------------------------------------------------------------------

' -----<Block Diagram>-----------------------------------------------------------------------------------
```

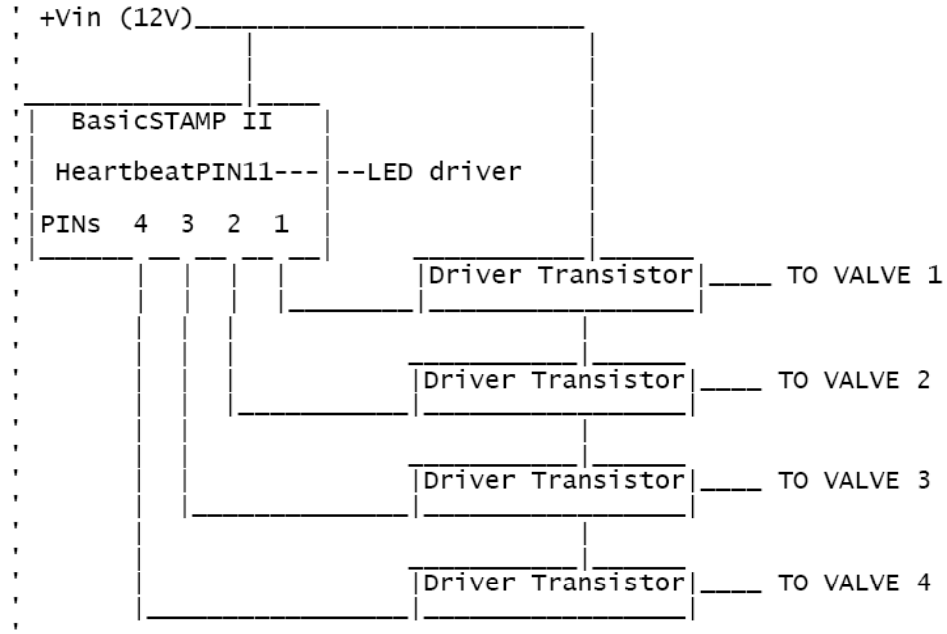


```
'-----</Block Diagram>----------------------------------------------------------------------------------

'-----<BS2 PIN assignment>------------------------------------------------------------------------------
DIRL = %1111000000000000
' pin 0
' pin 1 --- Valve 1
' pin 2 --- Valve 2
' pin 3 --- Valve 3
' pin 4 --- Valve 4
' pin 5
' pin 6
' pin 7
' pin 8
' pin 9
' pin 10
' pin 11
' pin 12
' pin 13
' pin 14
' pin 15
'-----</BS2 PIN assignment>-----------------------------------------------------------------------------
```

```
'-----<Variables>----------------------------------------------------------------------------------------
btnCHK VAR Byte ' workspace for BUTTON check, active LOW
SECONDs VAR Byte ' seconds basis
MINUTE VAR Byte ' establish minutes
V_Time VAR Byte ' PERIOD of VALVE switching set by user
V_1 VAR Byte ' counter Variable
V_2 VAR Byte
V_3 VAR Byte
V_4 VAR Byte
cyclic VAR Byte
'-----</Variables>---------------------------------------------------------------------------------------

'-----<Initialization>------------------------------------------------------------------------------------
Initialize:
btnCHK = 0
V_1 = 0
V_2 = 0
V_3 = 0
V_4 = 0
'HIGH 1 'valves off
HIGH 2
HIGH 3
HIGH 4
'LOW 1 ' reset VALVES to close
'LOW 2
'LOW 3
'LOW 4
'-----</Initialization>----------------------------------------------------------------------------------

'-----<Program Code>--------------------------------------------------------------------------------------
'-----<START switch>--------------------------------------------------------------------------------------
waitLoop:
' BUTTON 9, 0, 255, 250, btnCHK, 0, noPress 'goto noPress if PIN9 is LOW
'-----</START switch>-------------------------------------------------------------------------------------

Main:
'-----<TERMINATE switch>----------------------------------------------------------------------------------
' BUTTON 9, 0, 255, 250, btnCHK, 0, control 'goto terminate if PIN9 is LOW
' GOTO stopProc
control:
'-----</TERMINATE switch>---------------------------------------------------------------------------------

'-----<Program START>-------------------------------------------------------------------------------------
```

```
DEBUG CLS ' clear display SerialPort

'-----<LOOPing>----------------------------------------------------------------------------------------
DO

'-----<VALVE Control>----------------------------------------------------------------------------------
cyclic = cyclic + 1
IF cyclic = 9 THEN
LOW 4 'valve 1 'valve opens
ELSEIF cyclic = 12 THEN
HIGH 4
ELSEIF cyclic = 15 THEN
LOW 2
ELSEIF cyclic = 20 THEN
HIGH 2
ELSEIF cyclic = 21 THEN
LOW 4
ELSEIF cyclic = 24 THEN
HIGH 4
ELSEIF cyclic = 33 THEN
LOW 4
ELSEIF cyclic = 35 THEN
LOW 2
ELSEIF cyclic = 36 THEN
HIGH 4
ELSEIF cyclic = 40 THEN
HIGH 2
ELSEIF cyclic = 44 THEN
LOW 4
ELSEIF cyclic = 45 THEN
LOW 3
ELSEIF cyclic = 47 THEN
HIGH 4
ELSEIF cyclic = 55 THEN
LOW 2
ELSEIF cyclic = 57 THEN
LOW 4
ELSEIF cyclic = 60 THEN
cyclic = 1
HIGH 4
HIGH 2
HIGH 3
ENDIF
'-----</VALVE Control>---------------------------------------------------------------------------------
```

```
'-----<Print to SERIAL Port>-----------------------------------------------------------------------
DEBUG CRSRXY, 0 ,5, "status of valves --- (4, 3, 2, 1) : ", BIN IN4, BIN IN3, BIN IN2,
BIN IN1
'-----</Print to SERIAL Port>-----------------------------------------------------------------------

'-----<Establish Time BASE in 10 seconds>-----------------------------------------------------------
  FOR V_Time = 1 TO 1 ' establish VALVE Period basis
  PAUSE 1000 ' establish seconds basis ( 1000 )
NEXT
'-----</Establish Time BASE in 10 seconds>-----------------------------------------------------------

LOOP
'-----</LOOPing>-------------------------------------------------------------------------------------
'-----</Program START>-------------------------------------------------------------------------------

'-----<reset VALVES and END>-------------------------------------------------------------------------
stopProc:
terminate:      ' reset VALVES to close
'HIGH 1         'valves open
HIGH 2
HIGH 3
HIGH 4
'-----</reset VALVES and END>-----------------------------------------------------------------------

END             ' end program
'-----</Program Code>-------------------------------------------------------------------------------

noPress:
  GOTO waitLoop
END
```